Universitat Autònoma de Barcelona

Rational Design and Synthesis of New Nucleoside Analogues Bearing a Cyclohexane Core

Beatriz Domínguez Pérez

Ph.D. Thesis

Ph.D. in Chemistry

Supervisors:

Dr. Ramon Alibés Arqués

Dr. Félix Busqué Sánchez

Dr. Jean-Didier Márechal

Departament de Química

Facultat de Ciències

2015

Chapter V: Study of antiviral activity of prodrug candidates

1. Evaluation of the antiviral activity

In this work, a novel class of six-membered carbocyclic nucleoside analogues built on a bicyclo[4.1.0]heptane scaffold and bearing different nucleobases have been synthesised as anti-HSV agents (Figure V-1).

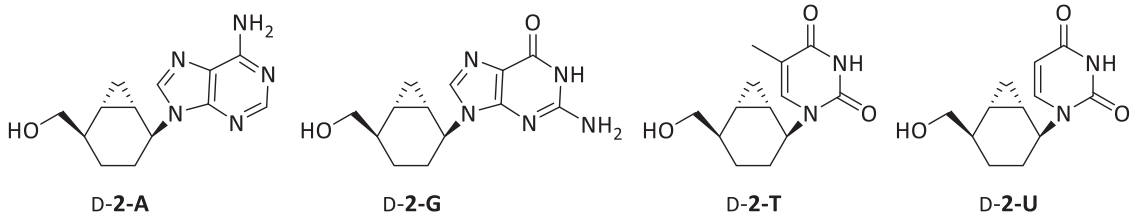

Figure V-1. Nucleoside analogues synthesised in the present dissertation.

The antiviral activity of all these nucleoside analogues has been evaluated against several viruses at the group leaded by Prof. Jan Balzarini at the Rega Institute for Medical Research, *Katholieke Universiteit Leuven*. Nucleosides D-**2-A**, D-**2-G**, D-**2-T** and D-**2-U** have been tested for antiviral activity against different viruses, such as HSV-1 (KOS), HSV-2 (G), HSV-1 resistant to ACV (TK^- KOS ACV^r) in human embryonic lung (HEL) cell cultures, among others (Tables V-1-5). Undoubtedly, results are at least confusing. On one side, all compounds but D-**2-U** (in MDK cell cultures, Table 4) have shown no cytotoxic activity. This shows a certain improvement regarding our previous families of antiviral candidates which displayed major cytotoxic effect, since these compounds are basically unharmful. On the other, the fact that D-**2-U** does display those effects in a given line confirms that this new series of compounds are able to pass the cellular membranes as predicted by the initial chemoinformatic analysis.

Unfortunately, though, this new family of compounds does not fulfil its major objective and none of them exhibit antiviral activity at concentrations up to 100 μg/mL.

Table V-1. Cytotoxicity and antiviral activity in: CRFK (Crandell-Rees Feline Kidney) cell cultures.

Compound	CC50[a] (µg/ml)	EC50[b]	
		Feline Corona Virus (FIPV)	Feline Herpes Virus
D-**2-A**	>100	>100	>100
D-**2-G**	>100	>100	>100
D-**2-T**	>100	>100	>100
D-**2-U**	>100	>100	>100
HHA	>100	18.0	9.8
UDA	>100	12.5	7.8
Ganciclovir (µM)	>100	>100	6.9

[a] 50% Cytotoxic concentration, as determined by measuring the cell viability with the colorimetric formazan-based MTS assay.

[b] 50% Effective concentration, or concentration producing 50% inhibition of virus-induced cytopathic effect, as determined by measuring the cell viability with the colorimetric formazan-based MTS assay.

Table V-2. Cytotoxicity and antiviral activity in: HEL cell cultures.

Compound	Min. cytotoxic concentration[a] (µg/mL)	EC_{50}[b]					
		Herpes simplex virus-1 (KOS)	Herpes simplex virus-2 (G)	Herpes simplex virus-1 TK^- KOS ACV^r	Vaccinia virus	Adeno virus-2	Vesicular stomatitis virus
D-**2-A**	≥100	>100	>100	>100	>100	>100	>100
D-**2-G**	>100	>100	>100	>100	>100	>100	>100
D-**2-T**	>100	>100	>100	>100	>100	>100	>100
D-**2-U**	100	>100	>100	>100	>100	>100	>100
Brivudin (µM)	>250	0.06	250	250	29	-	>250
Cidofovir (µM)	>250	2.0	2.0	2.0	29	10	>250
Acyclovir (µM)	>250	0.8	0.8	50	>250	-	>250
Ganciclovir (µM)	>100	0.03	0.08	4.0	>100	-	>100
Zalcitabine (µM)	>250	-	-	-	-	10	-
Alovudine (µM)	>250	-	-	-	-	5.8	-

[a] Required to cause a microscopically detectable alteration of normal cell morphology.

[b] Required to reduce virus-induced cytopathogenicity by 50 %.

Table V-3. Cytotoxicity and antiviral activity in: HeLa cell cultures.

Compound	Minimum cytotoxic concentration[a] (µg/ml)	EC_{50}[b]		
		Vesicular stomatitis virus	Coxsackie virus B4	Respiratory syncytial virus
D-**2-A**	>100	>100	>100	>100
D-**2-G**	>100	>100	>100	>100
D-**2-T**	>100	>100	>100	>100
D-**2-U**	>100	>100	>100	>100
DS-10.000	>100	1.8	100	2.0
Ribavirin (µM)	>250	22	112	5.0

[a] Required to cause a microscopically detectable alteration of normal cell morphology.

[b] Required to reduce virus-induced cytopathogenicity by 50 %.

Table V-4. Cytotoxicity and antiviral activity in: MDCK cell cultures.

Compound	Cytotoxicity		Antiviral EC_{50}[c]					
	CC_{50}[a]	Minimum cytotoxic concentration[b]	Influenza A/H1N1 A/Ned/378/05		Influenza A/H3N2 A/HK/7/87		Influenza B B/Ned/537/05	
			visual CPE score	MTS	visual CPE score	MTS	visual CPE score	MTS
D-**2-A**	>100	>100	>100	>100	>100	>100	>100	>100
D-**2-G**	>100	>100	>100	>100	>100	>100	>100	>100
D-**2-T**	>100	>100	>100	>100	>100	>100	>100	>100
D-**2-U**	49.8	100	>100	>100	>100	>100	>100	>100
Zanamivir (µM)	>100	>100	0.4	0.09	4.0	6.4	0.8	0.4
Ribavirin (µM)	76.8	≥100	6.8	2.8	6.8	1.9	4.0	1.5
Amantadine (µM)	>200	>200	8.0	3.8	1.6	1.1	>200	>200
Rimantadine (µM)	>200	>200	8.0	2.3	0.2	0.1	>200	>200

[a] 50% Cytotoxic concentration, as determined by measuring the cell viability with the colorimetric formazan-based MTS assay.

[b] Required to cause a microscopically detectable alteration of normal cell morphology.

[c] 50% Effective concentration, or concentration producing 50% inhibition of virus-induced cytopathic effect, as determined by measuring the cell viability with the colorimetric formazan-based MTS assay.

Table V-5. Cytotoxicity and antiviral activity in: Vero cell cultures.

Compound	Minimum cytotoxic concentration[a] (μg/mL)	EC_{50}[b]				
		Para-influenza-3 virus	Reovirus-1	Sindbis virus	Coxsackie virus B4	Punta Toro virus
D-**2-A**	>100	>100	>100	>100	>100	>100
D-**2-G**	>100	>100	>100	>100	>100	>100
D-**2-T**	>100	>100	>100	>100	>100	>100
D-**2-U**	>100	>100	>100	>100	>100	>100
DS-10.000	>100	>100	>100	>100	100	100
Ribavirin (μM)	>250	146	146	250	>250	112
Mycophenolic acid (μM)	>100	0.8	2.3	100	>250	50

[a] Required to cause a microscopically detectable alteration of normal cell morphology.

[b] Required to reduce virus-induced cytopathogenicity by 50 %.

2. Rationalisation of the antiviral activity

In order to shed light on this lack of activity, we decided to analyse back our approach and seek for the possible causes of failure.

One of the plausible causes could be the failure in the penetration through the cell membrane although all our compounds fulfil the Lipinski's rule of five. However, the fact that these compounds are chemically similar to potential drugs makes this hypothesis unlikely. Moreover, uracil derivative D-**2-U** shows cytotoxic effects which suggest penetration.

It has been reported that the major cause of failure in antiviral activity of nucleoside analogues is due to the activation process and more specifically to the first phosphorylation step.[1] Thus, the lack of activity of our compounds may be due to the failure of activation by the three kinases responsible for the triphosphorylation process. However, our theoretical calculations on the whole activation process reveal that the activation of our compounds seem quite feasible with a certain amount of uncertainly on results obtained on the third phosphorylation step. The same generality of the modelling process (magnesium, scoring function, flexibility) could be also part of the failure. A possible problem raises from the lack of experimental *in vitro* data to check modelling prediction.

Finally, another possible cause could be a higher specificity of HSV-1 DNA polymerase than generally expected, which would lead to a failure of our compounds to block the replication process. Therefore, to check whether the lack of activity was due to this step, a novel molecular docking was performed to study the interaction of the activated nucleosides with their target.

2.1. Interaction with DNA polymerase

Numerous evidences have led to consider failures in pharmacological activity of antiviral prodrug candidates based on nucleotide scaffolds raise from the lack of triphosphorylation. However, identifying molecules that could be activated by three enzymes in a stepwise process is by far a major tour de force. In this work, our primary objective was to generate molecules that could pass through this entire activation step. The major hypothesis of this framework was that DNA polymerase was promiscuous enough and should accept easily a triphosphorylated drug based on our scaffolds. In the view of the lack of activity of the compounds generated in this work, selectivity of DNA polymerase has become a possible cause. Protein-ligand docking was therefore further investigated to check how our compounds could act within the replication process.

To date, only the three dimensional structure of HSV DNA polymerase in its apo form is available in the Protein Data Bank. HSV-1 DNA polymerase (EC number: 2.7.7.7) is a homodimer with 1235 residues, which belongs to the polymerase α family. Each subunit is folded into six structure domains: a pre-NH_2-terminal, NH_2-terminal, 3'-5' exonuclease domain and polymerase thumb, fingers and palm domains (Figure V-2). It was reported that DNA polymerase interacts during DNA replication with an accessory factor, UL42, which increases the processivity of the polymerase.[2,3]

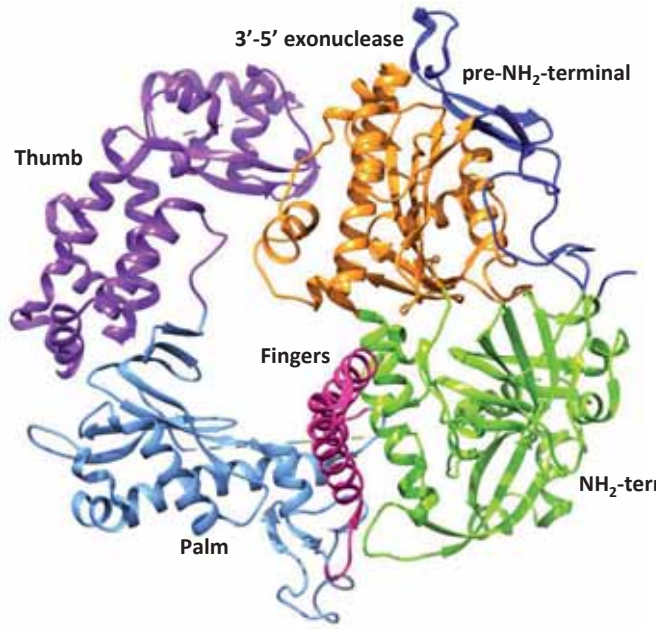

Figure V-2. Crystallographic structure of HSV-1 DNA polymerase (PDB code: 2GV9). Domains are depicted in different colours: pre-NH_2-terminal (blue), NH_2-terminal (green), 3'-5' exonuclease (orange), thumb (purple), palm (cyan) and fingers (pink).

Despite representing an important milestone in understanding the mechanism of action of the virus, this structure does not represent an interesting target for drug design. Indeed, this multidominial enzyme is known to perform major conformational changes upon DNA binding and a realistic docking experiment can only be achieved on a holo like structure. In the Protein Data Bank, only holo DNA polymerase of homologous systems are available. Therefore, a homology modelling like approach is needed to generate a three-dimensional structure of the replication complex of DNA polymerase with nucleotide drugs.

2.1.1. Homology modelling

Homology modelling, also known as comparative modelling, are computational tools to generate three-dimensional models of a given protein based on the primary sequence alignment with one or more proteins whose structures has been already resolved. This methodology is based on the principle that proteins with similar sequences have similar structures.[4,5] Despite the variety of homology modelling procedures, their general scheme could be summarised as: 1) identification of known structures of homologous molecules (templates) from the Protein Data Bank; 2) alignment of the target sequence to the template structure; 3) building the model based on the sequence alignment and 4) refinement of the model (Figure V-3). These steps may be repeated until a satisfactory model is build.[6]

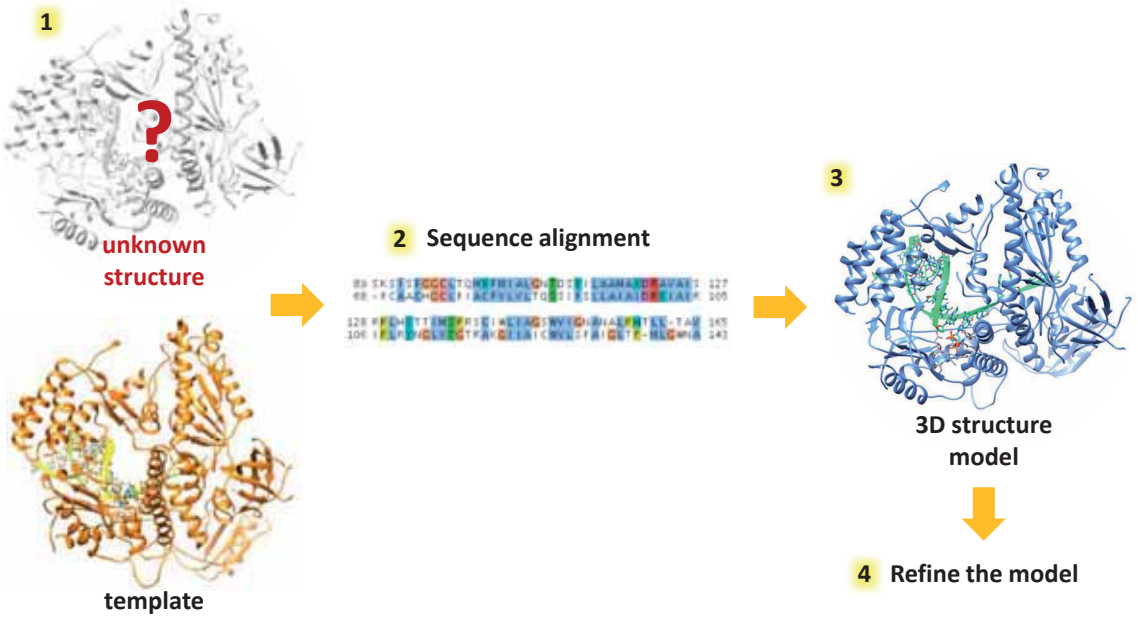

Figure V-3. Schematic representation of a homology modelling procedure.

In a large majority of cases, homology modelling is applied to the prediction of 3D structures of macromolecules based on a template. The resulting model presents a geometry similar to the initial model. In this case, the quality of the homology model relies on the level

of sequence similarity between the protein to study and the templates: the higher the sequence identity, the more accurate the resulting structure information.[7] It has been proved that if the sequence identity is greater than 30%, the resulting model is quite accurate and can be used in structure-based drug design whereas sequence identity of less than 30% leads to a less accurate model.

Homology modelling approaches also offers tools and techniques that can be used to manipulate one unique molecule and is generally applied to complex modelling whether alone or in combination with other methods. For example, homology modelling programs generally integrate loop optimization tools that are interesting allies in the exploration of the conformational space of proteins at the local minimum. However, homology modelling cannot generate major conformational changes in creating the model.

2.1.2. Generation of a model on an holo conformation of DNA polymerase

To carry out the homology modelling study, the first step was the search for known protein structures as templates for the desired model. As HSV-1 DNA polymerase belongs to polymerase α family, other polymerases of this family were evaluated as possible templates. In particular, we selected those with a crystallographic structure of the replication complex: from *Enterobacteriaphage RB69* (PDB code: 1IG9)[8] and yeast *Saccharomyces cerevisiae S288c* (PDB code: 4FYD)[9]. The sequence of DNA polymerase (PDB code: 2GV9)[10] was aligned to those of the templates in order to identify the best sequence identity, using the *UCSF Chimera* package.[11] The sequence identity between HSV-1 DNA polymerase and the RB69 polymerase amounts to 18%, while that between HSV-1 DNA polymerase and yeast amounts to 24%. As stated before, the sequence identity should be more than 30% in order to generate a reliable 3D model structure.

To overcome both the low sequence identity between our target and template, which include substantial missing parts of the structure between both species, and changes in conformation between the two homologous structures, we decided to use an approach based on morphing procedure.[12] Morphing consists in the generation of a trajectory from one 3D structure conformation to another by producing intermediate conformations. It has been widely used to demonstrate the motion of a protein as it changes between conformations.[12–14] As the amino acids of the binding site are almost identical (Figure V-4), this approximation allows to generate a holo like conformation at least at the region of interest for our docking process. Thus, a model of the replication complex of the target with DNA was created using the *Morph Conformations* tool of the *UCSF Chimera* package.

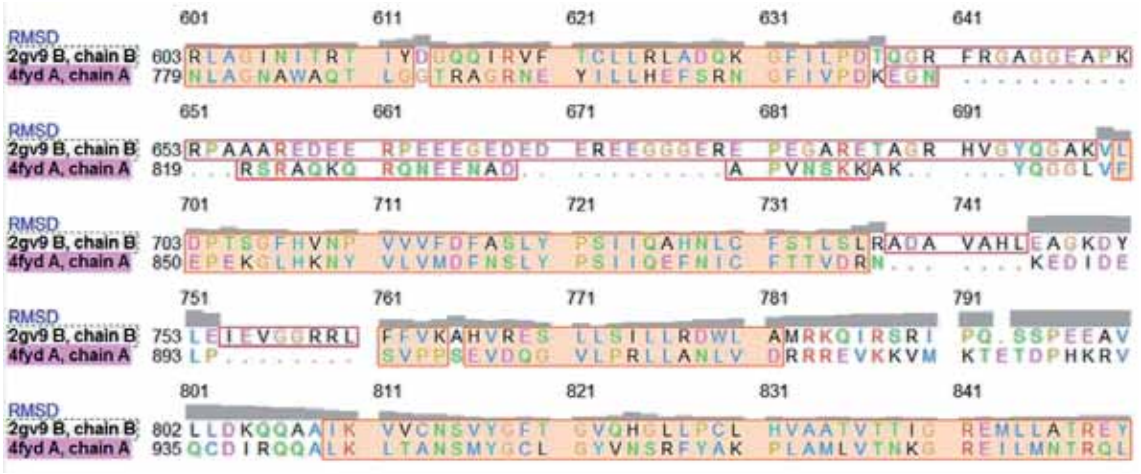

Figure V-4. Sequence alignemnt of the binding site of HSV-1 DNA polymerase (PDB: 2gv9) and yeast DNA polymerase (PDB: 4fyd).

The final homology model of the replication process of the target is shown in Figure V-5 along with its apo form. As one can see in the holo model of the replication state, the fingers domain has rotated close to the catalytic site in order to interact with the incoming nucleotide and the thumb domain has rotated to embrace the primer-template duplex.[10]

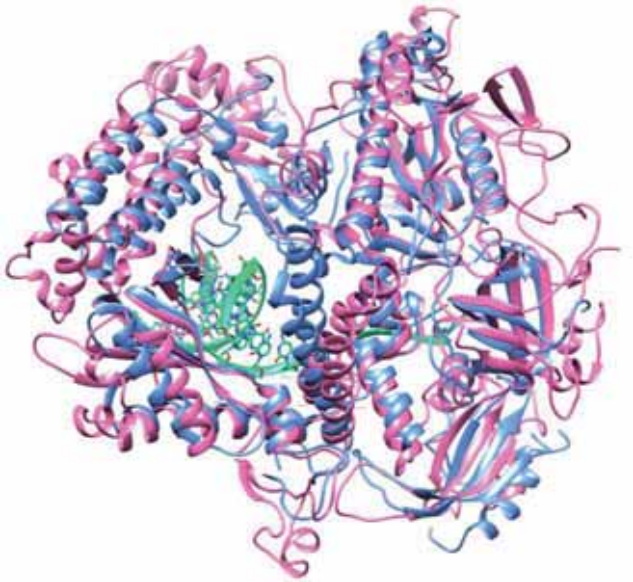

Figure V-5. The crystallographic structure of HSV-1 DNA polymerase in its apo form (pink) is shown along with the final homology model of the replication complex HSV-1 DNA polymerase with DNA (blue).

The generated model was used to carry out docking calculations on the synthesised ligands in order to evaluate their interactions with DNA polymerase.

2.1.3. Computational details

A trajectory that morphs the apo of the target to the template structure was generated with the *Morph Conformations* tool of the *UCSF Chimera* package.[11] Within the starting and

ending structures, intermediates were generated by interpolating the positions of the atoms in common. The interpolation of both structures is based on a RMS superposition of all atoms which minimises the RMS difference between Cα atoms in both conformations. Then, the pair of corresponding Cα atoms furthest apart are eliminated and the procedure is repeated until approximately half of the atoms in the protein have been eliminated. There are several interpolation methods available, but in our case the interpolation method used was *corkscrew* with a linear interpolation rate and in 20 steps. In this method, the two components interpolated are the rotation of groups of positions about a centre chosen to describe as much of the movement as possible, and the translation along the axis of rotation. This trajectory provided the homology model of the replication complex HSV DNA polymerase with DNA.

Protein-ligand docking calculations were used to predict all binding modes and energies. Those calculations were performed with the docking program GOLD (version 5.2.2),[15] and the scoring function used was *ChemPLP*.[16] Molecular graphics and visualization of docking results were performed with the *UCSF Chimera* package.[11]

The three-dimensional structures of the ligands were initially optimized using the *Marvin* work package[17] and the Merck molecular force field (MMFF) minimization.[18] Some modifications on the generated holo like structure of DNA polymerase must be performed with USCF Chimera before carrying out the docking calculations. All crystallographic waters, ions and ligands were also deleted from the enzyme. Hydrogen atoms were added and atom charges were assigned for the Amber force field using the Antechamber plugin of USCF Chimera.[19]

The central point of the docking cavity was set as Tyr722.B CD1 (radius 20 Å). Ligand flexibility was also considered in all the cases.

Finally, each nucleoside was docked into the enzyme and 20 predicted orientations were obtained and ranked. The results were analysed both in structural and energetic terms.

2.1.4. Docking results

- **Pyrimidine nucleoside analogues**

The interaction between dTTP and DNA polymerase in the binding site is detailed in Figure V-6. The incoming dTTP is pairing with the templating base, with the purine ring stacked against the base of the deoxynucleotide bound at the 3'-terminus of the primer strand. The phosphates are interacting via hydrogen bonds with Arg-789. Additionally, the 3'-OH is interacting with β-phosphate and Asn-815 via hydrogen bonds. It is worth noting that α-

phosphate is oriented towards the 3'-OH of the deoxynucleotide bound at the 3'-terminus of the primer strand.

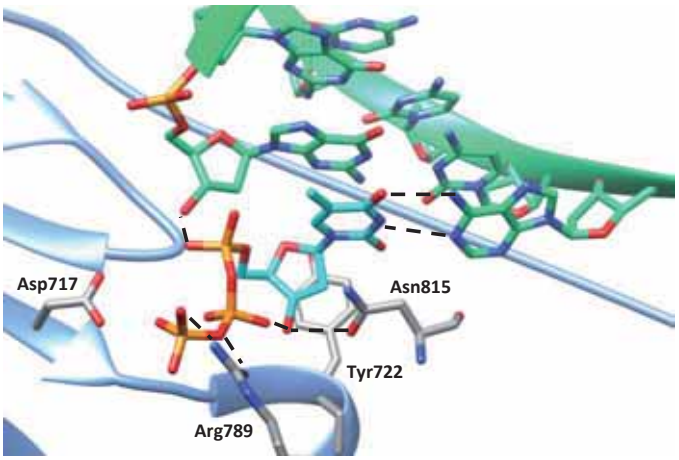

Figure V-6. Representation of the main interactions of dTTP (blue) in complex with DNA polymerase. X-ray residues shown in grey, DNA chains in green and backbone in blue. Hydrogen bonds are depicted as dotted lines. For the sake of clarity, crystallographic waters and hydrogen atoms are not shown.

Hence, the predicted orientations must present most of these interactions to be consistent with the catalysis, including the base paring with the corresponding nucleobase and the α-phosphate properly oriented.

We tested our docking protocol by carrying out calculations of the dTTP into the enzyme. The results showed that the lowest energy orientations with binding energies of -85 score units closely match the crystallographic structure of the template yeast *Saccharomyces cerevisiae S288c* (Figure V-7) and thus dTTP can be used as benchmark. It is therefore really encouraging to see that our objective to have a model of HSV-1 DNA polymerase consistent for pre-catalytic conformations has been fulfilled.

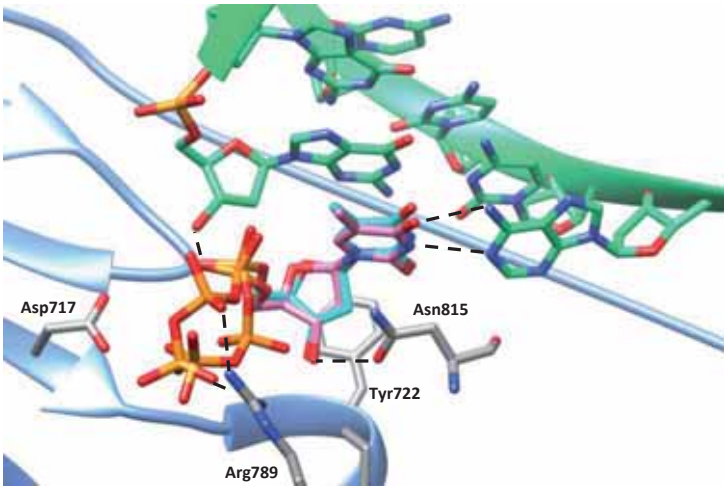

Figure V-7. dTTP (pink) superimposed to crystallographic dTTP (blue) in DNA polymerase nucleotide site (X-ray residues shown in grey). Hydrogen bonds are depicted as dotted lines. For the sake of clarity, crystallographic waters and hydrogen atoms are not shown.

Based on our initial results, dockings on our synthesised compounds were therefore carried out. For D-**2-TTP**, the lowest energy binding modes showed the thymine ring properly cleft and paired with the corresponding base. However, the α-phosphate was far away from the 3'-OH of the previous nucleotide and thus at distances unfavourable for the transfer of phosphate (Figure V-8a). On those grounds, although the binding energies are lower than those of dTTP (-92 score units), D-**2-TTP** is unlikely to be incorporated into the 3'-end of the growing primer stand.

On the other hand, docking calculations on D-**2-UTP** showed that the uracil moiety was pairing with the corresponding adenine and the α- and γ-phosphate were properly posed (Figure V-8b). D-**2-UTP** presents poses apparently consistent with catalysis with binding energies of -85 score units. The only difference between D-**2-TTP** and D-**2-UTP** is the methyl group of the thymine ring, which may cause a steric hindrance with the α-phosphate when it is properly posed, and so the α-phosphate could adopt another conformation to avoid the clash.

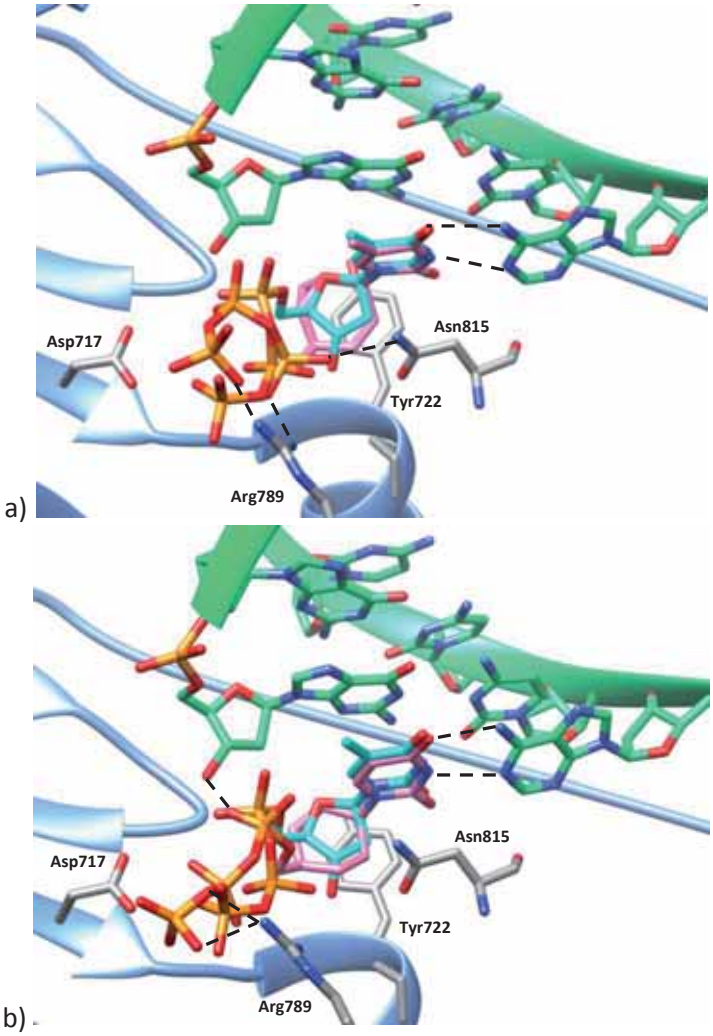

Figure V-8. a) D-**2-TTP** (pink) superimposed to crystallographic dTTP (blue) in DNA polymerase nucleotide site (X-ray residues shown in grey). b) D-**2-UTP** (pink) superimposed to crystallographic dTTP (blue) in DNA polymerase nucleotide site (X-ray residues shown in grey). Hydrogen bonds are depicted as dotted lines. For the sake of clarity, crystallographic waters and hydrogen atoms are not shown.

- **Purine nucleoside analogues**

The interaction between dGTP and DNA polymerase in the binding site are similar to dTTP (Figure V-9). The incoming dGTP is interacting with the templating base by three hydrogen bonds and the phosphates are hydrogen bonded to Arg-789. Additionally, the 3'-OH is interacting with β-phosphate and Asn-815 via hydrogen bonds, and the α-phosphate is pointing towards the 3'-OH of the deoxynucleotide bound at the 3'-terminus of the primer strand.

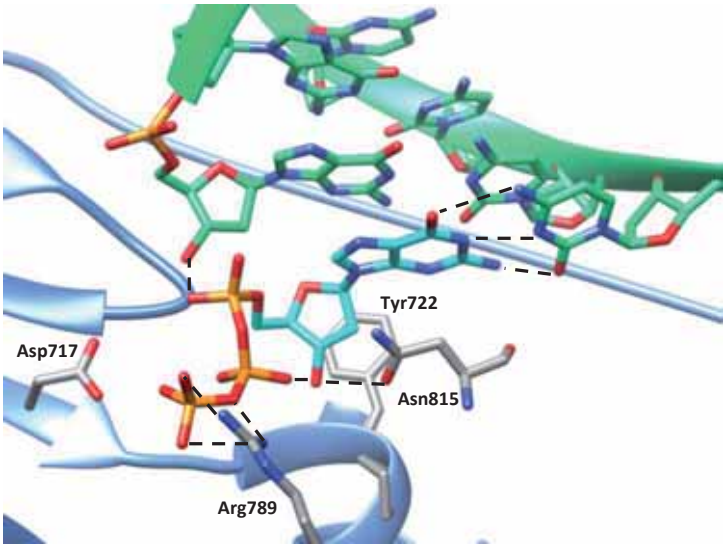

Figure V-9. Representation of the main interactions of dGTP (blue) in complex with DNA polymerase. X-ray residues shown in grey, DNA chains in green and backbone in blue. Hydrogen bonds are depicted as dotted lines. For the sake of clarity, crystallographic waters and hydrogen atoms are not shown.

Docking calculations of dGTP into the enzyme were performed to validate the docking protocol. The results showed that in lowest binding modes the guanine ring and the sugar moiety were perfectly overlapped with the crystallographic model and the α-phosphate is pointed towards 3'-OH of the previous nucleotide (Figure V-10).

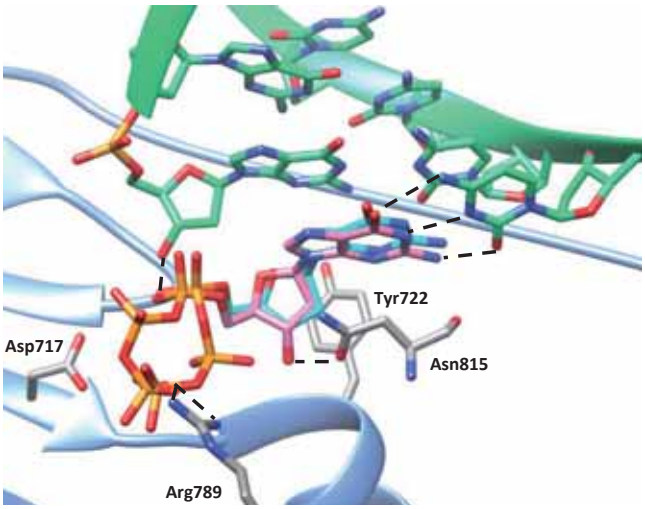

Figure V-10. dGTP (pink) superimposed to crystallographic dGTP (blue) in DNA polymerase nucleotide site (X-ray residues shown in grey). Hydrogen bonds are depicted as dotted lines. For the sake of clarity, crystallographic waters and hydrogen atoms are not shown.

To provide with structural and energetic benchmarks for purine derivatives, docking calculations of ACVTP and DCGTP into the model structure were also carried out. Results showed that the guanine moiety was correctly cleft in both cases. However, the phosphates were displaced from the crystallographic structure (Figure V-11) with particular emphasis on the α-phosphate which was not pointing towards the 3'-OH of the deoxynucleotide, and thus

they could not be used as benchmarks. Hence, dGTP was used as a benchmark for purine compounds, since the calculations of dGTP in the replication model showed that the lowest binding modes were consistent with the catalysis.

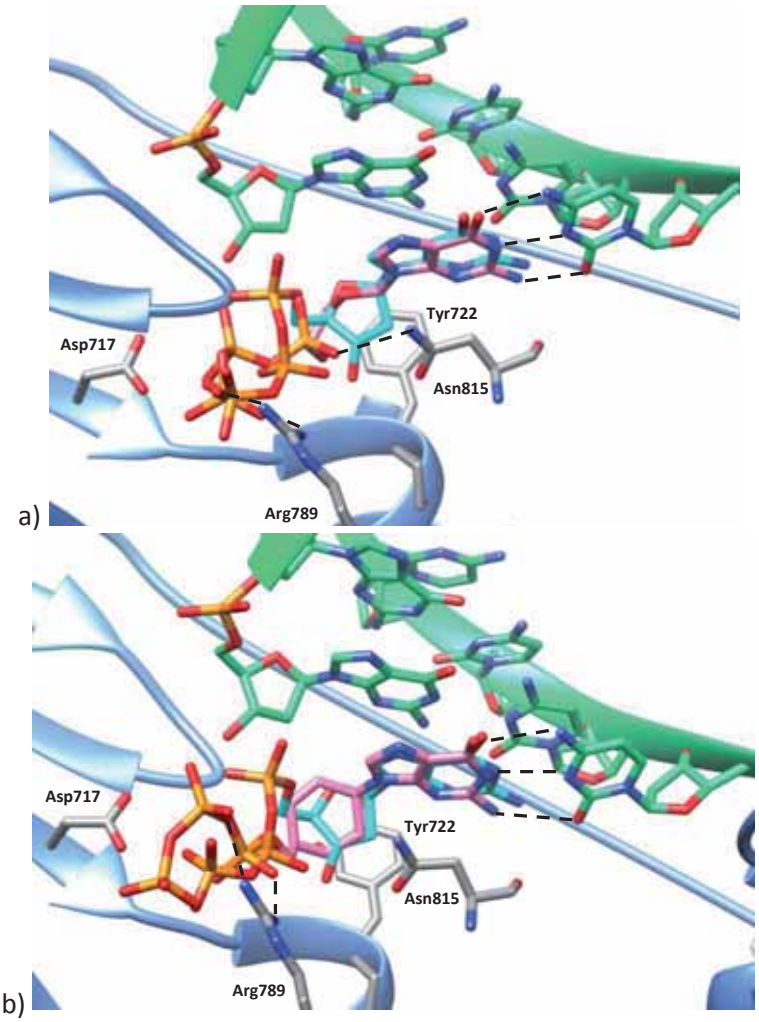

Figure V-11. a) AVCTP (pink) superimposed to crystallographic dGTP (blue) in DNA polymerase nucleotide site (X-ray residues shown in grey). b) DCGTP (pink) superimposed to crystallographic dGTP (blue) in DNA polymerase nucleotide site (X-ray residues shown in grey). Hydrogen bonds are depicted as dotted lines. For the sake of clarity, crystallographic waters and hydrogen atoms are not shown.

Regarding the purine derivatives synthesised in this work D-**2-G** and D-**2-A**, the lowest energy binding mode showed the purine ring properly cleft and paired with the corresponding base, however, the α-phosphate was far away from the 3'-OH of the previous nucleotide and the β- and γ-phosphates were pointing upwards instead of interacting with Arg-789 (Figure V-12). As a consequence, although the binding energies of the lowest predicted orientations of D-**2-G** and D-**2-A** were lower than those of dGTP (-100 and -95 score units for D-**2-G** and D-**2-A**, respectively, and -91 score units for dGTP), none of the predicted poses were consistent with the catalysis.

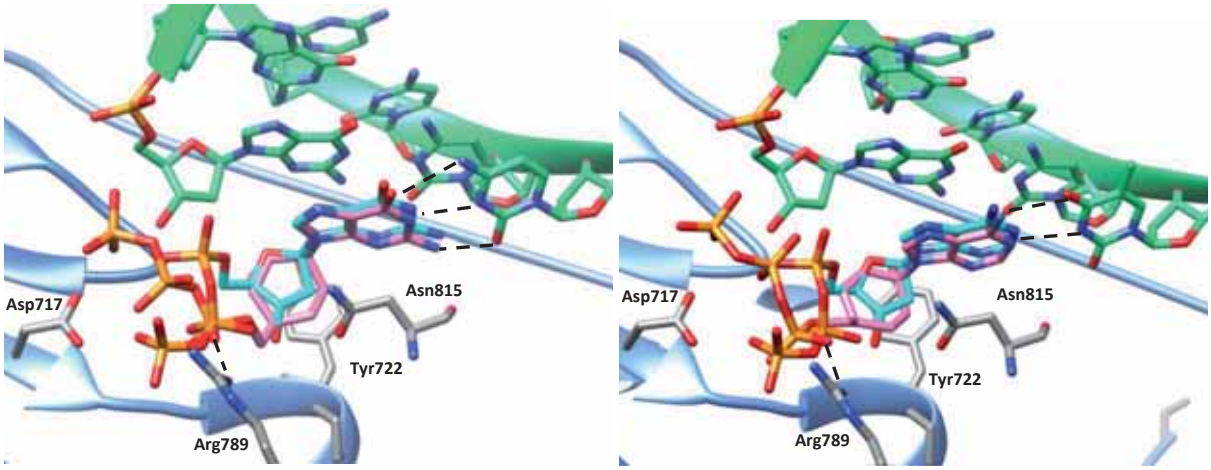

Figure V-12. a) lowest binding mode of D-**2-GTP** (pink) superimposed to crystallographic dGTP (blue) in DNA polymerase nucleotide site (X-ray residues shown in grey). b) lowest binding mode of D-**2-ATP** (pink) superimposed to crystallographic dATP (blue) in DNA polymerase nucleotide site (X-ray residues shown in grey). Hydrogen bonds are depicted as dotted lines. For the sake of clarity, crystallographic waters and hydrogen atoms are not shown.

3. Conclusions

The antiviral activity of the synthesised nucleosides D-**2-A**, D-**2-G**, D-**2-T** and D-**2-U** was evaluated against different viruses and unfortunately did not show activity up to µM. Interestingly, only D-**2-U** presented limited cytotoxic effects, which represents a major step forward regarding previous families produced in our group.

To rationalise the lack of antiviral activity, we extended our molecular docking study by exploring the interaction of our compounds with a model of the DNA polymerase involved in the replication process for HSV-1.

Regarding the interaction with DNA polymerase, due to the lack of a crystallographic structure of the target with DNA, a preliminary model of the replication complex with DNA was constructed by means of homology modelling like approach. Docking calculations on this model revealed that all the triphosphorylated nucleosides except D-**2-UTP** are not likely to be incorporated into the 3'-end of the growing primer stand, since the α-phosphate is not close to the 3'-OH of the primer deoxynucleotide. Nevertheless, it is important to recall that this is a preliminary model of the replication complex and thus other computational techniques must be performed to refine the complex, such as molecular dynamics.

In summary, this theoretical study is the first one which considers the whole activation process and the interaction with the target for the Herpes Simplex Virus type 1 (HSV-1). Those calculations suggested that the interaction of the nucleoside analogues with HSV DNA polymerase is more restrictive than the activation process, being responsible for the lack of

anti-HSV activity of D-**2-A**, D-**2-G** and D-**2-T**. On the other hand, docking calculations on D-**2-U** suggested that it is the third phosphoryl transfer which restricts its activity.

4. References

(1) Deville-Bonne, D.; El Amri, C.; Meyer, P.; Chen, Y.; Agrofoglio, L. A.; Janin, J. *Antiviral Res.* **2010**, *86*, 101–120.

(2) Zuccola, H. J.; Filman, D. J.; Coen, D. M.; Hogle, J. M. *Mol. Cell* **2000**, *5*, 267–278.

(3) Digard, P.; Bebrin, W. R.; Weisshart, K.; Coen, D. M. *J. Virol. Virol.* **1993**, *67*, 398–406.

(4) Johnson, M. S.; Srinivasan, N.; Sowdhamini, R.; Blundell, T. L. *Crit. Rev. Biochem. Mol. Biol.* **1994**, *29*, 1–68.

(5) Xu, D.; Xu, Y.; Uberbacher, E. *Curr. Protein Pept. Sci.* **2000**, *1*, 1–21.

(6) Martí-Renom, M. A.; Stuart, A. C.; Fiser, A.; Sánchez, R.; Melo, F.; Sali, A. *Annu. Rev. Biophys. Biomol. Struct.* **2000**, *29*, 291–325.

(7) Hillisch, A.; Pineda, L. F.; Hilgenfeld, R. *Drug Discov. Today* **2004**, *9*, 659–669.

(8) Franklin, M. C.; Wang, J.; Steitz, T. A. *Cell* **2001**, *105*, 657–667.

(9) Perera, R. L.; Torella, R.; Klinge, S.; Kilkenny, M. L.; Maman, J. D.; Pellegrini, L. *Elife* **2013**, *2*, e00482.

(10) Liu, S.; Knafels, J. D.; Chang, J. S.; Waszak, G. A.; Baldwin, E. T.; Deibel, M. R.; Thomsen, D. R.; Homa, F. L.; Wells, P. A.; Tory, M. C.; Poorman, R. A.; Gao, H.; Qiu, X.; Seddon, A. P. *J. Biol. Chem.* **2006**, *281*, 18193–18200.

(11) Pettersen, E. F.; Goddard, T. D.; Huang, C. C.; Couch, G. S.; Greenblatt, D. M.; Meng, E. C.; Ferrin, T. E. *J. Comput. Chem.* **2004**, *25*, 1605–1612.

(12) Krebs, W. G.; Gerstein, M. *Nucleic Acids Res.* **2000**, *28*, 1665–1675.

(13) Echols, N. *Nucleic Acids Res.* **2003**, *31*, 478–482.

(14) Castellana, N. E.; Lushnikov, A.; Rotkiewicz, P.; Sefcovic, N.; Pevzner, P. A.; Godzik, A.; Vyatkina, K. *Algorithms Mol. Biol.* **2013**, *8*, 19.

(15) GOLD 5.2.2, 2011, Cambrigde Crystallographic Data Centre (http://www.ccdc.cam.ac.uk).

(16) Korb, O.; Stu, T.; Exner, T. E. *J. Chem. Inf. Model.* **2009**, *49*, 84–96.

(17) Marvin 5.4, 2010, ChemAxon (http://www.chemaxon.com).

(18) Molecular, M.; Field, F.; Halgren, T. A. *J. Comput. Chem.* **1996**, *17*, 490–519.

(19) Wang, J.; Wang, W.; Kollman, P. A.; Case, D. A. *J. Mol. Graph. Model.* **2006**, *25*, 247–260.

Chapter VI: General conclusions

Conclusions

The computational and synthetic work presented in this thesis could be summarised in five major achievements:

i) A set of novel cyclohexenyl nucleoside analogues were modelled with the aim of being possible anti-HSV agents. Thus, the whole activation process of the prodrug candidates **1-6** were evaluated by means of molecular modelling techniques (Figure VI-1). The theoretical study was carried out using a novel concept for prodrug design, where all enzymes in the activation process were considered. This study revealed that pyrimidine nucleosides are more likely to be converted into their triphosphorylated derivatives than purine nucleosides. Additionally, these studies also proved that the fusion of a cyclopropane to a cyclohexanyl ring is not detrimental to the catalysis.

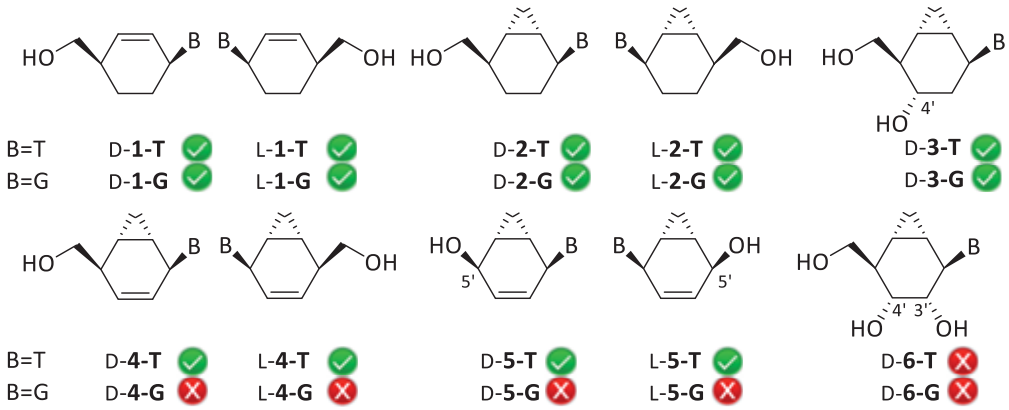

Figure VI-1. Summary of molecular docking results of possible drug candidates.

Considering those compounds more prone to be triphosphorylated, a new family of nucleoside analogues built on a bicyclo[4.1.0]heptane scaffold, **2**, was envisaged to be synthesised.

ii) A new practical, stereoselective procedure has been developed to synthesise allylic alcohol **8** starting from the commercially available 1,4-cyclohexanedione, **7**, in 3 steps and 66% overall yield (Scheme VI-1). This intermediate is the chiral precursor for the synthesis of bicyclo[4.1.0]hetptane nucleoside analogues **2**.

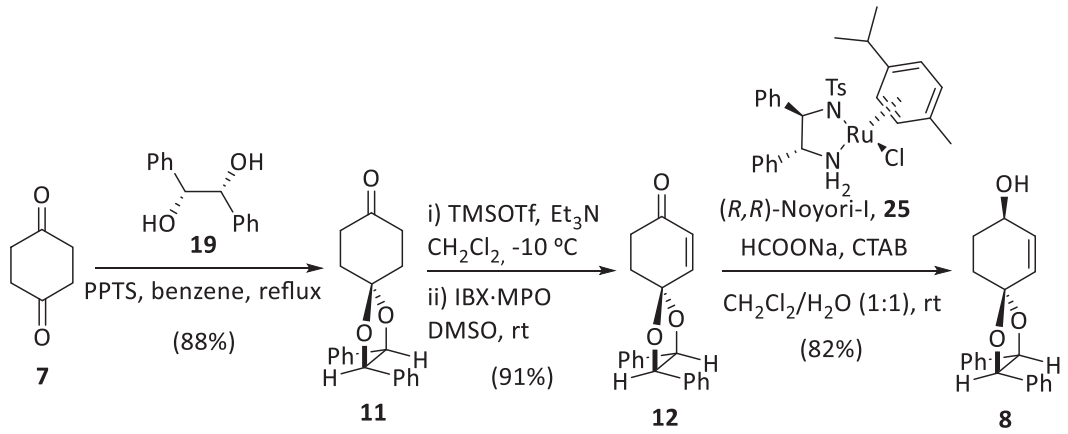

Scheme VI-1. Synthesis of allylic alcohol **8** starting from 1,4-cyclohexanedione **7**.

iii) Following the same strategy, a new synthetic approach towards the synthesis of both enantiomer of 4-hydroxy-2-cyclihexenone and their *O*-silyl derivatives has been established (Scheme VI-2). This procedure positively competes with the published methodologies, since (*R*)- and (*S*)-**29** were synthesised in 4 steps and 44% and 43% overall yield, respectively, as well as their *O*-silyl derivatives (*R*)- and (*S*)-**37** in 5 steps and 60% overall yield.

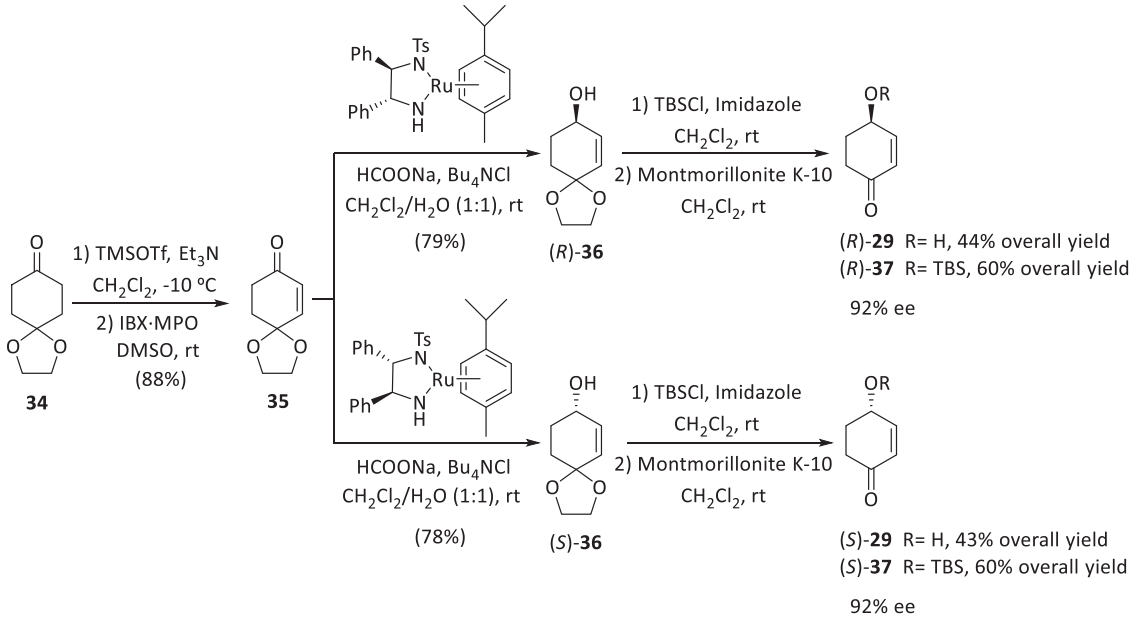

Scheme VI-2. Synthetic pathway to prepare both enantiomers of **X30** and their *O*-silyl derivatives.

iv) Finally, a new family of carbocyclic nucleosides built on a bicyclo[4.1.0]heptane scaffold has been synthesised following a divergent synthetic strategy (Scheme VI-3). The purine derivatives D-**2-G** and D-**2-A** have been achieved starting from 1,4-cyclohexanedione **7** in 16 steps and 5% and 10% overall yield, respectively. The pyrimidine derivatives D-**2-T** and D-**2-U** have been afforded in 14 and 15 steps and 5% and 2% global yield, respectively.

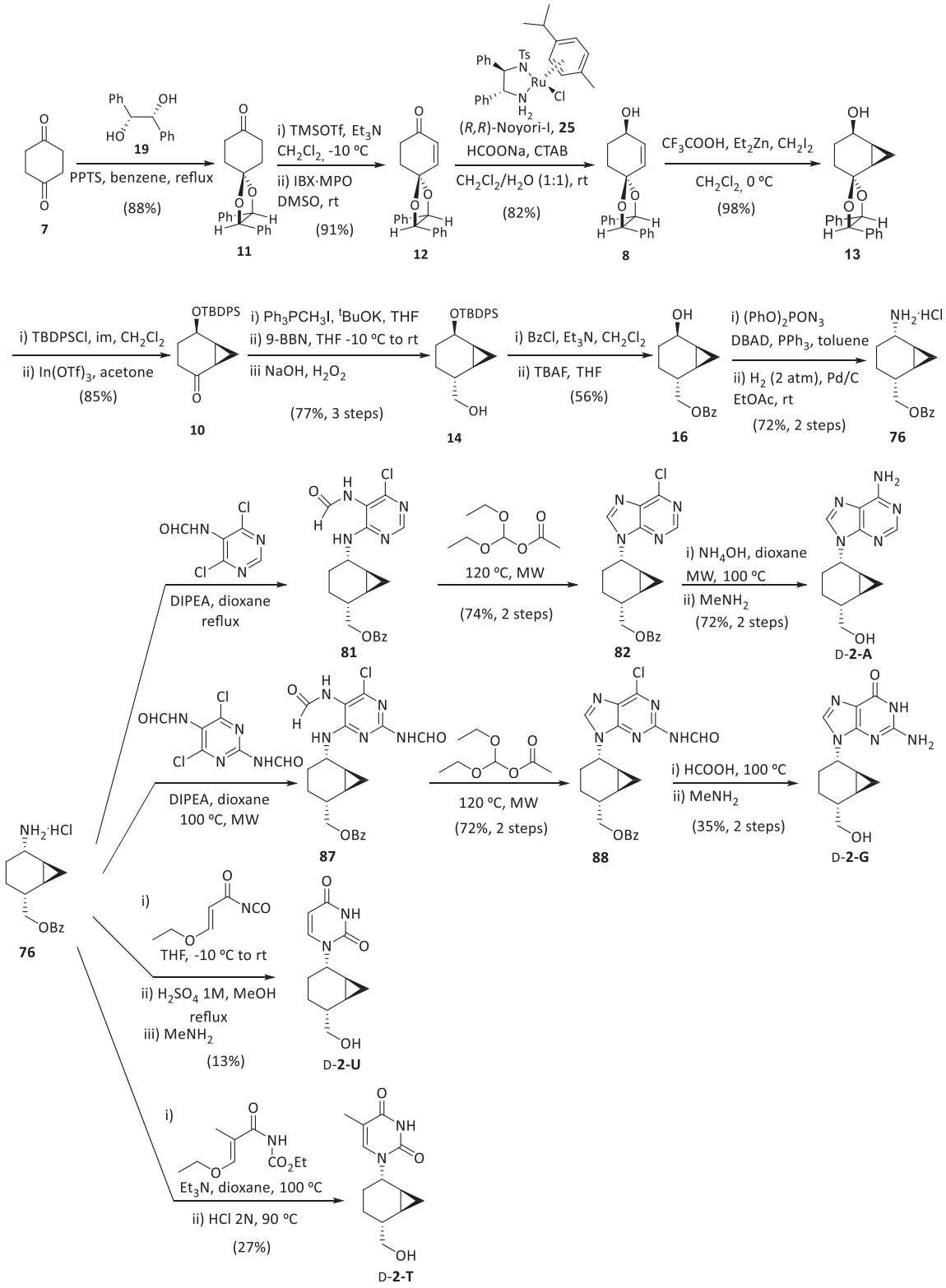

Scheme VI-3. Synthesis of bicyclo[4.1.0]heptane nucleoside analogues D-**2**.

v) The biological activity of these analogues against several viruses has been evaluated although none of them showed any significant activity. In order to rationalise the lack of activity, a molecular docking study has been carried out on their interaction with the HSV-1 DNA polymerase. As no crystallographic structure of the replication process of the target is

available, a 3D model structure has been constructed by means of a homology modelling like approach. The results derived from the theoretical study revealed that the antiviral activity of D-**2-A,** D-**2-G** and D-**2-T** is restricted by their incorporation into the viral DNA whereas D-**2-U** cannot be activated to the required triphosphorylated derivative.

This thesis had three major challenges: 1) the synthesis of a set of complex nucleoside analogues, 2) the set up and application of a cascade like docking protocol far beyond the limits of standard docking applications and 3) the reach of activity of prodrug candidates.

Although computation allowed to discard compounds that would likely not be recognised and metabolised by key enzymes in the activation process, the compounds that survival the screening were not successful for antiviral activity. Their synthesis though opened new opportunities for organic chemistry point of view. However, missing elements between the model of isolated enzymes and the real mechanism still remain. Identifying better where the protocol fails and which of our hypothesis could be wrong is one of the step forwards behind this Ph.D. dissertation.

Chapter VII: Experimental Section

1. Molecular modelling pre-study for the design of anti-HSV novel carbocyclic nucleosides

1.1. Drug-likeness

Table VII-1. Standard molecular descriptors of the studied compounds for "Lipinski's rule of 5".

Compound	H bond donors	H bond acceptors	MW	log P[1,2]
dT	3	5	242.23	-1.11
ACV	3	7	225.20	-1.59
1-T	2	3	236.27	0.2
2-T	2	3	250.29	0.2
3-T	3	4	266.30	-1.02
4-T	2	3	248.28	0.02
5-T	2	3	234.26	-0.2
6-T	4	5	282.30	-1.66
1-G	3	6	261.28	-0.62
2-G	3	6	275.31	-0.63
3-G	4	7	291.31	-1.84
4-G	3	6	273.30	-0.81
5-G	3	6	259.27	-1.03
6-G	5	8	307.31	-2.49
Lipinski's criterion	≤5	≤10	≤500	≤5

1.2. Activation process

1.2.1. Pyrimidine nucleoside analogues

Table VII-2. Predicted binding energies (score units) of pyrimidine compounds **1-6.**

Compounds		Activation process		
		OH→OMP	OMP→ODP	ODP→OTP
		1KIM	1VTK	1NDC
dT	Binding energy	-69.8	-72.7	-93.9
	Best pose	-69.8	-67.6	-89.3
D-**1-T**	Binding energy	-69.5	-71.5	-95.3
	Best pose	-66.7	-69.3	-91.6
L-**1-T**	Binding energy	-67.3	-68.7	-93.6
	Best pose	-67.3	-68.7	-93.2
D-**2-T**	Binding energy	-72.6	-80.4	-92.5
	Best pose	-72.6	-79.0	-92.5
L-**2-T**	Binding energy	-69.7	-67.4	-93.7
	Best pose	-63.4	-67.4	-93
D-**3-T**	Binding energy	-72.6	-70.3	-97.6
	Best pose	-72.2	-70.3	-93.8
D-**4-T**	Binding energy	-68.9	-71.6	-92.2
	Best pose	-68.9	-70.8	-90.8
L-**4-T**	Binding energy	-68.9	-67.7	-91.6
	Best pose	-68.9	-67.7	-91.4
D-**5-T**	Binding energy	-63.7	-67.5	-93.1
	Best pose	-63.7	-63.1	-93.1
L-**5-T**	Binding energy	-68.5	-62.5	-87.6
	Best pose	-68.5	-62.5	-87.1
D-**6-T**	Binding energy	-70.4	-66	-
	Best pose	-68.2	-66	-

1.2.2. Purine nucleoside analogues

Table VII-3. Predicted binding energies (score units) of purine compounds **1-6.**

Compounds		Activation process		
		OH→OMP	OMP→ODP	ODP→OTP
		2KI5	1LVG	1NUE
ACV	Binding energy	**-63.4**	**-86.7**	**-78.8**
	Best pose	**-63.4**	**-86.7**	**-76.6**
DCG	Binding energy	-66.3	-98.4	-91.0
	Best pose	-60.7	-97.7	-91.0
LCG	Binding energy	-65.4	-93.2	-84.5
	Best pose	-65.3	-93.2	-80.7
D-**1-G**	Binding energy	-65.0	-91.8	-82.0
	Best pose	-65.0	-91.1	-79.5
L-**1-G**	Binding energy	-63.9	-94.8	-88.9
	Best pose	-63.9	-94.4	-78.8
D-**2-G**	Binding energy	-70.1	-96.2	-79.9
	Best pose	-66	-92.8	-79.9
L-**2-G**	Binding energy	-65.3	-97.6	-79.7
	Best pose	-59.0	-97.0	-76.4
D-**3-G**	Binding energy	-	-99.0	-78.3
	Best pose	-	-99.0	-78.3
D-**4-G**	Binding energy	-	-95.9	-78.1
	Best pose	-	-95.9	-78.1
L-**4-G**	Binding energy	-	-99.1	-76.5
	Best pose	-	-97.1	-76.5
D-**5-G**	Binding energy	-	-92.0	-80.8
	Best pose	-	-90.4	-78.3
L-**5-G**	Binding energy	-	-99.0	-82.3
	Best pose	-	-96.1	-82.3
D-**6-G**	Binding energy	-	-	-82.1
	Best pose	-	-	-79.2

2. General procedures

All commercially available reagents were used as received. Solvents were dried by distillation over the appropriate drying agents: CH_2Cl_2 (CaH_2), THF (Na), ACN (CaH_2), toluene (Na). When required, reactions were performed avoiding moisture by standard procedures and under nitrogen or argon atmosphere.

Chromatography

All the reactions were monitored by analytical thin-layer chromatography (TLC) using silica gel 60 F254 pre-coated aluminium plates (0.25 mm thickness). Development was made using an UV lamp at 254 nm and/or using a $KMnO_4$/KOH aqueous solution or Vainillin solution. Column chromatography was performed using silica gel (230-400 mesh).

Spectroscopy

Nuclear magnetic resonance spectra (NMR) were registered at the *Servei de Ressonància Magnètica Nuclear* of the *Universitat Autònoma de Barcelona*. ^{1}H-NMR spectra were recorded on Bruker DPX250 (250 MHz), Bruker DPX360 (360 MHz) and Bruker AR430 (400 MHz) spectrometers. Proton chemical shifts (δ) are reported in ppm ($CDCl_3$, 7.26 ppm, MeOH-d_4, 3.31 ppm and DMSO-d_6, 2.50 ppm). ^{13}C-NMR spectra were recorded with complete proton decoupling on Bruker DPX250 (62.5 MHz), Bruker DPX360 (90 MHz) and Bruker AR430 (100.6 MHz) spectrometers. Carbon chemical shifts are reported in ppm ($CDCl_3$, 77.16 ppm, MeOH-d_4, 49.00 ppm and DMSO-d_6, 39.52 ppm). NMR signals were assigned with the help of COSY, dept135, HSQC, HMBC and NOESY experiments. All spectra were measured at 298 K.

The abbreviations used to describe signal multiplicities are: s (singlet), br s (broad singlet), d (doublet), t (triplet), br t (broad triplet), q (quartet), dd (double doublet), ddd (double double doublet), dddd (double double double doublet), ddddd (double double double double doublet), ddt (double double triplet), dtd (double triple doublet), dt (double triplet), dq (double quartet), dqd (double quartet doublet), td (triple doublet), tdd (triple double doublet), tt (triple triplet), m (multiplet) and *J* (coupling constant).

Infrared spectra (IR) were recorded on a Bruker Tensor 27 Spectrophotometer equipped with a Golden Gate Single Refraction Diamond ATR (Attenuated Total Reflectance) accessory at *Servei d'Anàlisi Química* of the *Universitat Autònoma de Barcelona*. Peaks are reported in cm^{-1}.

Mass Spectrometry

High resolution mass spectra (HRMS) were recorded at the *Servei d'Anàlisi Química* of the *Universitat Autònoma de Barcelona* in a Bruker micrOTOFQ spectrometer using ESIMS

(QTOF) or at *Parque Científico Tecnológico* of the *Universidad de Burgos* in a Micromass AutoSpec using EI-AR.

Optical Rotatory Power

Specific optical rotations ($[\alpha]_D$) were measured at 20 ± 2 °C and 589.6 nm using a JASCO J-715 polarimeter and using a 0.1-dm long cuvette.

Melting Points

Melting points were determined using a Koffler-Reichert apparatus and were not corrected.

Microwave

Microwave assisted reactions were performed using a *CEM Discover*® Microwave instrument, which operates between 0 and 300 W (Figure). Reactions were conducted in 10 mL glass vessels sealed with a septum. Temperature was measured with an infrared sensor placed under the reaction vessel. All experiments were performed using a stirring option whereby the contents of the vessel were stirred by means of a rotating magnetic plate located below the floor of the microwave cavity and a Telfon-coated magnetic stir bar in the vessel. During the experiments compressed nitrogen was used to cool the reactor when necessary (option PowerMAX^{TM} enabled).

Figure VII-1. CEM Discover® microwave instrument.

In this work some of the compounds prepared were already described in the literature. Therefore, only the physical and/or spectroscopic data necessary for their identification are presented.

3. Synthesis of nucleoside analogues built on a bicyclo[4.1.0]heptane scaffold

3.1. Preparation of allylic alcohol, 8

3.1.1. (2*R*,3*R*)-2,3-Diphenyl-1,4-dioxaspiro[4.5]decan-8-one, 11

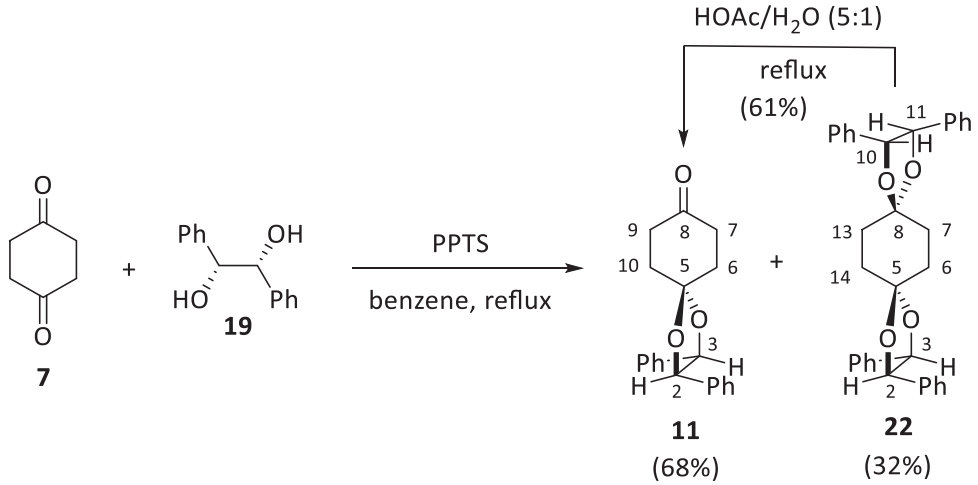

A solution of 1,4-cyclohexanedione **7** (17.6 g, 153 mmol), (*R*,*R*)-hydrobenzoin **19** (16.4 g, 76.6 mmol) and PPTS (1.92 g, 7.66 mmol) in benzene (300 mL) was stirred at the reflux temperature for 5 h in a Dean-Stark apparatus. The reaction mixture was cooled to room temperature and concentrated under vacuum, and the resulting oil was purified by column chromatography (hexanes-EtOAc, 8:1) to provide the monoketal **11** (16.1 g, 52.1 mmol, 68% yield) and the corresponding bisketal **22** (6.18 g, 12.3 mmol, 32% yield) both as white solids.

The bisketal **22** can be partially monohydrolised by dissolving it in a 5:1 mixture of acetic acid/water, and allowing it to stir at the reflux temperature for 6 h. Same work up as above, afforded an extra amount of the monoketal **11** (2.31 g, 7.47 mmol, 61% yield). Thus, the monoketal **11** was obtained in 88% overall yield.

Spectroscopic data of **11**

^{1}H-NMR (360 MHz, $CDCl_3$) δ: 7.38 – 7.28 (m, 6H, H-Ar), 7.28 – 7.18 (m, 4H, H-Ar), 4.87 (s, 2H, H-2, H-3), 2.69 (t br, $J_{7/9,6/10}$=7.0 Hz, 4H, H-7, H-9), 2.39 – 2.27 (m, 4H, H-6, H-10); **^{13}C-NMR** (100 MHz, $CDCl_3$) δ: 210.2 (C-8), 136.2/128.6/126.8 (C-Ar), 107.9 (C-5), 85.6 (C-2, C-3), 38.2 (C-7, C-9), 35.4 (C-6, C-10).

Spectroscopic data of **22**

^{1}H-NMR (250 MHz, $CDCl_3$) δ: 7.42 – 7.25 (m, 12H, H-Ar), 7.32 – 7.21 (m, 8H, H-Ar), 4.82 (s, 4H, H-2, H-3, H10, H-11), 2.29 (s, 8H, H-6, H-7, H-13, H-14); **^{13}C-NMR** (100 MHz, $CDCl_3$) δ: 137.1/128.5/128.4/126.8 (C-Ar), 109.2 (C-5, C-8), 85.4 (C-2, C-3, C-13, C-14), 33.8 (C-6, C-7, C-9, C-10).

3.1.2. *o*-Iodoxybenzoic acid, IBX, 23

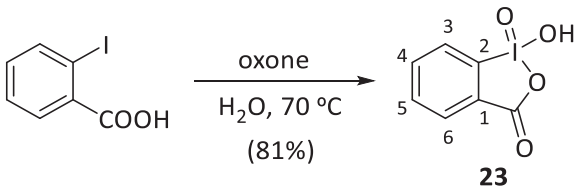

23

2-Iodobenzoic acid (15.05 g, 59.47 mmol) was added to a solution of oxone® (73.05 g, 118.82 mmol) in water (300 mL) and the reaction mixture was mechanically stirred at 70 ºC for 24 h. After that time, the suspension was cooled to 0 ºC and stirred slowly for a further 1 h. The mixture was then filtered, and the solid was washed with cooled water (6 x 20 mL) and acetone (2 x 20 mL) to furnish iodoxybenzoic acid **23** (13.46 g, 48.08 mmol, 81% yield) as a white solid.

Spectroscopic data of **23**

^{1}H-NMR (250 MHz, DMSO-d_6) δ: 8.15 (d, $J_{3,4}$=7.9 Hz, 1H, H-3), 8.04 (m, 2H, H-4, H-6), 7.84 (t, $J_{5,4}$=$J_{5,6}$=7.4 Hz, 1H, H-5).

3.1.3. (2*R*,3*R*)-2,3-Diphenyl-1,4-dioxaspiro[4.5]decan-6-ene-8-one, 12

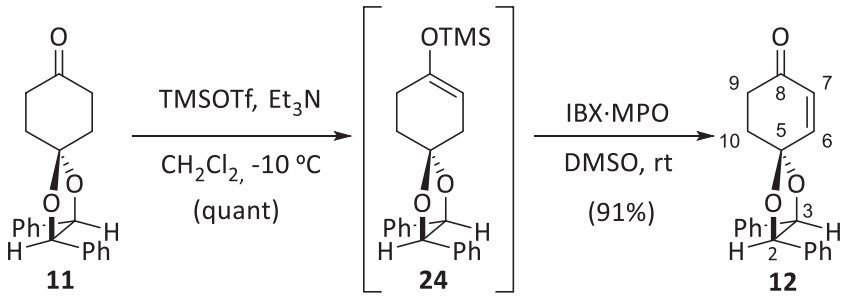

11 **24** **12**

To a stirred solution of monoketal **11** (6.70 g, 21.7 mmol) and Et_3N (4.50 mL, 32.6 mmol) in anhydrous CH_2Cl_2 (145 mL) at -10 °C, under nitrogen atmosphere, was added dropwise TMSOTf (5.90 mL, 32.6 mmol) and the reaction mixture was stirred for 2 h.

Then, a solution of IBX (10.2 g, 36.3 mmol) and MPO (4.21 g, 32.6 mmol) in DMSO (145 mL) was stirred during 1 h until becoming a clearly yellow solution, and then poured onto the

reaction mixture. After 1 h of stirring at room temperature a saturated aqueous $Na_2S_2O_3$ and $NaHCO_3$ solution (100 mL) was added and stirred for 30 min. After that time, diethyl ether (100 mL) was added, and the aqueous layer was extracted with more diethyl ether (2 x 100 mL). The organic phase was dried (Na_2SO_4) and concentrated under vacuum to provide enone **12** (6.08 g, 19.8 mmol, 91% yield) as a pale yellow solid.

Spectroscopic data of **12**

^{1}H-NMR (250 MHz, $CDCl_3$) δ: 7.40 – 7.25 (m, 6H, H-Ar), 7.25 – 7.10 (m, 4H, H-Ar), 6.93 (ddd, $J_{6,7}$=10.2 Hz, $J_{6,10}$=1.4 Hz, $J_{6,10}$=0.5 Hz, 1H, H-6), 6.13 (dd, $J_{7,6}$=10.2 Hz, $J_{7,9}$=0.8 Hz, 1H, H-7), 4.88 (d, $J_{3,2}$=8.5 Hz, 1H, H-3), 4.80 (d, $J_{2,3}$=8.5 Hz, 1H, H-2), 2.81 (ddt, J=16.8 Hz, J'=9.3 Hz, J''=6.4 Hz, 1H, H-9/H-10), 2.68 (dt, J=16.8 Hz, J'=J''=5.5 Hz, 1H, H-9/H-10), 2.60 – 2.40 (m, 2H, H-9, H-10); **^{13}C-NMR** (62.5 MHz, $CDCl_3$) δ: 198.6 (C-8), 146.7 (C-6), 135.6/135.4 (C-Ar), 130.8 (C-7), 128.7/128.6/126.6 (C-Ar), 104.5 (C-5), 85.8/85.2 (C-2, C-3), 35.2/34.0 (C-9, C-10).

3.1.4. (2*R*,3*R*,8*R*)-2,3-Diphenyl-1,4-dioxaspiro[4.5]decan-6-ene-8-ol, 8

3.1.4.1. Using tetrabutylammonium chloride as a phase-transfer catalyst

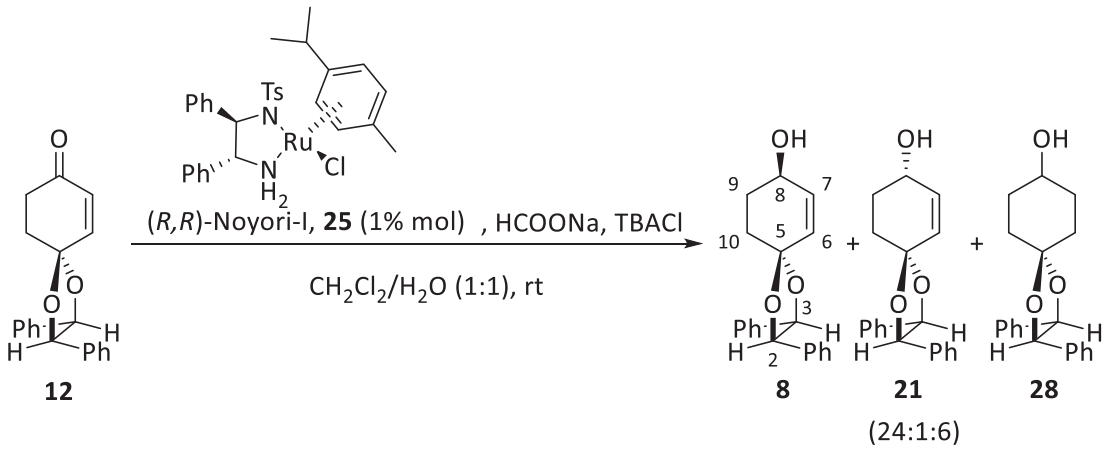

To a stirred solution of enone **12** (1.22 g, 3.99 mmol) in a biphasic media of CH_2Cl_2 (14 mL) and water (14 mL), tetrabutylammonium chloride (333 mg, 1.20 mmol), sodium formate (762 mg, 11.2 mmol) and (*R*,*R*)-Noyori-I catalyst **25** (25.5 mg, 0.040 mmol) were sequentially added at room temperature. The reaction mixture was allowed to stir for 24 h, when a TLC analysis (hexanes/ethyl acetate 1:1) shows totally consumption of the starting material. Then, the phases were separated and the organic layer was filtered through a short pad of silica. The volatiles were removed under reduced pressure affording a yellow oil, which was further purified by column chromatography (hexanes-EtOAc, 5:1) to afford an inseparable mixture of allylic alcohols **8** and **21** and alcohol **28** in a 24:1:6 ratio (1.10 g), as a white solid.

3.1.4.2. Using hexadecyltrimethylammonium bromide as a phase-transfer catalyst

To a stirred solution of enone **12** (1.76 g, 5.75 mmol) in a biphasic media of CH_2Cl_2 (10 mL) and water (10 mL), hexadecyltrimethylammonium bromide (628 mg, 1.72 mmol), sodium formate (589 mg, 8.62 mmol) and (*R*,*R*)-Noyori-I catalyst **25** (109 mg, 0.17 mmol) were sequentially added at room temperature. The reaction mixture was allowed to stir for 24 h. Then, the phases were separated and the volatiles were removed under reduced pressure affording a yellow oil, which was further purified by column chromatography (hexanes-EtOAc, 9:1 to 3:1) to deliver a 24:1:2.4 mixture of allylic alcohols **8** and **21** and alcohol **28** (1.46 g, 4.72 mmol, 82% yield) as a white solid.

Spectroscopic data of a mixture of **8**

^{1}H-NMR (400 MHz, $CDCl_3$) δ: 7.36 – 7.26 (m, 6H, H-Ar), 7.26 – 7.17 (m, 4H, H-Ar), 6.05 (ddd, $J_{7,6}$=10.1 Hz, $J_{7,8}$=2.0 Hz, $J_{7,9}$=1.2 Hz, 1H, H-7), 5.92 (dt, $J_{6,7}$=10.1 Hz, $J_{6,8}$=$J_{6,10}$=1.9 Hz, 1H, H-6), 4.79 (d, $J_{3,2}$=8.5 Hz, 1H, H-3), 4.69 (d, $J_{2,3}$=8.5 Hz, 1H, H-2), 4.29 (ddt, $J_{8,9ax}$=9.0 Hz, $J_{8,9eq}$=4.3 Hz, $J_{8,7}$=$J_{8,6}$=2.0 Hz, 1H, H-8), 2.29 – 2.18 (m, 2H, H-9, H-10), 2.11 – 2.01 (m, 1H, H-9/H-10), 1.93 – 1.80 (m, 1H, H-9/H-10); **^{13}C-NMR** (100 MHz, $CDCl_3$) δ: 136.3/136.2 (C-Ar), 135.7 (C-7), 129.5 (C-6), 128.5/128.4/128.3/126.8/126.6 (C-Ar), 105.7 (C-5), 85.5/85.1 (C-2, C-3), 66.6 (C-8), 32.8 (C-10), 31.0 (C-9).

3.2. Preparation of 4-hydroxy-2-cyclohexenone, 29

3.2.1. (2*R*,3*R*,8*R*)-5-(*tert*-butyldiphenylsilyloxy)-2,3-diphenyl-1,4-dioxaspiro[4.5]decan-6-ene-8-ol, 30

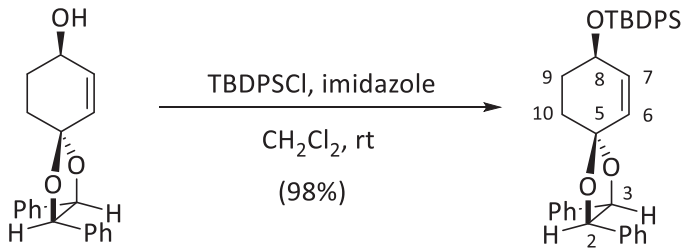

To a stirred solution of **8** (506 mg, 1.64 mmol) in CH_2Cl_2 (2.5 mL), imidazole (117 mg, 1.72 mmol) and TBDPSCl (455 µL, 1.72 mmol) were added at room temperature, allowing it to stir overnight. At this time, the volatiles were removed under vacuum and the resulting crude was purified by column chromatography (hexanes-EtOAc, 5:1) to furnish the silyl derivate **30** (880 mg, 1.61 mmol, 98% yield) as a colourless syrup.

Physical and spectroscopic data of **30**

$[\alpha]_D^{20}$= +45.1 (*c* 1.15, $CHCl_3$); **^{1}H-NMR** (400 MHz, $CDCl_3$) δ: 7.72 (ddd, *J*=8.0 Hz, *J*=3.2 Hz, *J*=1.5 Hz, 4H, H-Ar), 7.50 – 7.37 (m, 4H, H-Ar), 7.36 – 7.28 (m, 6H, H-Ar), 7.23 – 7.14 (m, 6H, H-Ar), 5.97 (ddd, $J_{7,6}$=10.2 Hz, $J_{7,8}$=1.9 Hz, $J_{7,9}$=1.2 Hz, 1H, H-7), 5.82 (dt, $J_{6,7}$=10.2 Hz, $J_{6,8}$=$J_{6,10}$=1.9 Hz, 1H, H-6), 4.77 (d, $J_{3,2}$=8.4 Hz, 1H, H-3), 4.67 (d, $J_{2,3}$=8.4 Hz, 1H, H-2), 4.32 (ddt, $J_{8,9ax}$=7.4 Hz, $J_{8,9eq}$=5.1 Hz, $J_{8,10eq}$=$J_{8,7}$=1.9 Hz, 1H, H-8), 2.20 (ddd, J_{gem}=12.8 Hz, $J_{10eq,9ax}$=$J_{10eq,9eq}$=3.7 Hz, $J_{10eq,6}$=1.9 Hz, 1H, H-10eq), 2.10 – 1.94 (m, 2H, H-9), 1.92 (td, J_{gem}=$J_{10ax,9ax}$=12.8 Hz, $J_{10ax,9eq}$= 3.1 Hz, 1H, H-10ax), 1.09 (s, 9H, H-^{t}Bu); **^{13}C-NMR** (100 MHz, $CDCl_3$) δ: 136.8 (C-7), 136.6/136.5/136.0/135.9/134.3/134.1/129.8/129.8/128.6/128.5 (C-Ar), 128.4 (C-6), 127.8/ 127.7/127.1/126.7 (C-Ar), 106.1 (C-5), 85.5/85.2 (C-2, C-3), 68.1 (C-8), 32.9 (C-10), 31.1 (C-9), 27.0 (C($\underline{C}H_3)_3$), 19.3 ($\underline{C}(CH_3)_3$); **COSY**, **dept135**, **HSQC** and **HMBC** experiments were recorded; **IR** (ATR): ν 3069, 3033, 2931, 2888, 2857, 1111, 1022, 760, 700 (cm^{-1}); **HRMS** (ESI+): Calcd. for $[C_{36}H_{38}O_3Si\text{-}C_4H_9]^+$: 489.1886, Found: 489.1887.

3.2.2. (1*R*,5*R*,6*S*)-5-(*tert*-butyldiphenylsilyloxy)bicyclo[4.1.0]heptan-2-one, 31

3.2.2.1. Using Montmorillonite K-10

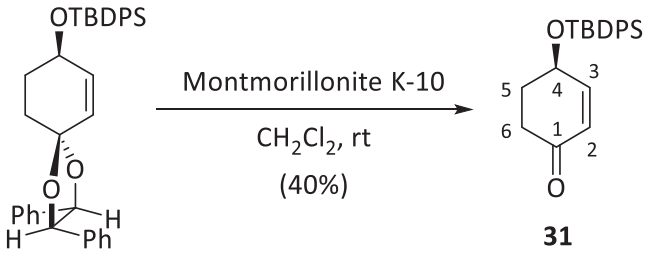

30 **31**

Montmorillonite K-10 (945 mg) was added to a solution of **30** (189 mg, 0.35 mmol) in CH_2Cl_2 (5.8 mL) and the mixture was stirred at room temperature for 3 h. Then, it was filtered and the solvent removed under vacuum to furnish enone **31** (46 mg, 0.13 mmol, 40% yield) as a yellowish oil.

3.2.2.2. Using indium(III)trifluoromethanesulfonate, $In(OTf)_3$

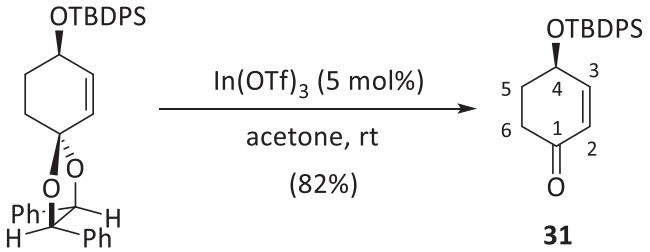

To a round-bottomed flask charged with **30** (404 mg, 0.74 mmol) in acetone (15 mL) was added $In(OTf)_3$ (21 mg, 0.04 mmol) and the mixture was stirred at room temperature for 16 h. Then, acetone was removed under vacuum and the residue was purified by column chromatography (hexanes-EtOAc, 8:1) to afford ketone **31** (225 mg, 0.64 mmol, 82% yield) as a pale yellow oil.

Physical and spectroscopic data of **31**

$[\alpha]_D^{20}$= +65.6 (*c* 0.9, $CHCl_3$); **^{1}H-NMR** (400 MHz, $CDCl_3$) δ: 7.74 – 7.66 (m, 4H, H-Ar), 7.49 – 7.37 (m, 6H, H-Ar), 6.80 (ddd, $J_{3,2}$=10.4 Hz, $J_{3,4}$=2.1 Hz, $J_{3,5}$=1.3 Hz, 1H, H-3), 5.87 (dt, $J_{2,3}$=10.4 Hz, $J_{2,4}$=$J_{2,6}$=1.1 Hz, 1H, H-2), 4.51 (ddd, $J_{4,5ax}$=7.5 Hz, $J_{4,5eq}$=4.4 Hz, $J_{4,3}$=2.1 Hz, 1H, H-4), 2.53 (dt, J_{gem}=16.3 Hz, $J_{6eq,5ax}$=$J_{6eq,5eq}$=4.5 Hz, 1H, H-6eq), 2.20 (ddd, J_{gem}=16.3 Hz, $J_{6ax,5ax}$=11.4 Hz, $J_{6ax,5eq}$=5.6 Hz, 1H, H-6ax), 2.12 – 2.07 (m, 2H, H-5), 1.10 (s, 9H, ^{t}Bu); **^{13}C-NMR** (100 MHz, $CDCl_3$) δ: 199.0 (C-1), 153.3 (C-3), 135.9/135.8/133.5/133.4/130.1/130.1 (C-Ar), 128.9 (C-2), 128.0/127.9 (C-Ar), 64.7 (C-4), 35.4 (C-6), 32.7 (C-5), 27.0 ($C(\underline{C}H_3)_3$), 19.3 ($\underline{C}(CH_3)_3$); **COSY**, **dept135**, **HSQC** and **HMBC** experiments were recorded; **IR** (ATR): ν 3070, 3048, 2956, 2930, 2892, 2857, 1718, 1104, 701, 615 (cm^{-1}); **HRMS** (ESI+): Calcd. for $[C_{22}H_{26}O_2Si\text{-}C_4H_9]^+$: 293.0998, Found: 293.1000.

3.3. Enantioselective synthesis of both enantiomers of cyclohexenone 29 and their derivatives

3.3.1. 1,4-Dioxaspiro[4.5]decan-6-en-8-one, 35

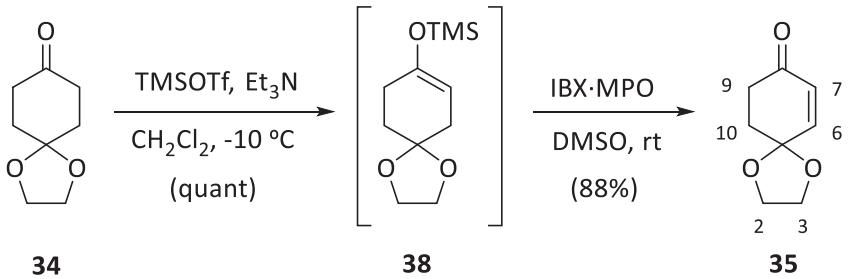

To a stirred solution of monoketal **34** (3.00 g, 18.7 mmol) and Et_3N (5.20 mL, 37.3 mmol) in dry CH_2Cl_2 (130 mL) at -10 °C, under nitrogen atmosphere, was added dropwise TMSOTf (4.20 mL, 23.2 mmol) and the reaction mixture was stirred for 2 h and then concentrated under reduced pressure to obtain crude **38**, which was used in the next step without further purification.

Then, a solution of the crude **38** in DMSO (50 mL) was poured onto a solution of IBX (10.4 g, 37.3 mmol) and MPO (4.82 mg, 37.3 mmol) in DMSO (35 mL), that had been previously stirred during 1 h until becoming a clearly solution. After 2 h of stirring at room temperature, CH_2Cl_2 (150 mL) and a saturated aqueous $NaHCO_3$ solution (150 mL) were added. The two phases were separated and the aqueous layer was extracted with CH_2Cl_2 (2 x 100 mL). The organic phase was concentrated under reduced pressure and washed with a solution of HCl 5% (100 mL) and brine (2 x 100 mL), dried (Na_2SO_4) , concentrated under vacuum to provide enone **35** (2.52 g, 16.4 mmol, 88% yield) as a yellow oil.

Physical and spectroscopic data of **35**

^{1}H-NMR (250 MHz, $CDCl_3$) δ: 6.60 (d, $J_{6,7}$=10.2 Hz, 1H, H-6), 5.99 (d, $J_{7,6}$=10.2 Hz, 1H, H-7), 4.11 – 3.98 (m, 4H, H-2, H-3), 2.62 (t, $J_{9,10}$=6.5 Hz, 2H, H-9), 2.19 (t, $J_{10,9}$=6.5 Hz, 2H, H-10); **^{13}C-NMR** (90 MHz, $CDCl_3$) δ: 198.7 (C=O), 146.4 (C-6), 130.6 (C-7), 104.0 (C-5), 65.1 (C-2, C-3), 35.3/32.9 (C-9, C-10).

3.2.3. (*8R*)-1,4-Dioxaspiro[4.5]decan-6-en-8-ol, (*R*)-36

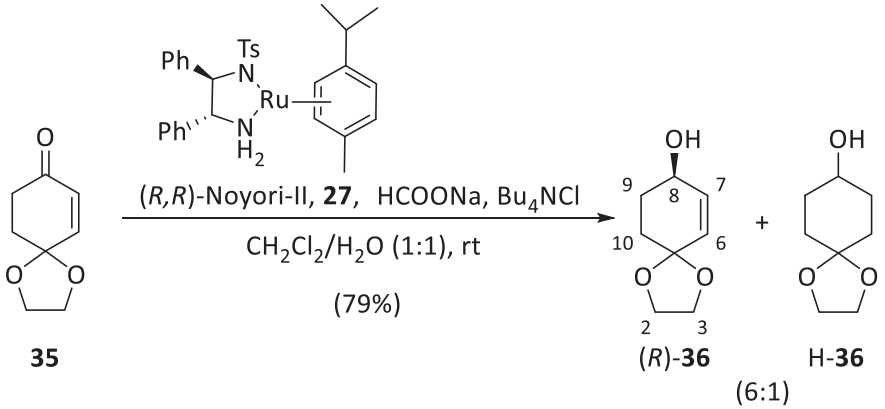

To a stirred solution of enone **35** (104 mg, 0.68 mmol) in a biphasic media of CH_2Cl_2 (2.3 mL) and water (2.3 mL), tetrabutylammonium chloride (57 mg, 0.20 mmol), sodium formate (139 mg, 2.04 mmol) and (*R*,*R*)-Noyori-II catalyst **27** (13 mg, 0.020 mmol) were sequentially added at room temperature. The reaction mixture was allowed to stir for 3 h, when TLC analysis (diethyl ether) shows totally consumption of the starting material. Then, the phases

were separated and the aqueous layer was extracted with more CH_2Cl_2 (2 x 2 mL) and the organic layers were concentrated under reduced pressure affording a yellow oil, which was purified by column chromatography (diethyl ether) to furnish allylic alcohol (*R*)-**36** and the totally hydrogenated derivative **H-36** in a 6:1 ratio (63 mg, 0.40 mmol, 59% yield) as a yellow oil. Considering the recovered starting material **35** (26 mg, 0.17 mmol) the yield arises until 79%.

Physical and spectroscopic data of (*R*)-**36**

$[\alpha]_D^{20}$= +39.0 (*c* 1.2, $CHCl_3$) [lit:[3] $[\alpha]_D^{20}$= -40.5 (*c* 1.24, $CHCl_3$) for its enantiomer]; **^{1}H-NMR** (250 MHz, $CDCl_3$) δ: 5.94 (ddd, $J_{7,6}$=10.1 Hz, $J_{7,8}$=2.8 Hz, $J_{7,9}$=1.1 Hz, 1H, H-7), 5.61 (dt, $J_{6,7}$= 10.1 Hz, $J_{6,8}$=$J_{6,10}$=1.5 Hz, 1H, H-6), 4.29 – 4.12 (m, 1H, H-8), 4.05 – 3.85 (m, 4H, H-2, H-3), 2.17 – 2.02 (m, 1H, H-9), 2.00 – 1.89 (m, 1H, H-9), 1.85 – 1.65 (m, 2H, H-10); **^{13}C-NMR** (90 MHz, $CDCl_3$) δ: 135.3 (C-7), 129.0 (C-6), 105.2 (C-5), 66.0 (C-8), 64.8/64.6 (C-2, C-3), 31.0/30.6 (C-9, C-10).

3.2.4. (8*S*)-1,4-Dioxaspiro[4.5]decan-6-en-8-ol, (*S*)-36

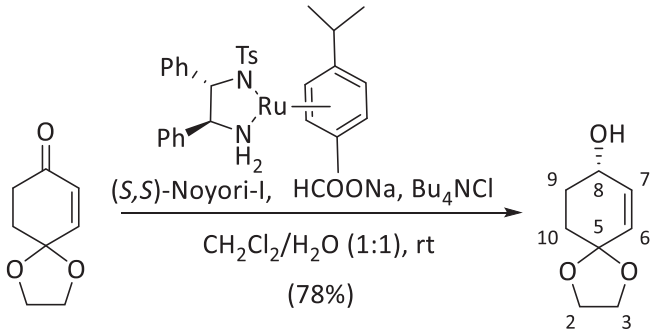

35 (*S*)-**36**

To a stirred solution of enone **35** (76 mg, 0.49 mmol) in a biphasic media of CH_2Cl_2 (1.3 mL) and water (1.3 mL), tetrabutylammonium chloride (45 mg, 0.16 mmol), sodium formate (140 mg, 2.06 mmol) and (*S*,*S*)-Noyori-II catalyst **39** (9.1 mg, 0.015 mmol) were sequentially added at room temperature. The reaction mixture was allowed to stir for 24 h. Then, the phases were separated and the aqueous layer was extracted with CH_2Cl_2 (2 x 10 mL) and the organic layers were concentrated under reduced pressure affording a yellow oil, which was purified by column chromatography (diethyl ether) to obtain allylic alcohol (*S*)-**36** (44 mg, 0.28 mmol, 57% yield) as a yellow oil. Considering the recovered starting material (20 mg, 0.13 mmol) the yield arises until 78%.

Spectroscopic data of (*S*)-**36**

^{1}H-NMR (250 MHz, $CDCl_3$) δ: 5.93 (ddd, $J_{7,6}$= 10.1 Hz, $J_{7,8}$ =2.8 Hz, $J_{7,9}$ =1.0 Hz, 1H, H-7), 5.60 (dt, $J_{6,7}$= 10.1 Hz, $J_{6,8}$=$J_{6,10}$=1.4 Hz, 1H, H-6), 4.26 – 4.16 (m, 1H, H-8), 4.05 – 3.85 (m, 4H, H-2, H-3), 2.19 – 2.05 (m, 1H, H-9), 2.04 – 1.90 (m, 1H, H-9), 1.90 – 1.68 (m, 2H, H-10).

3.2.5. (*4R*)-4-Hydroxycyclohex-2-en-1-one, (*R*)-29

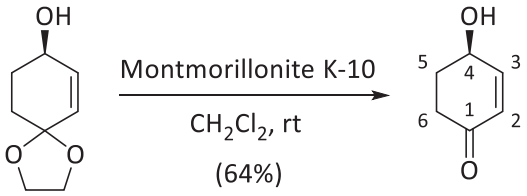

(*R*)-**36** (*R*)-**29**

Montmorillonite K-10 (832 mg) was added to a solution of (*R*)-**36** (77 mg, 0.49 mmol) in CH_2Cl_2 (7.6 mL) and the mixture was stirred at room temperature for 4 h. Then, it was filtered and the solvent removed under vacuum to furnish enone (*R*)-**29** (34 mg, 0.31 mmol, 64% yield) as a yellowish oil.

Physical and spectroscopic data of (*R*)-**29**

CHPLC (Daicel Chiralpak IC): 92% ee; **$[\alpha]_D^{20}$**= +90.0 (*c* 0.2, $CHCl_3$) [lit:[4,5] $[\alpha]_D^{20}$= +92.0 (*c* 1.0, $CHCl_3$)]; **^{1}H-NMR** (250 MHz, $CDCl_3$) δ: 6.95 (ddd, $J_{3,2}$=10.2 Hz, $J_{3,4}$=2.1 Hz, $J_{3,5eq}$=1.6 Hz, 1H, H-3), 5.98 (ddd, $J_{2,3}$=10.2 Hz, $J_{2,4}$=2.1 Hz, $J_{2,6}$=1.0 Hz, 1H, H-2), 4.58 (ddt, $J_{4,5ax}$=9.2 Hz, $J_{4,5eq}$=4.4 Hz, $J_{4,2}$=$J_{4,3}$=2.1 Hz, 1H, H-4), 2.60 (dt, J_{gem}=9.8 Hz, $J_{6eq,5}$=$J_{6eq,4}$=4.5 Hz, 1H, H-6eq), 2.45 – 2.28 (m, 2H, H-6ax, H-5eq), 2.10 – 1.90 (m, 1H, H-5ax); **^{13}C-NMR** (90 MHz, $CDCl_3$) δ: 199.4 (C-1), 153.6 (C-3), 129.0 (C-2), 66.2 (C-4), 35.4 (C-6), 32.4 (C-5).

3.2.6. (4*S*)-4-Hydroxycyclohex-2-en-1-one, (*S*)-29

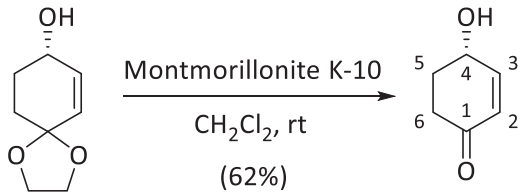

(*S*)-**36** (*S*)-**29**

Montmorillonite K-10 (852 mg) was added to a solution of (*R*)-**36** (79 mg, 0.50 mmol) in CH_2Cl_2 (7.8 mL) and the mixture was stirred at room temperature for 4 h. Then, it was filtered and the solvent removed under vacuum to furnish enone (*R*)-**29** (35 mg, 0.31 mmol, 62% yield) as a yellowish oil.

Physical and spectroscopic data of (S)-**29**

CHPLC (Daicel Chiralpak IC): 92% ee; **^{1}H-NMR** (250 MHz, $CDCl_3$) δ: 6.93 (ddd, $J_{3,2}$=10.2 Hz, $J_{3,4}$=2.4 Hz, $J_{3,5eq}$=1.6 Hz, 1H, H-3), 5.95 (ddd, $J_{2,3}$=10.2 Hz, $J_{2,4}$=2.0 Hz, $J_{2,6}$=1.0 Hz, 1H, H-2), 4.68 – 4.46 (m, 1H, H-4), 2.80 – 2.68 (m, 1H, OH), 2.57 (ddd, J_{gem}=9.8 Hz, $J_{6eq,4}$= 5.0Hz, $J_{6eq,5}$=4.0 Hz, 1H, H-6eq), 2.47 – 2.24 (m, 2H, H-6ax, H-5eq), 2.00 (ddd, J_{gem}=12.8 Hz, $J_{5ax,6ax}$=9.5 Hz, $J_{5ax,4}$=5.3 Hz, 1H, H-5ax).

3.2.7. (4*R*)-4-((*tert*-Butyldimethylsilyl)oxy)cyclohex-2-en-1-one, (*R*)-37

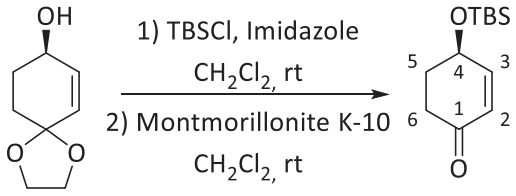

(*R*)-**36** (87%) (*R*)-**37**

To a stirred solution of (*R*)-**36** (102 mg, 0.65 mmol) in CH_2Cl_2 (0.5 mL) were added imidazole (56 mg, 0.82 mmol) and a solution of TBSCl (124 mg, 0.82 mmol) in CH_2Cl_2 (0.4 mL) at room temperature. The mixture was allowed to stir overnight. At this time, a saturated aqueous $NaHCO_3$ solution (1 mL) was added. The aqueous layer was extracted with CH_2Cl_2 (3 x 1 mL), and the organic layers were dried and concentrated under vacuum. The crude was dissolved in CH_2Cl_2 (4 mL) and Montmorillonite K-10 (513 mg) was added. The reaction mixture was allowed to stir at room temperature for 1 h. Then, it was filtered and the solvent removed under vacuum to furnish enone (*R*)-**37** (128 mg, 0.56 mmol, 87% yield) as a yellowish oil.

Physical and spectroscopic data of (*R*)-**37**

$[\alpha]_D^{20}$= +92.3 (*c* 1.02, $CHCl_3$) [lit:[6] $[\alpha]_D^{20}$= +101.0 (*c* 1.3, $CHCl_3$)]; **^{1}H-NMR** (400 MHz, $CDCl_3$) δ: 6.82 (ddd, $J_{3,2}$=10.2 Hz, $J_{3,4}$=2.1 Hz, $J_{3,5eq}$=1.6 Hz, 1H, H-3), 5.91 (ddd, $J_{2,3}$=10.2 Hz, $J_{2,4}$=2.1 Hz, $J_{2,6eq}$=1.0 Hz, 1H, H-2), 4.51 (ddt, $J_{4,5ax}$=9.1 Hz, $J_{4,5eq}$=4.6 Hz, $J_{4,2}$=$J_{4,3}$=2.1 Hz, 1H, H-4), 2.56 (dt, J_{gem}=16.8 Hz, $J_{6eq,5ax}$=$J_{6eq,5eq}$=4.5 Hz, 1H, H-6eq), 2.33 (ddd, J_{gem}=16.8 Hz, $J_{6ax,5ax}$=12.8 Hz, $J_{6ax,5eq}$=4.7 Hz, 1H, H-6ax), 2.20 (dqd, J_{gem}=12.8 Hz, $J_{5eq,4}$=$J_{5eq,6eq}$=$J_{5eq,6ax}$=4.6 Hz, $J_{5eq,3}$=1.6 Hz, 1H, H-5eq), 1.99 (tdd, J_{gem}=$J_{5ax,6ax}$=12.8 Hz, $J_{5ax,4}$=9.1 Hz, $J_{5ax,6eq}$=4.5 Hz, 1H, H-5ax), 0.90 (s, 9H, H-^{t}Bu), 0.12 (s, 3H, $SiCH_3$), (s, 3H, $SiCH_3$).

3.2.8. (4*S*)-4-((*tert*-Butyldimethylsilyl)oxy)cyclohex-2-en-1-one, (*S*)-37

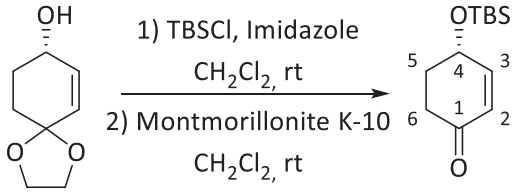

(*S*)-**36** (*S*)-**37**

To a stirred solution of (*S*)-**36** (49 mg, 0.32 mmol) in CH_2Cl_2 (0.4 mL) were added imidazole (34 mg, 0.49 mmol) and a solution of TBSCl (74 mg, 0.49 mmol) in CH_2Cl_2 (0.2 mL) at room temperature, allowing it to stir overnight. At this time, a saturated aqueous $NaHCO_3$ solution (1 mL) was added. The aqueous layer was extracted with more CH_2Cl_2 (3 x 1 mL), and the organic layers were dried and concentrated under vacuum. The crude was dissolved in CH_2Cl_2 (4 mL) and Montmorillonite K-10 (294 mg) was added. The reaction mixture was allowed to stir at room temperature for 1 h. Then, it was filtered and the solvent removed under reduced pressure to afford enone (*S*)-**37** (64 mg, 0.28 mmol, 88% yield) as a yellowish oil.

Spectroscopic data of (*S*)-**37**

^{1}H-NMR (250 MHz, $CDCl_3$) δ: 6.81 (ddd, $J_{3,2}$=10.2 Hz, $J_{3,4}$=2.1 Hz, $J_{3,5eq}$=1.6 Hz, 1H, H-3), 5.90 (ddd, $J_{2,3}$=10.2 Hz, $J_{2,4}$=2.1 Hz, $J_{2,6eq}$=1.0 Hz, 1H, H-2), 4.50 (ddt, $J_{4,5ax}$=9.0 Hz, $J_{4,5eq}$=4.8 Hz, $J_{4,3}$=$J_{4,2}$=2.1 Hz, 1H, H-4), 2.55 (dt, J_{gem}=16.7 Hz, $J_{6eq.5ax}$=$J_{6eq,5eq}$=4.8 Hz, 1H, H-6eq), 2.32 (ddd, J_{gem}=16.7 Hz, $J_{6ax,5ax}$=12.8 Hz, $J_{6ax,5eq}$=4.8 Hz, 1H, H-6ax), 2.19 (dqd, J_{gem}=12.8 Hz, $J_{5eq,6eq}$=$J_{5eq,4}$=$J_{5eq,6ax}$=4.8 Hz, $J_{5eq,3}$=1.6 Hz, 1H, H-5eq), 1.97 (tdd, J_{gem}=$J_{5ax,6ax}$=12.8 Hz, $J_{5ax,4}$=9.0 Hz, $J_{5ax,6eq}$=4.8 Hz, 1H, H-5ax), 0.89 (s, 9H, H-^{t}Bu), 0.11 (s, 3H, $SiCH_3$), 0.10 (s, 3H, $SiCH_3$).

3.3. Asymmetric Transfer Hydrogenation (ATH) Study

3.3.1. (4*R*)-4-hydroxycyclopent-2-en-1-one, (*R*)-48

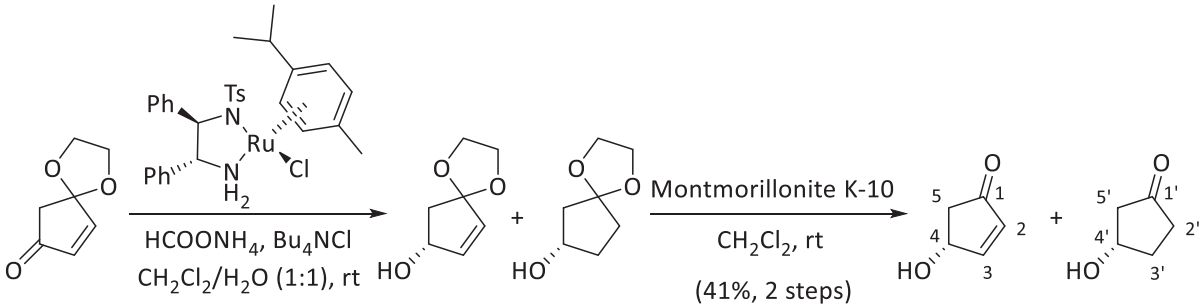

40 (*R*)-**112** **H-112** (*R*)-**48** **H-48**

To a stirred solution of enone **40** (28 mg, 0.20 mmol) in a biphasic media of CH_2Cl_2 (0.7 mL) and water (0.7 mL) and under a nitrogen flux, tetrabutylammonium chloride (19 mg, 0.07 mmol), ammonium formate (46.3 mg, 0.68 mmol) and (*R*,*R*)-Noyori-I catalyst **25** (4.3 mg, 0.007 mmol) were sequentially added at room temperature. The reaction mixture was allowed to stir for 5 h. Then, CH_2Cl_2 (1 mL) and water (1 mL) were added, the two phases were separated and the aqueous layer was extracted with CH_2Cl_2 (3 x 0.5 mL). The volatiles were removed under reduced pressure. The reaction crude was dissolved in CH_2Cl_2 (1.9 mL) and Montmorillonite K-10 (105 mg) was added. The mixture was stirred at room temperature for 2 h. Then, it was filtered and the solvent removed under vacuum to provide a 2:1 mixture of enone (*R*)-**48** and keto alcohol **H-48** (8 mg, 0.08 mmol, 41% yield for (*R*)-**48** the two steps) as a pale yellow oil.

Physical and spectroscopic data of the mixture of (*R*)-**48** and **H-48**

CHPLC (Daicel Chiralcel IC): 20% ee; **^{1}H-NMR** (250 MHz, $CDCl_3$) ((*R*)-**48**) δ: 7.56 (dd, $J_{3,2}$=5.7 Hz, $J_{3,4}$=2.4 Hz, 1H, H-3), 6.24 (dd, $J_{2,3}$= 5.7 Hz, $J_{2,4}$=1.3 Hz, 1H, H-2), 5.06 (br s, 1H, H-4), 2.79 (dd, J_{gem}=18.5 Hz, $J_{5,4}$=6.1 Hz, 1H, H-5), 2.28 (dd, J_{gem}=18.5 Hz, $J_{5,4}$=2.2 Hz, 1H, H-5); (**H-48**) δ: 4.64 (s, 1H, H-4'), 2.59 – 2.37 (m, 2H, H-5), 2.31 – 2.02 (m, 4H, H-2, H-3).

3.3.2. (4*R*)-4-Acetoxycyclohept-2-en-1-one, (*R*)-49

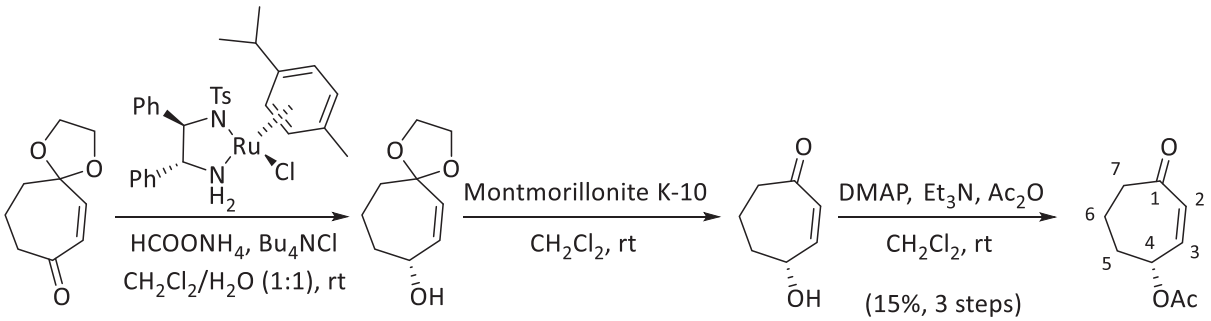

To a stirred solution of enone **41** (35 mg, 0.21 mmol) in a biphasic media of CH_2Cl_2 (0.69 mL) and water (0.69 mL) and under a nitrogen flux, tetrabutylammonium chloride (17 mg, 0.07 mmol), ammonium formate (42 mg, 0.62 mmol) and (*R*,*R*)-Noyori-I catalyst **25** (4 mg, 0.006 mmol) were sequentially added at room temperature. The reaction mixture was allowed to stir for 5h. Then, CH_2Cl_2 (20 mL) and water (20 mL) were added, the two phases were separated and the aqueous layer was extracted with CH_2Cl_2 (3 x 10 mL). The volatiles were removed under reduced pressure. The crude was dissolved in CH_2Cl_2 (2.6 mL) and montmorillonite K-10 (177 mg) was added. The mixture was stirred at room temperature for 2

h. Then, it was filtered and the solvent removed under vacuum to provide a 3:1 mixture of enone (*R*)-**49** and keto alcohol **H-49** as a pale yellow oil.

To a stirred solution of the crude in dry CH_2Cl_2 (0.16 mL) was added DMAP (0.59 mg, 4.75 μmol) and Et_3N (22 μL, 0.16 mmol) followed by acetic anhydride (10 μL, 0.11 mmol) dropwise. After stirring for 10 min, the reaction mixture was diluted with diethyl ether (1 mL) and a saturated aqueous $NaHCO_3$ solution (1 mL). After separation, the aqueous layer was extracted with diethyl ether (3 x 1 mL) and the combined organics were washed with a saturated aqueous $NaHCO_3$ solution and brine. The volatiles were removed under reduced pressure and purified by column chromatography (hexanes:EtOAc 4:1) to furnish the protected alcohol (*R*)-**114** (3 mg, 0.02 mmol, 15% yield for the three steps) as a yellowish oil.

Physical and spectroscopic data of (*R*)-**114**

CHPLC (Daicel Chiralcel AD-H): 70% ee; $[\alpha]_D^{20}$= +64.0 (*c* 0.27, $CHCl_3$) [lit:[8] $[\alpha]_D^{20}$= + 113.2 (*c* 0.5, $CHCl_3$), >98% ee]; **^{1}H-NMR** (250 MHz, $CDCl_3$) δ: 6.43 (ddd, $J_{3,2}$=12.6 Hz, $J_{3,4}$=3.4 Hz, $J_{3,5}$=1.1 Hz, 1H, H-3), 6.02 (dd, $J_{2,3}$=12.6 Hz, $J_{2,4}$=2.2 Hz, 1H, H-2), 5.67 – 5.51 (m, 1H, H-4), 2.71 – 2.56 (m, 2H, H-7), 2.27 – 2.12 (m, 1H, H-5), 2.10 (s, 3H, -CH_3), 1.96 – 1.81 (m, 3H, H-5, 2H-6).

3.3.3. (1*R*)-2-cyclohexen-1-ol, (*R*)-50

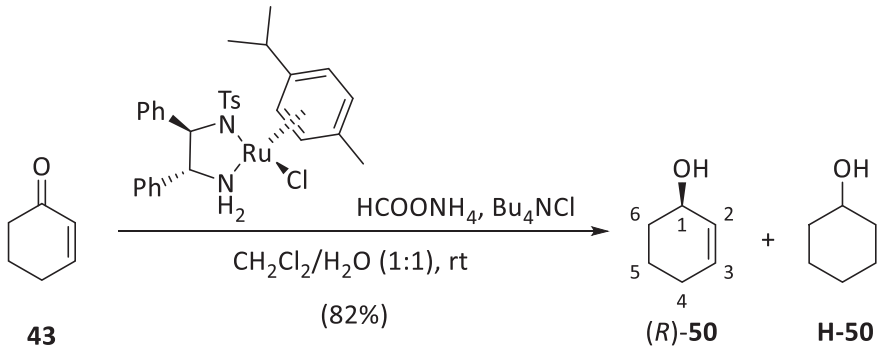

To a stirred solution of enone **43** (250 μL, 2.59 mmol) in a biphasic media of CH_2Cl_2 (8.6 mL) and water (8.6 mL) and under a nitrogen flux, tetrabutylammonium chloride (222 mg, 0.8 mmol), ammonium formate (532 mg, 7.82 mmol) and (*R*,*R*)-Noyori-I catalyst **25** (49.6 mg, 0.08 mmol) were sequentially added at room temperature. The reaction mixture was allowed to stir for 24 h. Then, CH_2Cl_2 (10 mL) and water (10 mL) were added, the two phases were separated and the aqueous layer was extracted with CH_2Cl_2 (3 x 5 mL). The volatiles were removed under reduced pressure and purified by column chromatography ($CHCl_3$) affording an inseparable

mixture of allylic alcohol (*R*)-**50** and cyclohexanol **H-50** (210 mg, 2.14 mmol, 82% yield for (*R*)-**50**) in a 2:1 ratio as a yellowish oil.

Physical and spectroscopic data of the mixture (*R*)-**50** and **H-50**

CHPLC (Daicel Chiralcel AD-H): 92% ee; **^{1}H-NMR** (250 MHz, $CDCl_3$) ((*R*)-**50**) δ: 5.82 (dtd, $J_{3,2}$=10.0 Hz, $J_{3,4eq}$=$J_{3,4ax}$=3.3 Hz, $J_{3,1}$=1.1 Hz, 1H, H-3), 5.73 (ddt, $J_{2,3}$=10.0, $J_{2,1}$=3.4, $J_{2,4}$=$J_{2,6}$=1.8 Hz, 1H, H-2), 4.42 – 4.13 (m, 1H, H-1), 2.07 – 1.89 (m, 1H, H-6), 1.92 – 1.81 (m, 1H, H-6), 1.79 – 1.64 (m, 2H, H-4, H-5), 1.64 – 1.48 (m, 2H, H-4, H-5); (**H-50**) δ: 3.66 – 3.52 (m, 1H, H-1'), 1.64 – 1.48 (m, 4H, H-2', H-6'), 1.38 – 0.96 (m, 6H, H-3', H-4', H-5').

3.3.4. Mixture of cyclopentan-1-one, 51, (1*R*)-cyclopentan-1-ol, 52, and 2-cyclopenten-1-one, 42

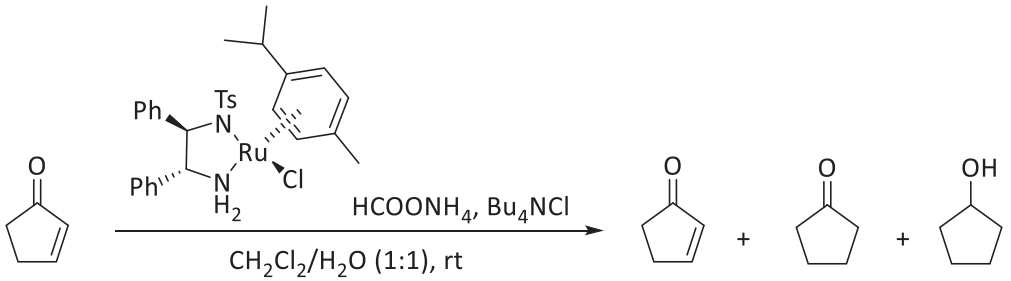

42 **42** **51** **52**

To a stirred solution of enone **42** (500 µL, 5.85 mmol) in a biphasic media of CH_2Cl_2 (19 mL) and water (19 mL) and under a nitrogen flux, tetrabutylammonium chloride (493 mg, 1.79 mmol), sodium formate (597 mg, 8.77 mmol) and (*R*,*R*)-Noyori-I catalyst **25** (110 mg, 0.18 mmol) were sequentially added at room temperature. The reaction mixture was allowed to stir for 24 h. After that time, catalyst **25** (110 mg, 0.18 mmol) was added and the reaction was stirred for further 24 h. Then, a third batch of catalyst **25** (110 mg, 0.18 mmol) was added and the mixture was stirred for 24 h. Then, CH_2Cl_2 (20 mL) and water (20 mL) were added, the two phases were separated and the aqueous layer was extracted with CH_2Cl_2 (3 x 20 mL). The volatiles were removed under reduced pressure to furnish a mixture of 1-cyclopentanone, **51**, 1-cyclopentanol, **52**, and starting material **42**, in a 3:3:2 ratio as a yellowish oil.

Spectroscopic data of the mixture of **42**, **51** and **52**

^{1}H-NMR (250 MHz, $CDCl_3$) (**42**) δ: 7.75 (dt, $J_{3,2}$=5.4 Hz, $J_{3,4}$=$J_{3,4}$=2.7 Hz, 1H, H-3), 6.23 (dt, $J_{2,3}$=5.4 Hz, $J_{2,5}$=$J_{2,5}$=2.3 Hz, 1H, H-2), 2.72 (dq, $J_{5,4}$=7.0 Hz, $J_{5,2}$=$J_{5,3}$=2.3 Hz, 2H, H-5), 2.41 – 2.35 (m, 2H, H-4); (**51**) δ: 2.25 – 2.11 (m, 4H, H-2, H-5), 2.05 – 1.90 (m, 4H, H-3, H-4); (**52**) δ: 4.48 – 4.26 (m, 1H, H-1), 3.38 (s, 1H, -OH), 1.85 – 1.72 (m, 4H, H-2, H-5), 1.66 – 1.54 (m, 4H, H-3, H-4).

3.3.5. (1*R*)-2-cyclohepten-1-ol, (*R*)-53

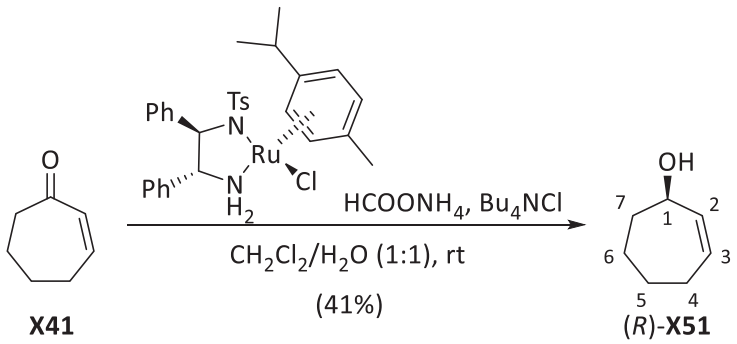

To a stirred solution of enone **44** (500 µL, 3.59 mmol) in a biphasic media of CH_2Cl_2 (12 mL) and water (12 mL) and under a nitrogen flux, tetrabutylammonium chloride (299 mg, 1.08 mmol), ammonium formate (732 mg, 10.8 mmol) and (*R*,*R*)-Noyori-I catalyst **25** (68.5 mg, 0.11 mmol) were sequentially added at room temperature. The reaction mixture was allowed to stir for 24 h. Then, CH_2Cl_2 (12 mL) and water (12 mL) were added, the two phases were separated and the aqueous layer was extracted with CH_2Cl_2 (3 x 5 mL). The volatiles were removed under reduced pressure and purified by column chromatography ($CHCl_3$) to furnish a 7:1 mixture of allylic alcohol (*R*)-**53** and the totally hydrogenated derivative **H-53** (165 mg, 1.47 mmol, 41% yield for (*R*)-**53**) as a yellowish oil.

Physical and spectroscopic data of (*R*)-**53**

CHPLC (Daicel Chiralcel IC): 83% ee; $[\alpha]_D^{20}$= +10.5 (*c* 1.4, $CHCl_3$) [lit:[9] $[\alpha]_D^{20}$= +28.2 (*c* 1.03, $CHCl_3$), >99% ee]; **^{1}H-NMR** (400 MHz, $CDCl_3$) δ: 5.79 – 5.69 (m, 2H, H-2, H-3), 4.42 – 4.36 (m, 1H, H-1), 2.23 – 2.13 (m, 1H, H-7), 2.08 – 1.97 (m, 1H, H-7), 1.96 – 1.82 (m, 2H, H-4), 1.71 – 1.51 (m, 3H, 2H-6, H-5), 1.41 – 1.30 (m, 1H, H-5); **^{13}C-NMR** (100 MHz, $CDCl_3$) δ: 138.0 (C-2), 130.3 (C-3), 72.3 (C-1), 36.9 (C-7), 28.8 (C-4), 27.0/26.9 (C-5, C-6).

3.3.6. (1*R*)-3-methyl-2-cyclohexen-1-ol, (*R*)-54

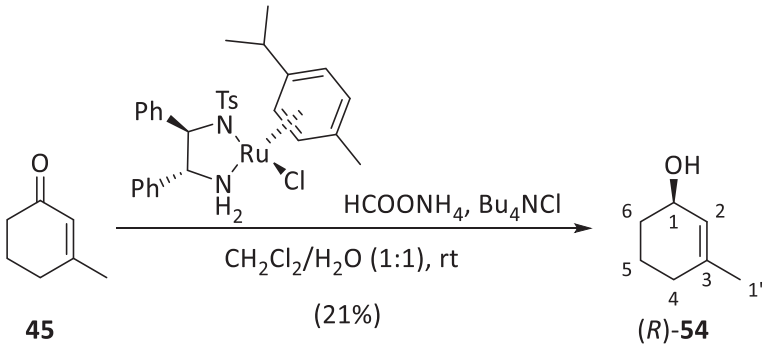

To a stirred solution of enone **45** (510 µL, 4.40 mmol) in a biphasic media of CH_2Cl_2 (14.7 mL) and water (14.7mL) and under a nitrogen flux, tetrabutylammonium chloride (367 mg, 1.32 mmol), ammonium formate (899 mg, 13.2 mmol) and (*R*,*R*)-Noyori-I catalyst **25** (84 mg, 0.13 mmol) were sequentially added at room temperature. The reaction mixture was allowed to stir for 72 h. Then, CH_2Cl_2 (10 mL) and water (10 mL) were added, the two phases were separated and the aqueous layer was extracted with CH_2Cl_2 (3 x 5 mL). The volatiles were removed under reduced pressure and purified by column chromatography ($CHCl_3$) yielding allylic alcohol (*R*)-**54** (89 mg, 0.795 mmol, 21% yield) as a yellowish oil.

Physical and spectroscopic data of (*R*)-**54**

CHPLC (Daicel Chiralcel IC): 88% ee; $[\alpha]_D^{20}$= +89.8 (*c* 0.1, $CHCl_3$) [lit:[10] $[\alpha]_D^{20}$= +62.4 (*c* 1.0, $CHCl_3$), 96% ee]; **^{1}H-NMR** (250 MHz, $CDCl_3$) δ: 5.47 (dq, $J_{2,1}$=3.3 Hz, $J_{2,1'}$=1.6 Hz, 1H, H-2), 4.22 – 4.02 (m, 1H, H-1), 2.06 – 1.81 (m, 2H, H-6), 1.86 – 1.57 (m, 2H, H-5), 1.67 (s, 3H, H-1'), 1.64 – 1.34 (m, 2H, H-4).

3.3.7. (1*R*)-1,2,3,4-tetrahydro-1-naphthalenol (*R*)-55

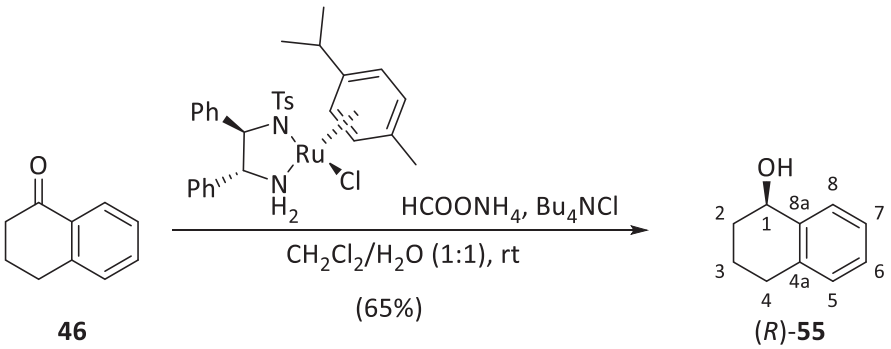

46 (*R*)-**55**

To a stirred solution of ketone **46** (100 µL, 0.73 mmol) in a biphasic media of CH_2Cl_2 (2.4 mL) and water (2.4 mL) and under a nitrogen flux, tetrabutylammonium chloride (61 mg, 0.22 mmol), ammonium formate (149 mg, 2.19 mmol) and (*R*,*R*)-Noyori-I catalyst **25** (13.9 mg, 0.022 mmol) were sequentially added at room temperature. The reaction mixture was allowed to stir during 24 h. Then, CH_2Cl_2 (2 mL) and water (2 mL) were added, the two phases were separated and the aqueous layer was extracted with CH_2Cl_2 (3 x 1 mL). The volatiles were removed under reduced pressure and purified by column chromatography ($CHCl_3$) yielding alcohol (*R*)-**55** (71 mg, 0.476 mmol, 65% yield) as a yellowish oil.

Physical and spectroscopic data of (*R*)-**55**

CHPLC (Daicel Chiralcel OD-H): 94% ee; $[\alpha]_D^{20}$= -36.5 (*c* 0.98, $CHCl_3$) [lit:[10] $[\alpha]_D^{20}$= -33.2 (*c* 1.0, $CHCl_3$), 99% ee]; **^{1}H-NMR** (250 MHz, $CDCl_3$) δ: 7.43 (dd, $J_{8,7}$=5.5 Hz, $J_{8,6}$=3.5 Hz, 1H, H-8), 7.25 –

7.17 (m, 2H, H-6, H-7), 7.11 (dd, $J_{5,6}$=5.5 Hz, $J_{5,7}$=3.5 Hz 1H, H-5), 4.76 (t, $J_{1,2ax}$=$J_{1,2eq}$=4.5 Hz, 1H, H-1), 2.94 – 2.62 (m, 2H, H-4), 2.05 – 1.84 (m, 4H, H-2, H-3); **^{13}C-NMR** (100 MHz, $CDCl_3$) δ: 138.9 (C-8a), 137.3 (C-4a), 129.2/128.8 (C-5, C-8), 127.7/126.3 (C-6, C-7), 68.3 (C-1), 32.4 (C-2), 29.4 (C-4), 18.9 (C-3).

3.3.8. (5*R*)-5-Methyldihydro-2(*3H*)-furanone (*R*)-56

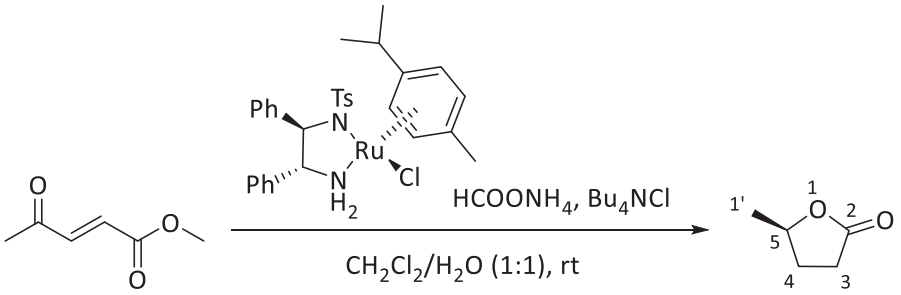

47 (96%) (*R*)-**56**

To a stirred solution of **47** (101 mg, 0.79 mmol) in a biphasic media of CH_2Cl_2 (2.6 mL) and water (2.6 mL) and under a nitrogen flux, tetrabutylammonium chloride (68 mg, 0.24 mmol), ammonium formate (557 mg, 8.19 mmol) and (*R*,*R*)-Noyori-I catalyst **25** (15.1 mg, 0.024 mmol) were sequentially added at room temperature. The reaction mixture was allowed to stir during 24h. Then, CH_2Cl_2 (2 mL) and water (2 mL) were added, the two phases were separated and the aqueous layer was extracted with CH_2Cl_2 (3 x 1 mL). The volatiles were removed under reduced pressure and purified by column chromatography ($CHCl_3$) providing lactone (*R*)-**56** (86 mg, 0.75 mmol, 96% yield) as a yellowish oil.

Physical and spectroscopic data of (*R*)-**56**

$[\alpha]_D^{20}$= +20.3 (*c* 0.73, $CHCl_3$) [lit:[12] $[\alpha]_D^{20}$= +33.7 (c 1.75, CH_2Cl_2)]; **^{1}H-NMR** (250 MHz, $CDCl_3$) δ: 4.63 (dq, $J_{5,4ax}$=7.7 Hz, $J_{5,1'}$=$J_{5,4eq}$=6.3 Hz, 1H, H-5), 2.61 – 2.44 (m, 2H, H-3), 2.34 (dt, $J_{4eq,4ax}$=12.6 Hz, $J_{4eq,5}$=6.3 Hz, 1H, H-4eq), 1.81 (dtd, $J_{4ax,4eq}$=12.6 Hz, $J_{4ax,3ax}$=9.1 Hz, $J_{4ax,5}$=7.7 Hz, 1H, H-4ax), 1.40 (d, $J_{1',5}$=6.3 Hz, 3H, H-1').

3.4. Synthesis of the alcohol 16

3.4.1. (1*R*,4'*R*,5*R*,5'*R*,6*S*)-4',5'-diphenylspiro[bicyclo[4.1.0]heptane-2,2'-[1,3]dioxolan]-5-ol, 13

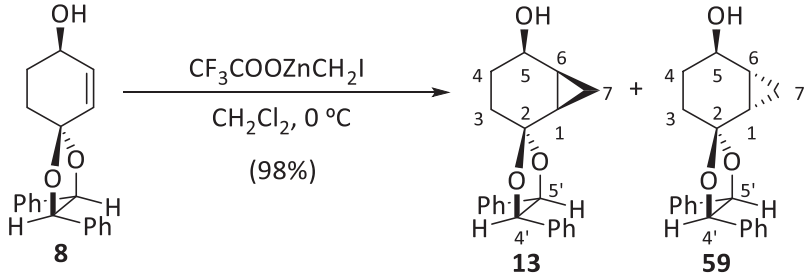

An ice-cooled solution of Et_2Zn (6.48 mL, 6.480 mmol, 1.0 M in hexanes) in CH_2Cl_2 (45 mL) was stirred for 15 min under nitrogen atmosphere. Then, to the mixture and, after stirring trifluoroacetic acid (504 µL, 6.480 mmol) was dropwise added for another 20 min, then diiodomethane (523 µL, 6.480 mmol) was dropwise added and stirred for 20 min more. At that time, a solution of alcohol **8** (1.0 g, 3.240 mmol) in CH_2Cl_2 (20 mL) was introduced at 0 °C. The resulting mixture was stirred for 2 h, quenched by the addition of saturated aqueous Na_2EDTA solution (80 mL) and extracted with CH_2Cl_2 (2 x 60 mL). The organic layers were dried (Na_2SO_4), concentrated under reduced pressure and purified by column chromatography (hexanes-EtOAc, 4:1) to provide cyclohexanol **13** (1.126 g, 3.492 mmol, 98% yield) as a white solid.

Physical and spectroscopic data of **13**

m.p.: 103-105 °C (diethyl ether); $[\alpha]_D^{20}$= +25.5 (*c* 1.1, $CHCl_3$); **^{1}H-NMR** (400 MHz, $CDCl_3$) δ: 7.37 – 7.28 (m, 8H, H-Ar), 7.23 – 7.19 (m, 2H, H-Ar), 4.83 (d, $J_{5',4'}$=9.0 Hz, 1H, H-5'), 4.70 (d, $J_{4',5'}$=9.0 Hz, 1H, H-4'), 4.35 (q, $J_{5,4ax}$=$J_{5,4eq}$=$J_{5,6}$=5.5 Hz, 1H, H-5), 1.94 – 1.81 (m, 3H, 2H-3, H-4eq), 1.70 – 1.55 (m, 2H, H-1, H-6), 1.56 – 1.41 (m, 1H, H-4ax), 0.96 (q, $J_{7endo,1}$=$J_{7endo,6}$=J_{gem}=5.7 Hz, 1H, H-7endo), 0.83 (td, $J_{7exo,1}$=$J_{7exo,6}$=9.4 Hz, J_{gem}=5.7 Hz, 1H, H-7exo); **^{13}C-NMR** (100 MHz, $CDCl_3$) δ: 136.9/136.6 (C-Ar), 128.5/128.5/128.4 (C-Ar), 127.0/126.7 (C-Ar), 108.7 (C-2), 85.5/85.2 (C-4',C-5'), 65.4 (C-5), 31.8 (C-3), 27.5 (C-4), 23.4 (C-1), 19.4 (C-6), 4.2 (C-7); **COSY**, **dept135**, **HSQC**, **HMBC** and **NOESY** experiments were recorded; **IR** (ATR): 3496, 2930, 1454, 1258, 1086, 1062, 965, 752, 700 (cm^{-1}); **HRMS** (ESI+): Calcd. for $[C_{21}H_{22}O_3Na]^+$: 345.1461, Found: 345.1448.

Spectroscopic data of **59**

^{1}H-NMR (360 MHz, $CDCl_3$): δ 7.38 – 7.31 (m, 8H, H-Ar), 7.31 – 7.21 (m, 2H, H-Ar), 4.88 (d, $J_{5',4'}$=8.5 Hz, 1H, H-5'), 4.77 (d, $J_{4',5'}$=8.5 Hz, 1H, H-4'), 4.10 (s br, 1H, H-5), 2.09 – 1.99 (m, 2H, H-3), 1.89 – 1.74 (m, 2H, H-4eq, H-6), 1.67 (td, $J_{1,6}$=$J_{1,7exo}$=9.0 Hz, $J_{1,7endo}$=5.8 Hz, 1H, H-1), 1.49 (tdd, J_{gem}=$J_{4ax,3ax}$=10.5 Hz, $J_{4ax,5}$=5.8 Hz, $J_{4ax,3eq}$=2.1 Hz, 1H, H-4ax), 0.87 (td, $J_{7exo,1}$=$J_{7exo,6}$=9.0 Hz,

$J_{7exo,7endo}$=5.8 Hz, 1H, H-7exo), 0.57 (q, $J_{7endo,1}$=$J_{7endo,6}$=$J_{7endo,7exo}$=5.8 Hz, 1H, H-7endo); **^{13}C-NMR** (90 MHz, $CDCl_3$): δ 136.6/136.6 (C-Ar), 128.5/128.4/128.4 (C-Ar), 126.9/126.8 (C-Ar), 109.9 (C-2), 85.4/85.3 (C-4',C-5'), 66.2 (C-5), 28.6 (C-3), 27.9 (C-4), 21.0 (C-1), 20.6 (C-6), 7.6 (C-7); **NOESY** experiment was recorded.

3.4.2. (1*R*,5*R*,6*S*)-5-hydroxybicyclo[4.1.0]heptan-2-one, 60

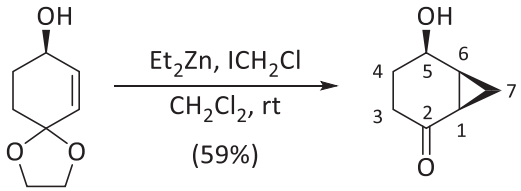

(*R*)-**36** **60**

To a stirred solution of allylic alcohol (*R*)-**36** (38 mg, 0.24 mmol) in anhydrous CH_2Cl_2, ICH_2Cl (240 µL, 3.18 mmol) was added and the mixture was stirred 20 min at 0 °C. At this time, Et_2Zn (1.6 mL, 1.6 mmol) was dropwise added at 0 °C, and the mixture was stirred for 5 h, allowing it to warm to room temperature. Then, a saturated aqueous $NaHCO_3$ solution (6 mL) was added, and the aqueous layer was extracted with diclohomethane (3 x 6 mL). The organic layer was dried (Na_2SO_4), concentrated under reduced pressure and purified by column chromatography (pentane:diethyl ether 4:1)furnishing compound **60** (18 mg, 0.14 mmol, 59% yield) as a colourless oil.

Physical and spectroscopic data of **60**

$[\alpha]_D^{20}$= +78.5 (*c* 0.65, $CHCl_3$) [lit:[7] $[\alpha]_D^{20}$= -80.7 (*c* 1.37, $CHCl_3$), for its enantiomer]; **^{1}H-NMR** (400 MHz, $CDCl_3$) δ: 4.42 (dddd, $J_{5,4ax}$=10.1 Hz, $J_{5,6}$=5.2 Hz, $J_{5,4eq}$=4.1 Hz, $J_{5,3ax}$=0.8 Hz, 1H, H-5), 2.37 (ddd, J_{gem}=18.4 Hz, $J_{3eq,4ax}$=5.6 Hz, $J_{3eq,4eq}$=3.6 Hz, 1H, H-3eq), 2.15 (dddd, J_{gem}=18.4 Hz, $J_{3ax,4ax}$=12.1 Hz, $J_{3ax,4eq}$=6.6 Hz, $J_{3ax,5}$=0.8 Hz, 1H, H-3ax), 1.98 – 1.83 (m, 3H, H-1, H-6, H-4eq), 1.63 (dddd, J_{gem}=13.8 Hz, $J_{4ax,3ax}$=12.1 Hz, $J_{4ax,5}$=10.3 Hz, $J_{4ax,3eq}$=5.6 Hz, 1H, H-4ax), 1.44 (q, J_{gem}=$J_{7endo,1}$=$J_{7endo,6}$=5.4 Hz, 1H, H-7endo), 1.14 (ddd, $J_{7exo,1/6}$=9.8 Hz, $J_{7exo,1/6}$=7.7 Hz, J_{gem}=5.4 Hz, 1H, H-7exo); **^{13}C-NMR** (100 MHz, $CDCl_3$) δ: 207.5 (C-2), 65.3 (C-5), 34.8 (C-3), 26.8 (C-1), 26.7 (C-4), 23.3 (C-6), 8.0 (C-7); **COSY**, **dept135**, **HSQC** and **NOESY** experiments were recorded; **IR** (ATR): 3359, 2919, 2850, 1659, 1345, 1066, 1041 (cm^{-1}); **HRMS** (ESI+): Calcd. for $[C_7H_{10}O_2Na]^+$: 149.0573, Found: 149.0576.

3.4.3. (1*R*,4'*R*,5*R*,5'*R*,6*S*)-5-(*tert*-Butyldiphenylsilyloxy)-4',5'-diphenylspirobicyclo[4.1.0]heptane-2,2'-[1,3]dioxolane, 9

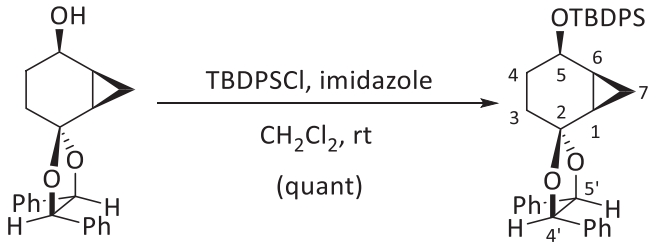

To a stirred solution of **13** (1.55 g, 4.81 mmol) in CH_2Cl_2 (32 mL) were added imidazole (360 mg, 5.290 mmol) and TBDPSCl (1.3 mL, 5.05 mmol) at room temperature, allowing it to stir overnight. At this time, the volatiles were removed under vacuum and the resulting crude was purified by column chromatography (hexanes-EtOAc, 5:1) to furnish the silyl derivate **9** (2.70 g, 4.81 mmol, quantitative yield) as a colourless syrup.

Physical and spectroscopic data of **9**

$[\alpha]_D^{20}$= +38.1 (*c* 1.05, $CHCl_3$); **^{1}H-NMR** (400 MHz, $CDCl_3$) δ: 7.77 (dd, *J*=7.3 Hz, *J*=5.8 Hz, 4H, H-Ar), 7.50 – 7.37 (m, 6H, H-Ar), 7.37 – 7.28 (m, 8H, H-Ar), 7.21 (dd, *J*=6.8 Hz, *J*=2.9 Hz, 2H, H-Ar), 4.84 (d, $J_{5',4'}$=8.5 Hz, 1H, H-5'), 4.74 (d, $J_{4',5'}$=8.5 Hz, 1H, H-4'), 4.40 (q, $J_{5,4ax}$=$J_{5,4eq}$=$J_{5,6}$=5.8 Hz, 1H, H-5), 1.98 (t, J_{gem}=$J_{3eq,4ax}$=$J_{3eq,4eq}$=10.8 Hz, 1H, H-3eq), 1.86 – 1.72 (m, 2H, H-3ax, H-4eq), 1.70 – 1.62 (m, 1H, H-4ax), 1.49 (td, $J_{1,6}$=$J_{1,7exo}$=9.3 Hz, $J_{1,7endo}$=5.8 Hz 1H, H-1), 1.32 (tt, $J_{6,7exo}$=$J_{6,1}$= 9.3 Hz, $J_{6,7endo}$=$J_{6,5}$=5.8 Hz, 1H, H-6), 1.19 (q, $J_{7endo,1}$=$J_{7endo,6}$=J_{gem}=5.8 Hz, 1H, H-7endo), 1.13 (s, 9H, H-*t*Bu), 0.83 (td, $J_{7exo,1}$=$J_{7exo,6}$=9.3 Hz, J_{gem}=5.8 Hz, 1H, H-7exo); **^{13}C-NMR** (100 MHz, $CDCl_3$) δ: 137.2/136.9 (C-Ar), 136.0/135.9 (C-Ar), 135.3/134.9/134.8/134.7 (C-Ar), 129.8/129.7 (C-Ar), 128.6/128.5/128.4 (C-Ar), 127.8/127.7/127.6/127.0/126.7 (C-Ar), 109.6 (C-2), 85.5/85.3 (C-4',C-5'), 66.2 (C-5), 30.7 (C-3), 28.9 (C-4), 27.1 ($C(\underline{C}H_3)_3$), 23.1 (C-1), 19.4 (C-6), 19.1 ($\underline{C}(CH_3)_3$), 5.7 (C-7); **COSY**, **dept135**, **HSQC** and **NOESY** experiments were recorded; **IR** (ATR): 3068, 2930, 1695, 1427, 1104, 1074, 869, 697 (cm^{-1}); **HRMS** (ESI+): Calcd. for $[C_{37}H_{40}O_3SiNa]^+$: 583.2639, Found: 583.2636.

3.4.4. (1*R*,5*R*,6*S*)-5-(*tert*-Butyldiphenylsilyloxy)bicyclo[4.1.0]heptan-2-one, 10

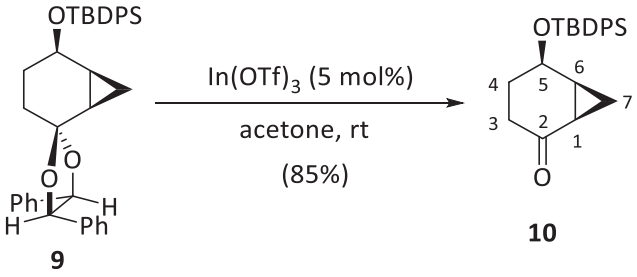

To a solution of **9** (6.01 g, 10.7 mmol) in acetone (228 mL) was added $In(OTf)_3$ (258 mg, 0.459 mmol) and the mixture was stirred at room temperature for 16 h. Then, acetone was removed under vacuum and the residue was purified by column chromatography (hexanes-EtOAc, 8:1) to afford ketone **10** (3.33 mg, 9.13 mmol, 85% yield) as a white solid.

Physical and spectroscopic data of **10**

m.p.: 49-51 °C (diethyl ether); $[\alpha]_D^{20}$= +136.7 (*c* 0.3, $CHCl_3$); **^{1}H-NMR** (400 MHz, $CDCl_3$) δ: 7.72 (dd, *J*=14.1 Hz, *J*=6.9 Hz, 4H, H-Ar), 7.41 (dd, *J*=13.7 Hz, *J*=7.0 Hz, 6H, H-Ar), 4.39 (q, $J_{5,4ax}$=$J_{5,4eq}$=$J_{5,6}$=6.9 Hz, 1H, H-5), 2.32 (dt, J_{gem}=17.6 Hz, $J_{3eq,4ax}$=$J_{3eq,4eq}$=5.2 Hz, 1H, H-3eq), 1.98 (dt, J_{gem}=17.6 Hz, $J_{3ax,4ax}$=$J_{3ax,4eq}$=8.6 Hz, 1H, H-3ax), 1.82 – 1.72 (m, 2H, H-4), 1.72 – 1.62 (m, 2H, H-1, H-6), 1.52 (q, $J_{7endo,1}$=$J_{7endo,6}$=J_{gem}=5.5 Hz, 1H, H-7endo), 1.10 (s, 10H, 9H-*t*Bu, H-7exo); **^{13}C-NMR** (100 MHz, $CDCl_3$) δ: 208.0 (C-2), 135.8/135.8 (C-Ar), 134.2/134.0 (C-Ar), 129.9/129.8 (C-Ar), 127.8/127.7 (C-Ar), 66.4 (C-5), 34.5 (C-3), 27.8 (C-4), 27.0 ($C(CH_3)_3$), 27.0 (C-1), 23.9 (C-6), 19.3 ($C(CH_3)_3$), 9.2 (C-7); **COSY**, **dept135**, **HSQC** and **HMBC** experiments were recorded; **IR** (ATR): 3069, 2927, 1689, 1427, 1080, 967, 820, 701 (cm^{-1}); **HRMS** (ESI+): Calcd. for $[C_{23}H_{28}O_2SiNa]^+$: 387.1751, Found: 387.1744.

3.4.4.1. From keto alcohol 60

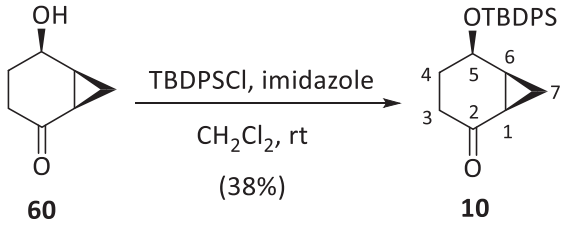

To a stirred solution of **60** (19 mg, 0.15 mmol) in CH_2Cl_2 (1 mL) were added imidazole (13 mg, 0.19 mmol) and TBDPSCl (42 µL, 0.16 mmol) at room temperature, allowing it to stir overnight. At this time, the volatiles were removed under vacuum and the resulting crude was

purified by column chromatography (pentane-Et_2O, 4:1) to furnish the silyl derivate **10** (21 mg, 0.06 mmol, 38% yield) as a white solid.

3.4.5. ((1'*S*,2'*R*,5'*R*,6'*S*)-5'-(*tert*-Butyldiphenylsilyloxy)bicyclo[4.1.0]hept-2'-yl)methanol, 14 and its (2'*S*)-diastereomer 15

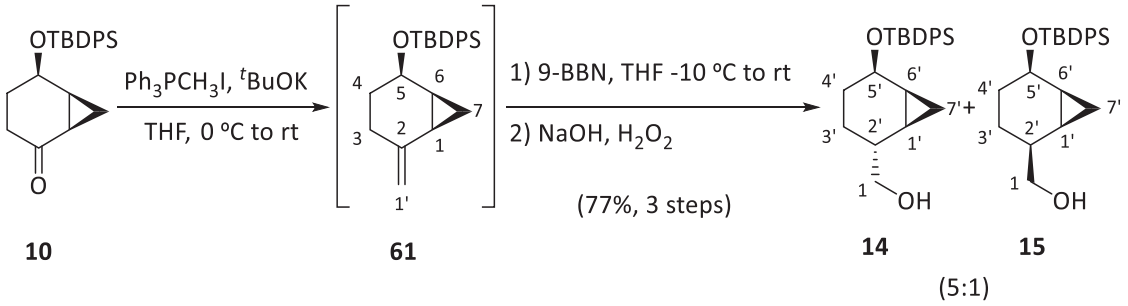

To a stirring solution of Ph_3PCH_3I (587 mg, 1.41 mmol) in anhydrous THF (1.6 mL) at 0 ºC, ^{t}BuOK (160 mg, 1.36 mmol) was added, under nitrogen atmosphere, and the resulting yellow mixture was allowed to react for 1 h. At this time, a solution of ketone **10** (102 mg, 0.28 mmol) in THF (1.6 mL) was added and the mixture was stirred for 3 h. Then, diethyl ether (3 mL) was added and the crude filtered through a thin pad of silica and Celite®, using more diethyl ether (15 mL) as eluent. The volatiles were removed under vacuum to obtain an orange oil as a crude, which was directly used for the next step without further purification.

In order to avoid isomerization, crude alkene **61** was rapidly dissolved in anhydrous THF (2.9 mL) and 9-BBN (1.68 mL, 0.84 mmol, 0.5 M in THF) was added at -10 ºC. The mixture was allowed to stir overnight and then, water (0.6 mL), NaOH (1.1 mL, 3 M in water) and H_2O_2 (1 mL, 30% in water) were added at 0 ºC. After stirring for 15 min, the mixture was diluted with brine (10 mL) and CH_2Cl_2 (10 mL) and the aqueous phase was extracted with more CH_2Cl_2 (2 x 10 mL). The organic layers were dried (Na_2SO_4), concentrated under reduced pressure and purified by column chromatography (hexanes-EtOAc, 4:1 to 2:1) to provide a chromatographycally inseparable mixture of alcohols **14** and **15** (94 mg, 0.25 mmol, 88% yield) in a *ca.* 5:1 diastereomeric ratio.

Physical and spectroscopic data of **61**

$[\alpha]_D^{20}$= +22.0 (*c* 1.0, $CHCl_3$); **^{1}H-NMR** (360 MHz, $CDCl_3$) δ: 7.75 (dd, *J*=18.0 Hz, *J*=7.2 Hz, 4H, H-Ar), 7.41 (dd, *J*=11.4 Hz, *J*=6.9 Hz, 6H, H-Ar), 4.84 (s, 1H, H-1'), 4.75 (s, 1H, H-1'), 4.34 (q, $J_{5,4ax}$=$J_{5,4eq}$=$J_{5,6}$=6.1 Hz, 1H, H-5), 2.21 (dt, J_{gem}=14.8 Hz, $J_{3eq,4ax}$=$J_{3eq,4eq}$=6.0 Hz, 1H, H-3eq), 1.95 (dt, J_{gem}=14.8 Hz, $J_{3ax,4ax}$=$J_{3ax,4eq}$=7.2 Hz, 1H, H-3ax), 1.66 (td, $J_{1,6}$=$J_{1,7exo}$=8.7 Hz, $J_{1,7endo}$=5.0 Hz, 1H, H-1), 1.56 – 1.46 (m, 2H, H-4), 1.35 – 1.21 (m, 1H, H-6), 1.12 (s, 9H, H-*t*Bu), 0.94 (q,

$J_{7endo,1}$=$J_{7endo,6}$=J_{gem}=5.0 Hz, 1H, H-7endo), 0.75 (td, $J_{7exo,1}$=$J_{7exo,6}$=8.7 Hz, J_{gem}=5.0 Hz, 1H, H-7exo); **^{13}C-NMR** (90 MHz, $CDCl_3$) δ: 146.4 (C-2), 136.0/135.9 (C-Ar) 134.9/134.8 (C-Ar), 129.6/129.6/127.6/127.5 (C-Ar), 108.2 (C-1'), 67.4 (C-5), 31.1 (C-4), 27.9 (C-3), 27.1 (C(CH_3)$_3$), 20.3 (C-6), 20.2 (C-1), 19.4 (C(CH_3)$_3$), 9.1 (C-7); **COSY**, **dept135**, **HSQC**, **HMBC** and **NOESY** experiments were recorded; **IR** (ATR): 3070, 2930, 1471, 1427, 1106, 1067, 739, 702 (cm^{-1}); **HRMS** (ESI+): Calcd. for $[C_{24}H_{30}OSiNa]^+$: 385.1958 Found: 385.1950.

Spectroscopic data of a mixture of **14** and **15**

^{1}H-NMR (400 MHz, $CDCl_3$) (*ca.* 83% **14**) δ: 7.78 – 7.64 (m, 4H, H-Ar), 7.46 – 7.31 (m, 6H, H-Ar), 4.26 – 4.13 (m, 1H, H-5'), 3.51 (d, $J_{1,2'}$=6.6 Hz, 2H, H-1), 1.73 – 1.58 (m, 2H, H-2', H-4'eq), 1.57 – 1.39 (m, 1H, H-3'eq), 1.07 (s, 10H, H-*t*Bu, H-4'eq), 0.96 (ddd, $J_{6',7'exo}$=8.8 Hz, $J_{6',7'endo}$=5.3 Hz, $J_{6',1'}$=3.0 Hz, 1H, H-6'), 0.82 – 0.69 (m, 2H, H-1', H-3'ax), 0.65 (td, $J_{7'exo,1'}$=$J_{7'exo,6'}$=8.8, J_{gem}=5.3 Hz, 1H, H-7'exo), 0.50 (q, J_{gem}=$J_{7'endo,1'}$=$J_{7'endo,6'}$= 5.3 Hz, 1H, H-7'endo); (*ca.* 17% **15**, observable signals) δ: 7.78 – 7.64 (m, 4H, H-Ar), 7.46 – 7.31 (m, 6H, H-Ar), 4.31 (dt, $J_{5',6'}$=6.5 Hz, $J_{5',4'ax}$=$J_{5',4'eq}$=4.5 Hz, 1H, H-5'), 3.61 – 3.46 (m, 2H, H-1), 2.04 – 1.94 (m, 1H, H-2'), 1.88 – 1.78 (m, 1H, H-4'), 0.38 (td, $J_{7'exo,1'}$=$J_{7'exo,6'}$=9.0 Hz, J_{gem}=4.9 Hz, 1H, H-7'exo); **^{13}C-NMR** (100 MHz, $CDCl_3$) (*ca.* 83% **X13**) δ: 136.0/135.9 (C-Ar), 135.2/135.0 (C-Ar), 129.6/129.5/127.6/127.5 (C-Ar), 69.8 (C-5), 68.2 (C-1), 38.1 (C-2'), 28.4 (C-4'), 27.2 (C($\underline{C}H_3$)), 25.7 (C-3'), 19.4 ($\underline{C}$(CH_3)), 18.2(C-6'), 16.4 (C-1'), 8.6 (C-7'); (*ca.* 17% **X64**, observable signals) δ: 136.0/135.9 (C-Ar), 135.0/134.9 (C-Ar), 129.8/129.6/127.9/127.7 (C-Ar), 67.7 (C-1), 66.4 (C-5'), 35.1 (C-2'), 30.9 (C-4'), 27.2 (C($\underline{C}H_3$)), 22.8 (C-3'), 19.4 ($\underline{C}$(CH_3)), 17.2 (C-6'), 14.5 (C-1'), 2.5(C-7'); **COSY**, **dept135**, **HSQC**, **HMBC** and **NOESY** experiments were recorded; **IR** (ATR): 3358, 3070, 2930, 2856, 1427, 1109, 1070, 820, 739, 699 (cm^{-1}); **HRMS** (ESI+): Calcd. for $[C_{24}H_{32}O_2Si\text{-}C_4H_9]^+$: 323.1467, Found: 323.1469.

3.4.6. ((1'*S*,2'*R*,5'*R*,6'*S*)-5'-(*tert*-Butyldiphenylsilyloxy)bicyclo[4.1.0]heptan-2'-yl)methyl benzoate, 63 and its (2'*S*)-diastereomer 64

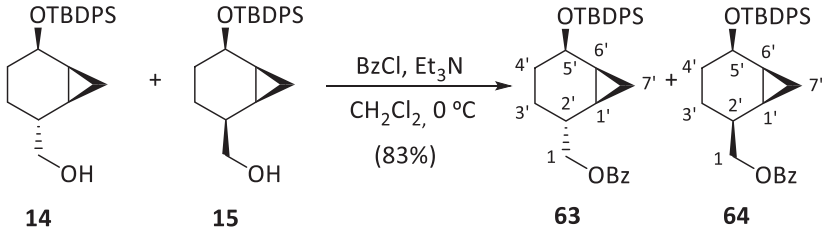

To a stirred solution of **14** and **15** (1.00 g, 2.63 mmol) in dry CH_2Cl_2 (30 mL) at 0 °C, anhydrous Et_3N (310 mL, 2.68 mmol) and benzoyl chloride (0.38 mL, 2.68 mmol) were

sequentially added under argon atmosphere and the mixture was allowed to stir overnight. Then, HCl 10% solution (30 mL) and CH_2Cl_2 (30 mL) were added, the two phases were separated and the aqueous phase was extracted with CH_2Cl_2 (2 x 30 mL). The organic layers were washed with brine (100 mL), dried (Na_2SO_4), concentrated under reduced pressure and purified by column chromatography (hexanes-EtOAc, 8:1) to afford a 11:1 diastereomeric mixture of **63** and **64** (1.06 g, 2.19 mmol, 83% yield) as a yellowish syrup.

Physical and spectroscopic data of **63**

$[\alpha]_D^{20}$= +46.9 (*c* 0.83, $CHCl_3$); **^{1}H-NMR** (400 MHz, $CDCl_3$) δ: 8.01 (dd, *J*=8.3 Hz, *J*=1.3 Hz, 2H, H-Bz), 7.76-7.34 (m, 4H, H-Ar), 7.58 – 7.52 (m, 1H, H-Bz), 7.45 – 7.34 (m, 8H, H-Ar, H-Bz), 4.22 (dt, $J_{5',6'}$=8.9 Hz, $J_{5',4'ax}$=$J_{5',4'eq}$=6.9 Hz, 1H, H-5'), 4.19 (dd, $J_{1,2'}$=7.0 Hz, $J_{1,1'}$=4.1 Hz, 2H, H-1), 1.97 (ddd, $J_{2',3'ax}$=12.0 Hz, $J_{2',1}$=7.0 Hz, $J_{2',3'eq}$=3.4 Hz, 1H, H-2'), 1.68 – 1.57 (m, 2H, H-4'eq, H-3'eq), 1.15 (ddd, J_{gem}=12.7 Hz, $J_{4'ax,5'}$=7.4 Hz, $J_{4'ax,3'}$=2.4 Hz, 1H, H-4'ax), 1.07 (s, 9H, H-*t*Bu), 0.99 (tt, $J_{6',7'exo}$=$J_{6',5'}$=8.9 Hz, $J_{6',7'endo}$=$J_{6',1'}$=5.3 Hz, 1H, H-6'), 0.93 – 0.82 (m, 2H, H-1', H-3'ax), 0.66 (td, $J_{7'exo,1'}$=$J_{7'exo,6'}$=8.9 Hz, J_{gem}=5.3 Hz, 1H, H-7'exo), 0.55 (q, $J_{7'endo,1'}$=$J_{7'endo,6'}$=J_{gem}=5.3 Hz, 1H, H-7'endo); **^{13}C-NMR** (100 MHz, $CDCl_3$) δ: 166.77 (C=O), 136.0/135.9 (C-Ar) 135.1/135.0 (C-Ar), 133.0/130.5/129.7 (C-Bz), 129.6/129.6 (C-Ar), 128.5 (C-Bz), 127.6/127.6 (C-Ar), 69.5 (C-1), 69.4 (C-5'), 34.6 (C-2'), 28.2 (C-4'), 27.2 (C($\underline{C}H_3$)$_3$), 25.8 (C-3'), 19.4 ($\underline{C}$(CH_3)$_3$), 18.0 (C-6'), 16.3 (C-1'), 8.4 (C-7'). **COSY**, **dept135**, **HSQC** and **HMBC** experiments were recorded; **IR** (ATR): 3069, 3000, 2931, 2856, 1718, 1270, 1106, 1068, 700 (cm^{-1}); **HRMS** (ESI+): Calcd. for $[C_{31}H_{36}O_3Si\text{-}C_4H_9]^+$: 427.1725 Found: 427.1723.

3.4.7. ((1'*S*,2'*R*,5'*R*,6'*S*)-5'-Hydroxybicyclo[4.1.0]heptan-2'-yl)methyl benzoate, 16

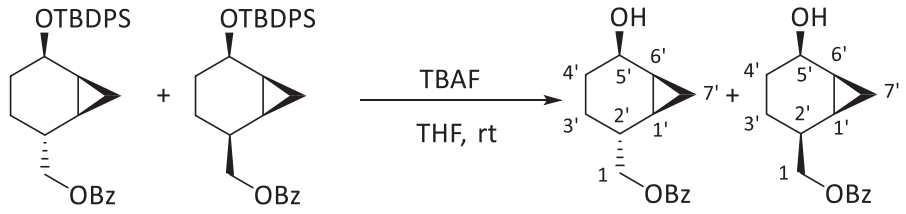

To a stirring solution of the 11:1 mixture of **63** and **64** (1.06 g, 2.19 mmol) in THF (44 mL) at room temperature, was added TBAF (6.6 mL, 6.57 mmol, 1 M in THF) and stirred overnight. Then, the solvent was removed and the crude was purified by column chromatography (hexanes-EtOAc, 10:1) to afford alcohol **16** (369 mg, 1.50 mmol, 68% yield) as a colourless syrup and **65** (25 mg, 0.1 mmol, 5% yield) as a colourless syrup.

Physical and spectroscopic data of **16**

[α]$_D^{20}$= +44.9 (*c* 0.88, $CHCl_3$); **^{1}H-NMR** (400 MHz, $CDCl_3$) δ: 8.05 (dd, *J*=8.3 Hz, *J*=1.3 Hz, 2H, H-Ar), 7.61 – 7.51 (m, 1H, H-Ar), 7.44 (t, *J*=7.6 Hz, 2H, H-Ar), 4.28 (dd, $J_{1,2'}$=6.8 Hz, $J_{1,1'}$=2.0 Hz, 2H, H-1), 4.20 (dt, $J_{5',6'}$=8.8 Hz, $J_{5',4'ax}$=$J_{5',4'eq}$=6.9 Hz, 1H, H-5'), 2.05 – 1.91 (m, 1H, H-2'), 1.86 – 1.72 (m, 1H, H-4'eq), 1.70 – 1.61 (m, 2H, H-3'), 1.33 (tt, $J_{6',5'}$=$J_{6',7'exo}$=8.8 Hz, $J_{6',1'}$=$J_{6',7'endo}$=5.3 Hz, 1H, H-6'), 1.13 – 0.87 (m, 2H, H-1', H-4'ax), 0.71 (td, $J_{7'exo,1'}$=$J_{7'exo,6'}$=8.8 Hz, J_{gem}=5.3 Hz, 1H, H-7'exo), 0.40 (q, $J_{7'endo,1'}$=$J_{7'endo,6'}$=J_{gem}=5.3 Hz, 1H, H-7'endo); **^{13}C-NMR** (100 MHz, CDCl3) δ: 166.8 (C=O), 133.1/130.4/129.7/128.5 (C-Ar), 69.4 (C-1), 68.0 (C-5'), 34.5 (C-2'), 28.0 (C-4'), 26.0 (C-3'), 18.1 (C-6'), 16.2 (C-1'), 7.6 (C-7'); **COSY**, **dept135**, **HSQC**, **HMBC** and **NOESY** experiments were recorded; **IR** (ATR): ν 3366, 3066, 3003, 2937, 2869, 1715, 1269, 1110, 1026, 708 (cm^{-1}); **HRMS** (ESI+): Calcd. for $[C_{15}H_{18}O_3]^+$: 246.1256, Found: 246.1258.

Physical and spectroscopic data of **65**

[α]$_D^{20}$= -7.2 (*c* 1.03, $CHCl_3$); **^{1}H-NMR** (400 MHz, $CDCl_3$) δ: 8.05 (d, *J*=7.2 Hz, 2H, H-Ar), 7.56 (t, *J*=7.4 Hz, 1H, H-Ar), 7.44 (t, *J*=7.6 Hz, 2H, H-Ar), 4.34 (dt, $J_{5',4'ax}$=7.3 Hz, $J_{5',4'eq}$=$J_{5',6'}$=4.7 Hz, 1H, H-5'), 4.29 (dd, J_{gem}=10.7 Hz, $J_{1,2'}$=6.9 Hz, 1H, H-1), 4.18 (dd, J_{gem}=10.7 Hz, $J_{1,2'}$=6.9 Hz, 1H, H-1), 2.36 (dq, $J_{2',3'ax}$=12.6 Hz, $J_{2',1}$=$J_{2',1}$=$J_{2',3'eq}$=6.9 Hz, 1H, H-2'), 1.51 - 1.37 (m, 4H, H-6', 2H-4', H-3'eq), 1.27 (tt, $J_{1',2'}$=$J_{1',7'exo}$=8.9 Hz, $J_{1',7'endo}$=$J_{1',6'}$=5.3 Hz, 1H, H-1'), 1.23 - 1.13 (m, 1H, H-3'ax), 0.57 (q, J_{gem}=$J_{7'endo,6'}$=$J_{7'endo,1'}$=5.3 Hz, 1H, H-7'endo), 0.46 (td, $J_{7'exo,1'}$=$J_{7'exo,6'}$=8.9 Hz, J_{gem}=5.3 Hz, 1H, H-7'exo); **^{13}C-NMR** (100 MHz, $CDCl_3$) δ: 166.8 (C=O), 133.0/130.6/129.7/128.5 (C-Ar), 68.9 (C-1), 64.7 (C-5'), 31.7 (C-2'), 29.9 (C-4'), 19.4 (C-3'), 17.1 (C-1'), 14.7 (C-6'), 1.7 (C-7'); **COSY**, **dept135**, **HSQC**, **HMBC** and **NOESY** experiments were recorded; **IR** (ATR): ν 3410, 3069, 3009, 2938, 1715, 1273, 1114, 712, 630 (cm^{-1}); **HRMS** (ESI+): Calcd. for $[C_{15}H_{20}O_3]^+$: 246.1256, Found: 246.1252.

3.5. Introduction of the base moiety

3.5.1. Nucleophilic substitution S_N2

3.5.1.1. ((1'*R*,2'*R*,6'*R*)-Bicyclo[4.1.0]hept-4'-en-2'-yl)methyl benzoate, 69

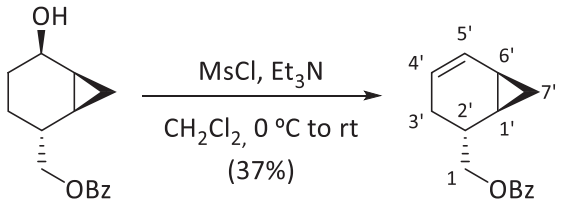

16 **69**

To a solution of **16** (33 mg, 0.13 mmol) in dry CH_2Cl_2 (1.5 mL), anhydrous Et_3N (37 µL, 0.27 mmol) and mesyl chloride (17 µL, 0.23 mmol) were sequentially added at 0 ºC, under argon atmosphere, and stirred overnight. Then, HCl 5% solution (2 mL) and CH_2Cl_2 (0.5 mL) were added. The two phases were separated and the aqueous layer was extracted with CH_2Cl_2 (2x2 mL). The organic layers were dried (Na_2SO_4), concentrated under reduced pressure and purified by column chromatography (hexanes-EtOAc, 20:1) to afford **69** (11 mg, 0.048 mmol, 37% yield) as a colourless syrup.

Physical and spectroscopic data of **69**

$[\alpha]_D^{20}$= -21.7 (*c* 0.17, $CHCl_3$); **^{1}H-NMR** (400 MHz, $CDCl_3$) δ: 8.09 (dd, *J*=8.5 Hz, *J*=1.3 Hz, 2H, H-Ar), 7.62 – 7.53 (m, 1H, H-Ar), 7.47 (tt, *J*=6.8 Hz, *J*=1.3 Hz, 2H, H-Ar), 6.08 (dddd, $J_{5',4'}$=9.9 Hz, $J_{5',6'}$=5.1 Hz, $J_{5',3'ax}$=2.7 Hz, $J_{5',3'eq}$=1.8 Hz, 1H, H-5'), 5.33 (ddd, $J_{4',5'}$=9.9 Hz, $J_{4',3'eq}$=6.6 Hz, $J_{4',3'ax}$=2.7 Hz, 1H, H-4'), 4.30 (dd, J_{gem}=10.6 Hz, $J_{1,2'}$=6.4 Hz, 1H, H-1), 4.20 (dd, J_{gem}=10.6 Hz, $J_{1,2'}$=8.3 Hz, 1H, H-1), 2.68 – 2.53 (m, 1H, H-2'), 2.11 (ddt, J_{gem}=17.3 Hz, $J_{3'eq,4'}$=6.6 Hz, $J_{3'eq,2'}$=$J_{3'eq,5'}$=1.8 Hz, 1H, H-3'eq), 2.00 (ddt, J_{gem}=17.3 Hz, $J_{3'ax,2'}$=6.9 Hz, $J_{3'ax,5'}$=$J_{3'ax,4'}$=2.7 Hz, 1H, H-3'ax), 1.33 – 1.23 (m, 2H, H-1', H-6'), 0.92 (td, $J_{7'exo,1'}$=$J_{7'exo,6'}$=8.5 Hz, J_{gem}=5.7 Hz, 1H, H-7'exo), 0.75 (dt, $J_{7'endo,6'}$=$J_{7'endo,1'}$=5.7 Hz, J_{gem}=4.4 Hz, 1H, 1H, H-7'endo); **^{13}C-NMR** (100 MHz, $CDCl_3$) δ: 166.8 (C=O), 133.0/130.7/ 129.7 (C-Ar), 129.4 (C-5'), 128.5 (C-Ar), 119.8 (C-4'), 68.1 (C-1), 29.0 (C-2'), 23.4 (C-3'), 16.1 (C-6'), 15.4 (C-1'), 11.2 (C-7'); **COSY**, **dept135**, **HSQC** and **HMBC** experiments were recorded; **IR** (ATR): ν 3031, 2924, 2852, 2363, 1720, 1270, 1114, 711 (cm^{-1}).

3.5.2. Mitsunobu reaction

3.5.2.1. ((1'*S*,2'*R*,5'*S*,6'*S*)-5'-((3''-Benzoyl-5''-methyl-4''-oxo-3'',4''-dihydropyrimidin-2''-yl)oxy)bicyclo[4.1.0]heptan-2'-yl)methyl benzoate, 72, and ((1'*S*,2'*R*,5'*S*,6'*S*)-5'-(benzoyloxy)bicyclo[4.1.0]heptan-2'-yl)methyl benzoate, 73

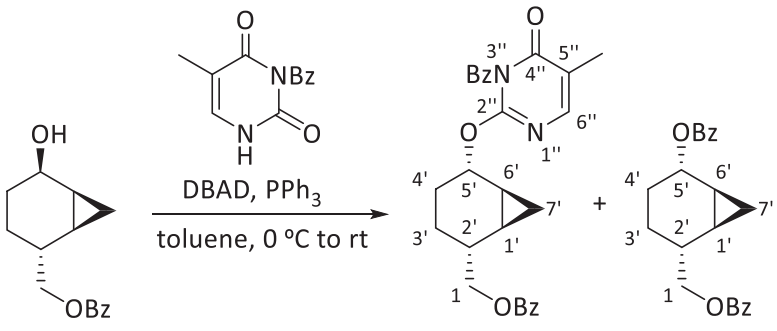

16 **72** **73**

To a suspension of Ph_3P (56 mg, 0.20 mmol) in dry ACN (1 mL) at 0 °C, DBAD (47 mg, 0.20 mmol) was slowly added and the mixture was stirred for 30 min at 0 °C. Then, *N3*-benzoyl-thymine (43 mg, 0.19 mmol) and alcohol **16** (33 mg, 0.13 mmol) in dry toluene (0.8 mL) were slowly added to the pre-formed complex at 0 °C under argon atmosphere. The reaction was warmed to room temperature and stirred overnight. The solvent was removed under vacuum and the resulted residue was purified by column chromatography (hexanes-EtOAc, 20:1) to provide an inseparable mixture of DBAD and **72** (7 mg, 15 µmol, 11% yield) as a white solid and protected alcohol **73** (8.5 mg, 0.024 mmol, 18% yield) as a colourless syrup.

Physical and spectroscopic data of the mixture of DBAD and **72**

^{1}H-NMR (400 MHz, $CDCl_3$) δ: 8.41 (s, 1H, H-6''), 8.19 (dd, *J*=8.3 Hz, *J*=1.2 Hz, 2H, H-Ar), 8.09 – 7.98 (m, 3H, H-Ar), 7.69 – 7.59 (m, 1H, H-Ar), 7.52 (t, *J*=7.9 Hz, 4H, H-Ar), 7.46 – 7.36 (m, 4H, H-Ar), 5.48 (br s, 1H, H-5'), 4.33 (d, $J_{1,2'}$=7.0 Hz, 2H, H-1), 2.14 (s, 3H, CH_3), 2.13 – 2.05 (m, 1H, H-2'), 1.99 – 1.90 (m, 2H, H-4'), 1.61 – 1.50 (m, 2H, H-3'), 1.42 – 1.29 (m, 1H, H-6'), 0.98 (dtd, $J_{1',7'exo}$=9.3 Hz, $J_{1',7'endo}$=$J_{1',6'}$=5.4 Hz, $J_{1',2'}$=1.4 Hz, 1H, H-1'), 0.84 (td, $J_{7'exo,1'}$=$J_{7'exo,6'}$=9.3 Hz, J_{gem}=5.4 Hz, 1H, H-7'exo), 0.13 (q, J_{gem}=$J_{7'endo,1'}$=$J_{7'endo,6'}$=5.4 Hz, 1H, H-7'endo); **^{13}C-NMR** (100 MHz, $CDCl_3$) δ: 166.8 (C=O), 165.5 (C-4''), 164.1 (C-2''), 163.4 (C=O), 161.9 (C-6''), 134.4/133.3/132.9/130.6/130.1/129.8/129.1/128.9/128.5/128.5 (C-Ar), 115.5 (C-5''), 72.4 (C-5'), 69.7 (C-1), 34.3 (C-2'), 24.1 (C-4'), 20.1 (C-3'), 15.0 (C-6'), 12.8 (C-1'), 12.3 (-CH_3), 9.7 (C-7'); **COSY**, **dept135**, **HSQC** and **HMBC** experiments were recorded.

Physical and spectroscopic data of **73**

$[\alpha]_D^{20}$= -3.1 (*c* 0.85, $CHCl_3$); **^{1}H-NMR** (400 MHz, $CDCl_3$) δ: 8.08 (d, *J*=7.4 Hz, 5H, H-Ar), 7.55 (dd, *J*=8.0 Hz, *J*=5.4 Hz, 2H, H-Ar), 7.41 (dd, *J*=17.6 Hz, *J*=7.9 Hz, 5H, H-Ar), 5.53 (br s, 1H, H-5'), 4.39 (d, $J_{1,2'}$=6.4 Hz, 2H, H-1), 2.16 (dq, $J_{2',3'ax}$=12.3 Hz, $J_{2',1}$=$J_{2',1}$=$J_{2',3'eq}$=6.4 Hz 1H, H-2'), 1.92 – 1.76 (m, 1H, H-4'eq), 1.56 – 1.40 (m, 3H, 2H-3', H-4'ax), 1.37 – 1.20 (m, 1H, H-6'), 1.03 (ddd, $J_{1',7'exo}$=9.3 Hz, $J_{1',6'}$=8.0 Hz, $J_{1',7'endo}$=5.4 Hz, 1H, H-1'), 0.88 (td, $J_{7'exo,1'}$=$J_{7'exo,6'}$=9.3 Hz, J_{gem}=5.4 Hz, 1H, H-7'exo), 0.19 (q J_{gem}=$J_{7'endo,1'}$=$J_{7'endo,6'}$=5.4 Hz, 1H, H-7'endo); **^{13}C-NMR** (100 MHz, $CDCl_3$) δ: 166.9 (C=O), 166.4 (C=O), 133.1/133.0/131.0/130.5/129.7/129.7/128.5/128.5 (C-Ar), 69.8 (C-5'), 69.6 (C-1), 34.2 (C-2'), 24.4 (C-4'), 20.4 (C-3'), 15.2 (C-6'), 12.7 (C-1'), 9.7 (C-7'); **COSY**, **dept135**, **HSQC**, **HMBC** and **NOESY** experiments were recorded; **IR** (ATR): ν 3065, 3005, 2944, 1712, 1267, 1109, 707 (cm^{-1}); **HRMS** (ESI+): Calcd. for $[C_{22}H_{22}O_4]^+$: 350.1518, Found: 350.1520.

3.5.2.2. ((1'*R*,2'*R*,5'*S*,6'*S*)-5'-(1''-Benzoyl-5''-methyl-2'',4''-dioxo-3'',4''-dihydropyrimidin-3''(2*H*)-yl)bicyclo[4.1.0]heptan-2'-yl)methyl benzoate, 74

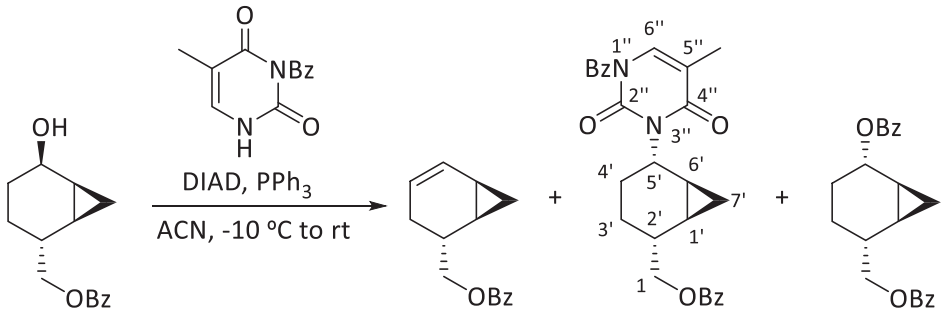

To a suspension of Ph_3P (68 mg, 0.26 mmol) in dry ACN (1.5 mL) at 0 °C, DIAD (53 µL, 0.26 mmol) was slowly added and the mixture was stirred for 30 min at 0 °C. This preformed complex was slowly added to a suspension of the 3-*N*-benzoylthymine (55 mg, 0.24 mmol) and alcohol **16** (42 mg, 0.17 mmol) in dry ACN (1.4 mL) at -10 °C under argon atmosphere. The reaction was warmed to room temperature and stirred overnight. The solvent was removed under vacuum and the resulting crude was purified by column chromatography (hexanes-EtOAc, 5:1) to afford **74** (18 mg, 0.039 mmol, 23% yield) as a white solid, **69** (7 mg, 0.029 mmol, 17% yield) and **73** (9 mg, 0.027 mmol, 16% yield).

Physical and spectroscopic data of **74**

$[\alpha]_D^{20}$= +13.9 (*c* 0.9, $CHCl_3$); **^{1}H-NMR** (400 MHz, $CDCl_3$) δ: 8.05 (dd, *J*=8.4 Hz, *J*=1.3 Hz, 2H, H-Ar), 7.94 (dd, *J*=8.4 Hz, *J*=1.2 Hz, 2H, H-Ar), 7.66 (dddd, *J*=8.7 Hz, *J*=7.1 Hz, *J*=4.3 Hz, *J*=1.2 Hz, 1H, H-Ar), 7.60 – 7.54 (m, 1H, H-Ar), 7.52 – 7.42 (m, 5H, H-Ar, H-6''), 5.07 (dt, $J_{5',4'ax}$=11.7 Hz, $J_{5',6'}$=$J_{5',4'eq}$=5.0 Hz, 1H, H-5'), 4.32 (d, $J_{1,2'}$=6.5 Hz, 2H, H-1), 2.12 (dtd, $J_{2',3ax'}$=10.1 Hz, $J_{2',1}$=6.5 Hz, $J_{2',3eq'}$=4.7 Hz, 1H, H-2'), 1.99 (d, $J_{CH3,4''}$=1.0 Hz, 3H, CH_3), 1.86 (ddt, J_{gem}=16.0 Hz, $J_{4'eq,5'}$=5.0 Hz, $J_{4'eq,3'ax}$=$J_{4'eq,3'ax}$=1.5 Hz 1H, H-4'eq), 1.33 – 1.22 (m, 4H, 2H-3', H-4'ax, H-6'), 1.15 (dtd, $J_{1',7'exo}$=9.4 Hz, $J_{1',7'endo}$=$J_{1',6'}$=5.4 Hz, $J_{1',2'}$=1.5 Hz, 1H, H-1'), 1.05 (td, $J_{7'exo,1'}$=$J_{7'exo,6'}$=9.4 Hz, J_{gem}=5.4 Hz, 1H, H-7'exo), 0.63 (q, J_{gem}=$J_{7'endo,1'}$=$J_{7'endo,6'}$=5.4 Hz, 1H, H-7'endo); **^{13}C-NMR** (100 MHz, $CDCl_3$) δ: 169.4 (C=O), 166.7 (C=O), 162.9 (C-4'), 150.5 (C-2''), 136.6 (C-6''), 135.0/133.3/131.9/130.6/130.2/129.7/129.3/128.6 (C-Ar), 110.5 (C-5''), 69.1 (C-1), 53.2 (C-5'), 34.6 (C-2'), 27.1 (C-4'), 24.3 (C-3'), 14.7 (C-6'), 13.9 (C-1') , 13.0 (-CH_3), 10.4 (C-7'); **COSY**, **dept135** and **HSQC** experiments were recorded; **IR** (ATR): ν 3057, 2991, 2930, 1745, 1714, 1694, 1651, 1437, 1181, 1118, 750, 719, 693 (cm^{-1}).

3.5.2.3. ((1'*R*,2'*R*,5'*S*,6'*S*)-5'-(3''-benzoyl-5''-methyl-2'',4''-dioxo-3'',4''-dihydropyrimidin-1''(2*H*)-yl)bicyclo[4.1.0]heptan-2'-yl)methyl benzoate, 71

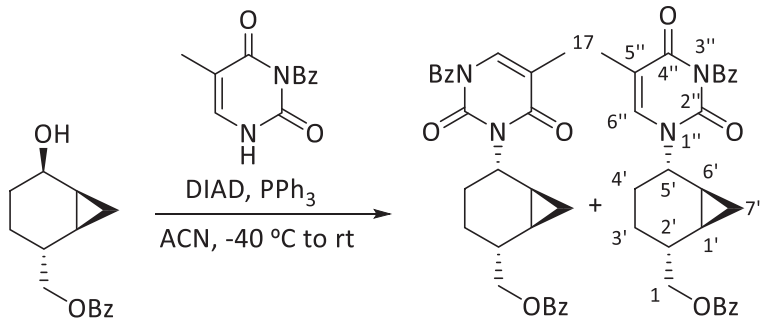

To a suspension of Ph_3P (65 mg, 0.25 mmol) in dry ACN (1.4 mL) at 0 °C, DIAD (51 µL, 0.25 mmol) was slowly added and the mixture was stirred for 30 min at 0 °C. This preformed complex was slowly added to a suspension of the *N3*-benzoylthymine (53 mg, 0.23 mmol) and alcohol **16** (40 mg, 0.16 mmol) in dry ACN (1.4 mL) at -40 °C under argon atmosphere. The reaction was warmed to room temperature and stirred overnight. The solvent was removed under vacuum and the resulting residue was purified by column chromatography (hexanes-EtOAc, 5:1) to furnish **74** (4.9 mg, 0.011 mmol, 7% yield) as a white solid and **71** (4.1 mg, 8.9 µmol, 6% yield) also as a white solid.

Physical and spectroscopic data of **71**

m.p.: 100-103 °C (EtOAc); $[\alpha]_D^{20}$= +59.5 (*c* 0.41, $CHCl_3$); **^{1}H-NMR** (400 MHz, $CDCl_3$) δ: 8.08 (dd, *J*=8.4 Hz, *J*=1.4 Hz, 2H, H-Ar), 7.93 (dd, *J*=8.4 Hz, *J*=1.2 Hz, 2H, H-Ar), 7.64 (ddd, *J*=8.6 Hz, *J*=5.6 Hz, *J'*=1.6 Hz, 1H, H-Ar), 7.60 (ddd, *J*=8.7 Hz, *J*=5.7 Hz, *J*=1.3 Hz, 1H, H-Ar), 7.56 (d, $J_{6'',CH3}$=1.1 Hz, 1H, H-6''), 7.51 (t, *J*=7.0 Hz, 2H, H-Ar), 7.47 (t, *J*=8.1 Hz, 2H, H-Ar), 4.88 (br t, $J_{5',4'ax}$=$J_{5',4'eq}$=4.9 Hz, 1H, H-5'), 4.46 (dd, J_{gem}=8.7 Hz, $J_{1,2'}$=4.4 Hz, 1H, H-1), 4.44 (dd, J_{gem}=8.7 Hz, $J_{1,2'}$=4.4 Hz, 1H, H-1), 2.33 – 2.22 (m, 1H, H-2'), 1.89 (d, $J_{CH3,6''}$=1.1 Hz, 3H, CH_3), 1.81 – 1.69 (m, 1H, H-4'eq), 1.58 – 1.42 (m, 2H, H-3',H-4'ax), 1.38 – 1.19 (m, 2H, H-3', H-6'), 1.06 – 0.94 (m, 2H, H-1', H-7'exo), 0.35 (q, J_{gem}=$J_{7'endo,1'}$=$J_{7'endo,6'}$=5.4 Hz, 1H, H-7'endo); **^{13}C-NMR** (100 MHz, $CDCl_3$) δ: 169.4 (C=O), 166.9 (C=O), 163.0 (C-4''), 150.1 (C-2''), 137.9 (C-6''), 135.1/133.4/131.9/130.6/130.2/129.7/129.3/128.7 (C-Ar), 110.4 (C-5''), 68.7 (C-1), 51.2 (C-5'), 33.2 (C-2'), 24.1 (C-4'), 19.6 (C-3'), 14.4 (C-6'), 12.9/12.8 (C-1', -CH_3), 10.1 (C-7'); **COSY**, **dept135**, **HSQC**, **HMBC** and **NOESY** experiments were recorded; **IR** (ATR): 3280, 3246, 2979, 2922, 2850, 1735, 1667, 1655, 1523, 1251, 1107, 1050 (cm^{-1}).

3.5.3. Stepwise construction of the base moiety

3.5.3.1. ((1'*R*,2'*R*,5'*S*,6'*S*)-5'-Azidobicyclo[4.1.0]hept-2'-yl)methyl benzoate, 75

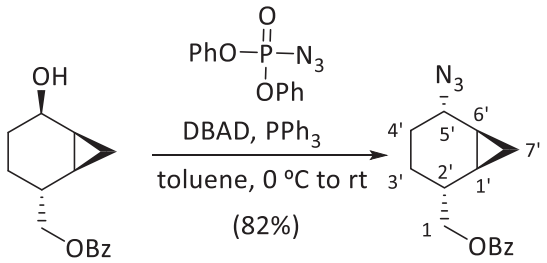

16 **75**

To a stirred suspension of Ph_3P (360 mg, 1.36 mmol) in dry toluene (9 mL), DBAD (313 mg, 1.36 mmol) was slowly added under argon atmosphere and the mixture was stirred for 45 min at 0 °C. After 15 min, a suspension appeared. Then, diphenylphosphoryl azide (216 µL, 0.97 mmol) and a solution of **16** (223 mg, 0.91 mmol) in dry toluene (2 mL) were sequentially added. The mixture was allowed to warm to room temperature and stirred overnight. Then, the solvent was removed and the crude was purified by column chromatography (hexanes-EtOAc, 20:1) to obtain azide **75** (201 mg, 0.74 mmol, 82% yield) as a yellowish syrup.

Physical and spectroscopic data of **75**

$[\alpha]_D^{20}$= -36.2 (*c* 1.01, $CHCl_3$); **^{1}H-NMR** (400 MHz, $CDCl_3$) δ: 8.07 (d, *J*=7.0 Hz, 2H, H-Ar), 7.56 (t, *J*=7.5 Hz, 1H, H-Ar), 7.45 (t, *J*=7.9 Hz, 2H, H-Ar), 4.32 (d, $J_{1,2'}$=6.8 Hz, 2H, H-1), 4.01 (br s, 1H, H-5'), 2.19 – 2.00 (m, 1H, H-2'), 1.70 – 1.58 (m, 1H, H-4'), 1.45 – 1.31 (m, 3H, 2H-3', H-4'), 1.21 – 1.12 (m, 1H, H-6'), 0.99 (dddd, $J_{1',7'exo}$=9.3 Hz, $J_{1',6'}$=7.5 Hz, $J_{1',7'endo}$=5.4 Hz, $J_{1',2'}$=1.3 Hz, 1H, H-1'), 0.85 (td, $J_{7'exo,1'}$=$J_{7'exo,6'}$=9.3 Hz, J_{gem}=5.4 Hz, 1H, H-7'exo), 0.15 (q, J_{gem}=$J_{7'endo,1'}$=$J_{7'endo,6'}$=5.4 Hz, 1H, H-7'endo); **^{13}C-NMR** (100 MHz, $CDCl_3$) δ: 166.8 (C=O), 133.1/130.5/129.7/128.5 (C-Ar), 69.4 (C-1), 57.0 (C-5'), 34.0 (C-2'), 24.5 (C-4'), 20.2 (C-3'), 14.7 (C-6'), 12.6 (C-1'), 9.9 (C-7'); **COSY**, **dept135**, **HSQC**, **HMBC** and **NOESY** experiments were recorded; **IR** (ATR): ν 2925, 2089, 1716, 1270, 1110, (cm^{-1}); **HRMS** (ESI+): Calcd. For $[C_{13}H_{17}N_3O_2]^+$: 271.1321, Found: 271.1324.

3.5.3.2. (1*S*,2*S*,5*R*,6*R*)-5-(benzoyloxymethyl)bicyclo[4.1.0]heptan-2-amonium chloride, 76

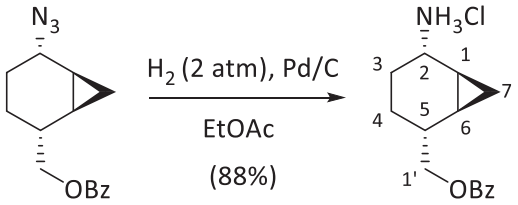

75 **76**

A stirred solution of azide **75** (200 mg, 0.74 mmol) in EtOAc (2.5 mL) at room temperature, was hydrogenated in the presence of 10% Pd/C (20 mg) at 2 atm for 24 h. Then, the mixture was filtered through a short pad of Celite® and washing it with more EtOAc. The solvent was evaporated under reduced pressure and the crude was treated with 2M HCl/Et_2O (1 mL, 2 mmol), stirred for 2h and filtered to furnish the amonium salt **76** (184 mg, 0,65 mmol, 88% yield) as a brown solid.

Physical and spectroscopic data of **76**

m.p.: 130-132 °C (diethyl ether); **[α]$_D^{20}$**= +14.6 (*c* 1.03, $CHCl_3$); **^{1}H-NMR** (400 MHz, $CDCl_3$) δ: 8.69 (s, 3H, NH_3), 8.08 – 7.97 (m, 2H, H-Ar), 7.56 – 7.50 (m, 1H, H-Ar), 7.44 – 7.36 (m, 2H, H-Ar), 4.45 (d, $J_{1',2}$=7.7 Hz, 2H, H-1'), 3.84 (br s, 1H, H-2), 2.15 – 1.89 (m, 2H, H-5, H-4), 1.60 – 1.46 (m, *J*=7.8 Hz, 3H, 2H-3, H-4), 1.31 – 1.22 (m, 1H, H-1), 1.12 – 1.02 (m, 1H, H-6), 0.91 (td, $J_{7exo,1}$=$J_{7exo,6}$=9.1 Hz, J_{gem}=5.5 Hz, 1H, H-7exo), 0.19 (q, J_{gem}=$J_{7endo,1}$=$J_{7endo,6}$=5.5 Hz, 1H, H-7endo); **^{13}C-NMR** (100 MHz, $CDCl_3$) δ: 166.6 (C=O), 133.0/130.4/129.7/128.5 (C-Ar), 69.0 (C-1'), 47.1 (C-2), 33.9 (C-5), 23.2 (C-4), 19.4 (C-3), 14.0 (C-1), 12.5 (C-6), 10.4 (C-7); **COSY**, **dept135**, **HSQC** and **HMBC** experiments were recorded; **IR** (ATR): ν 3404, 2929, 1712, 1273, 1113, 713 (cm^{-1}); **HRMS** (ESI+): Calcd. for $[C_{15}H_{18}NO_2]^+$: 244.1338, Found: 244.1335.

3.5.3.3. 6-chloro-9-((1'*S*,2'*S*,5'*R*,6'*R*)-5'-(benzoyloxymethyl)bicyclo[4.1.0]heptan-2'-yl)-9*H*-purine, 82

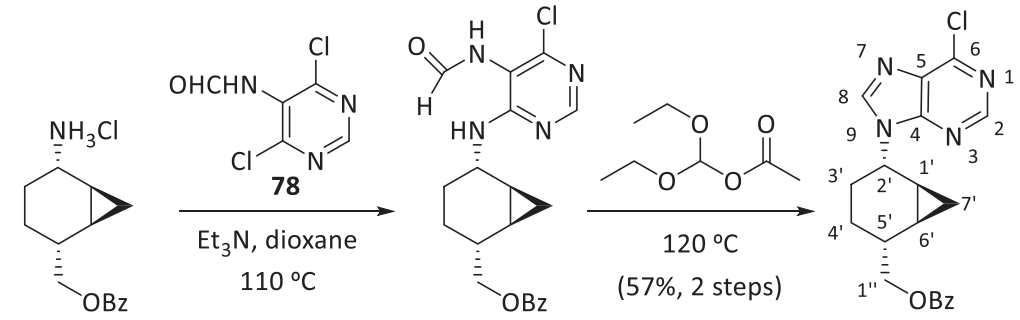

A **76** **81** **82**

solution of compound **76** (20 mg, 0.07 mmol) and *N*-(4,6-dichloropyrimidin-5-yl)formamide, **78**, (17 mg, 0.09 mmol) in 1,4-dioxane (1 mL) was treated with Et_3N (40 µL, 0.23 mmol) and heated at 110 °C overnight. The mixture was evaporated in vacuo, and the residue was extracted with EtOAc (2 mL), washed with brine, dried (Na_2SO_4), filtered, and evaporated in vacuo. The crude **81** was then dissolved in diethoxymethyl acetate (1 mL) and heated at 120 °C for 12 h. After the volatiles were removed in vacuo, the residue was purified by column chromatography (Hexane-EtOAc , 5:1) to afford **82** (16 mg, 0.04 mmol, 57% yield) as a white solid.

3.5.3.3.1. Under microwave irradiation

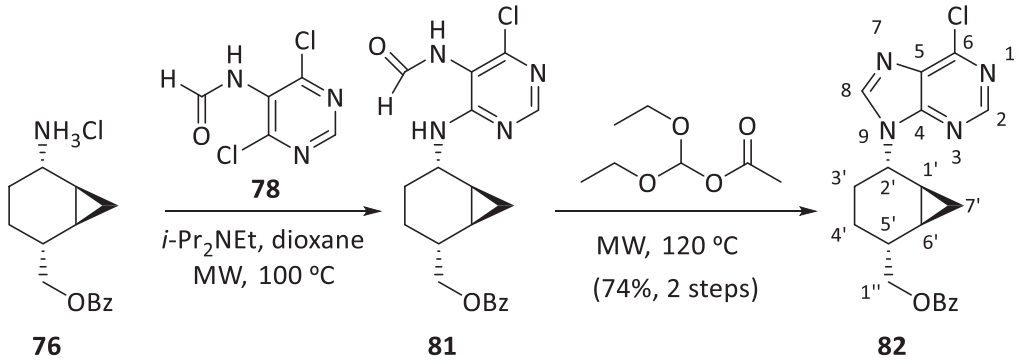

76 **81** **82**

A solution of compound **76** (32 mg, 0.11 mmol) and *N*-(4,6-dichloropyrimidin-5-yl)formamide, **78**, (34 mg, 0.18 mmol) in 1,4-dioxane (0.8 mL) was treated with *i*-Pr_2NEt (110 µL, 0.64 mmol) and heated in a microwave reactor at 100 °C for 40 min. The mixture was evaporated in vacuo, and the residue was extracted with EtOAc (2 mL), washed with brine, dried (Na_2SO_4), filtered, and evaporated in vacuo. The crude **81** was then dissolved in diethoxymethyl acetate (0.8 mL) and heated in a microwave reactor at 120 °C for 120 min. After the volatiles were removed in vacuo, the residue was purified by column chromatography (Hexane-EtOAc , 1:1) to afford **82** (32 mg, 0.084 mmol, 74% yield) as a white solid.

Physical and spectroscopic data of **82**

m.p.: 210-213 °C (EtOAc); $[\alpha]_D^{20}$= +53.1 (*c* 0.39, $CHCl_3$); **^{1}H-NMR** (400 MHz, $CDCl_3$) δ: 8.76 (s, 1H, H-2), 8.50 (s, 1H, H-8), 8.06 (dd, *J*=8.3 Hz, *J*=1.4 Hz, 2H, H-Ar), 7.58 (ddt, *J*=8.7 Hz, *J*=2.6 Hz, *J*=1.3 Hz, 1H, H-Ar), 7.48 (t, *J*=7.6 Hz, 2H, H-Ar), 5.24 (t, $J_{2',3'ax}=J_{2',3'eq}$=3.4 Hz, 1H, H-2'), 4.46 (dd, J_{gem}=11.8 Hz, $J_{1'',5'}$=7.5 Hz, 1H, H-1''), 4.42 (dd, J_{gem}=11.8 Hz, $J_{1'',5'}$=7.5 Hz, 1H, H-1''), 2.30 (dtd, $J_{5',4'ax}$=12.0 Hz, $J_{5',1''}=J_{5',1''}$=7.5 Hz, $J_{5',4'eq}$=5.7 Hz 1H, H-5'), 2.04 – 1.94 (m, 1H, H-3'eq), 1.71 (ddt, J_{gem}=14.5 Hz, $J_{3'ax,4'ax}$=12.3 Hz, $J_{3'ax,2'}=J_{3'ax,4'eq}$=3.4 Hz, 1H, H-3'ax), 1.49 (dtd, J_{gem}=14.5 Hz, $J_{4'eq,3'eq}=J_{4'eq,5'}$=5.7 Hz, $J_{4'eq,3'ax}$=3.4 Hz, 1H, H-4'eq), 1.42 – 1.27 (m, 2H, H-1', H-6'), 1.19 – 1.04 (m, 2H, H-

4'ax, H-7'exo), 0.48 (q, J_{gem}=$J_{7'endo,1'}$=$J_{7'endo,6'}$=5.3 Hz, 1H, H-7'endo); **^{13}C-NMR** (100 MHz, $CDCl_3$) δ: 166.8 (C=O), 152.0 (C-2), 151.6/151.2 (C-6, C-4), 144.4 (C-8), 133.3 (C-Ar), 132.0 (C-5), 130.1/129.7/128.7 (C-Ar), 67.0 (C-1''), 50.9 (C-2'), 33.7 (C-5'), 24.7 (C-3'), 19.8 (C-4'), 14.8 (C-1'), 12.9 (C-6'), 10.4 (C-7'); **COSY**, **dept135**, **HSQC, HMBC** and **NOESY** experiments were recorded; **IR** (ATR): 3064, 2931, 1716, 1590, 1560, 1272, 1115, 714 (cm^{-1}); **HRMS** (ESI+): Calcd. for $[C_{20}H_{19}N_4O_2Cl]^+$: 382.1197, Found: 382.1175.

3.3.1.1. 6-amino-9-((1'*S*,2'*S*,5'*R*,6'*R*)-5'-(hydroxymethyl)bicyclo[4.1.0]heptan-2'-yl)-9*H*-purine, D-2-A

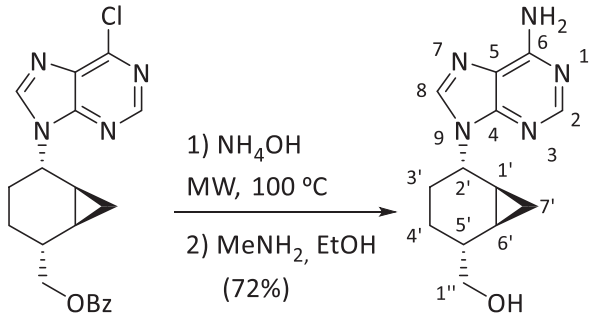

82 D-**2-A**

Compound **82** (11 mg, 28 µmol) was dissolved in a mixture of 1,4-dioxane and NH_4OH (0.5 mL, 1:1, v/v) and heated in a microwave reactor at 100 °C for 40 min. After the volatiles were removed in vacuo, the residue was dissolved in a 33% solution of methylamine in EtOH and stirred overnight. Then, the mixture was concentrated under reduce pressure and purified by column chromatography (CH_2Cl_2-MeOH, 15:1) to provide D-**2-A** (5.3 mg, 20 µmol, 72% yield) as a white solid.

Physical and spectroscopic data of D-**2-A**

m.p.: 226-230 °C (MeOH); **[α]$_D^{20}$**= +73.9 (*c* 0.3, $CHCl_3$); **^{1}H-NMR** (400 MHz, MeOD) δ: 8.49 (s, 1H, H-2), 8.22 (s, 1H, H-8), 5.09 (br t, $J_{2',3'ax}$=$J_{2',3'eq}$=3.5 Hz, 1H, H-2'), 3.68 (dd, J_{gem}=10.7 Hz, $J_{1'',5'}$=5.7 Hz, 1H, H-1''), 3.63 (dd, J_{gem}=10.7 Hz, $J_{1'',5'}$=5.7 Hz, 1H, H-1''), 1.92 (dq, $J_{5',4'ax}$=13.6 Hz, $J_{5',1''}$=$J_{5',1''}$=$J_{5',4'eq}$=5.7 Hz, 1H, H-5'), 1.83 (ddt, J_{gem}=14.5 Hz, $J_{3'eq,4'eq}$=4.0 Hz, $J_{3'eq,2'}$=$J_{3'eq,4'ax}$=3.5 Hz 1H, H-3'eq), 1.66 (ddt, J_{gem}=14.5 Hz, $J_{3'ax,4'ax}$=11.0 Hz, $J_{3'ax,4'eq}$=$J_{3'ax,2'}$=3.5 Hz, 1H, H-3'ax), 1.42 – 1.26 (m, 2H, H-4'eq, H-1'), 1.23 (dddd, $J_{6',7'exo}$=9.3 Hz, $J_{6',1'}$=7.3 Hz, $J_{6',7'endo}$=5.4 Hz, $J_{6',5'}$=1.5 Hz, 1H, H-6'), 1.06 (tdd, J_{gem}=$J_{4'ax,5'}$=13.6 Hz, $J_{4'ax,3'ax}$=11.0 Hz, $J_{4'ax,3'eq}$=3.5 Hz, 1H, H-4'ax), 0.98 (td, $J_{7'exo,1'}$=$J_{7'exo,6'}$=9.3 Hz, J_{gem}=5.4 Hz, 1H, H-7'exo), 0.43 (q, J_{gem}=$J_{7'endo,1'}$=$J_{7'endo,6'}$=5.4 Hz, 1H, H-7'endo); **^{13}C-NMR** (100 MHz, MeOD) δ: 157.1 (C-5), 153.1 (C-8), 150.5 (C-4), 142.4 (C-2), 120.5 (C-6), 67.9 (C-1''), 51.8 (C-2'), 37.9 (C-5'), 25.8 (C-3'), 20.3 (C-4'), 16.1 (C-1'), 14.3 (C-6'), 10.8 (C-7'); **COSY**, **dept135**, **HSQC** and **HMBC** experiments were recorded; **IR** (ATR): ν 3273, 3102, 293,

2882, 2362, 1675, 1601, 1334, 1312 (cm^{-1}); **HRMS** (EI-HR): Calcd. for [$C_{13}H_{17}N_5O$]: 259.1433, Found: 259.1430.

3.3.1.1. 6-chloro-2-formamido-9-((1'*S*,2'*S*,5'*R*,6'*R*)-5'-(benzoyloxymethyl)bicyclo[4.1.0]heptan-2'-yl)-9*H*-purine, 88

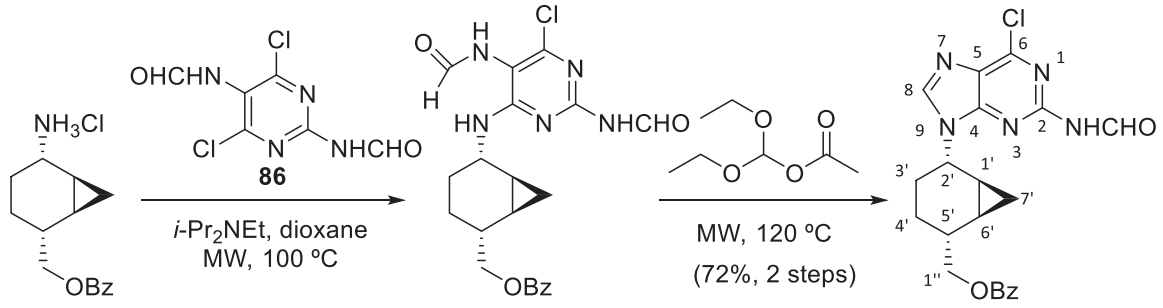

A solution of compound **76** (50 mg, 0.18 mmol) and *N*,*N*'-(4,6-dichloropyrimidine-2,5-diyl)diformamide (46 mg, 0.20 mmol) in 1,4-dioxane (0.9 mL) was treated with *i*-Pr_2NEt (125 µL, 0.71 mmol) and heated in a microwave reactor at 100 °C for 40 min. The mixture was evaporated in vacuo, and the residue was extracted with EtOAc (2 mL), washed with brine, dried (Na_2SO_4), filtered, and evaporated in vacuo. The crude **87** was then dissolved in diethoxymethyl acetate (0.9 mL) and heated in a microwave reactor at 120 °C for 120 min. After the volatiles were removed in vacuo, the residue was purified by column chromatography (CH_2Cl_2-MeOH, 15:1) to afford **88** (54 mg, 0.13 mmol, 72% yield) as a white solid.

Physical and spectroscopic data of **88**

m.p.: 240-243 °C (MeOH); **$[\alpha]_D^{20}$=** +40.5 (*c* 0.6, $CHCl_3$); **^{1}H-NMR** (400 MHz, $CDCl_3$) δ: 9.54 (d, $J_{CHO,NH}$=10.5 Hz, 1H, CHO), 8.29 (s, 1H, H-8), 8.08 (dd, *J*=8.3 Hz, *J*=1.2 Hz, 2H, H-Ar), 7.65 – 7.55 (m, 1H, H-Ar), 7.48 (t, *J*=7.6 Hz, 2H, H-Ar), 5.04 (t, $J_{2',3'ax}$=$J_{2',3'eq}$=4.6 Hz, 1H, H-2'), 4.56 (dd, J_{gem}=10.9 Hz, $J_{1'',5'}$=7.1 Hz, 1H, H-1''), 4.45 (dd, J_{gem}=10.9 Hz, $J_{1'',5'}$=6.3 Hz, 1H, H-1''), 2.34 (dq, $J_{5',4'ax}$=12.7 Hz, $J_{5',4'eq}$=$J_{5',1''}$=$J_{5',1''}$=6.4 Hz, 1H, H-5'), 2.02 – 1.91 (m, 1H, H-3'eq), 1.75 – 1.60 (m, 1H, H-3'ax), 1.50 (dtd, J_{gem}=14.9 Hz, $J_{4'eq,5'}$=$J_{4'eq,3'eq}$=6.4 Hz, $J_{4'eq,3'ax}$=2.9 Hz, 1H, H-4'eq), 1.38 – 1.25 (m, 2H, H-6', H-1'), 1.19 (tdd, J_{gem}=$J_{4'ax,3'ax}$=14.9 Hz, $J_{4'ax,5'}$=12.7 Hz, $J_{4'ax,3'eq}$=3.0 Hz, 1H, H-4'ax), 1.05 (td, $J_{7'exo,1'}$=$J_{7'exo,6'}$=9.4 Hz, J_{gem}=5.4 Hz, 1H, H-7'exo), 0.46 (q, J_{gem}=$J_{7'endo,1'}$=$J_{7'endo,6'}$=5.4 Hz, 1H, H-7'endo); **^{13}C-NMR** (100 MHz, $CDCl_3$) δ: 166.9 (C=O), 162.7 (-NH**C**HO), 152.5 (C-6), 151.9 (C-2), 151.8 (C-4), 143.8 (C-8), 133.4 (C-Ar), 130.1 (C-5), 129.8/129.4/128.7 (C-Ar), 68.9 (C-1''), 51.1 (C-2'), 33.2 (C-5'), 24.3 (C-3'), 19.7 (C-4'), 14.7 (C-1'), 13.0 (C-6'), 10.2 (C-7'); **COSY**,

dept135 and **HSQC** experiments were recorded; **IR** (ATR): ν 3214, 3111, 2922, 1714, 1695, 1262, 1236, 1202 (cm^{-1}); **HRMS** (ESI+): Calcd. for $[C_{21}H_{20}N_5O_3Cl]^+$: 425.1255, Found: 425.1235.

3.3.1.2. 2-amino-9-((1'*S*,2'*S*,5'*R*,6'*R*)-5'-(hydroxymethyl)bicyclo[4.1.0]heptan-2'-yl)-1,9-dihydro-6*H*-purin-6-one, D-2-G

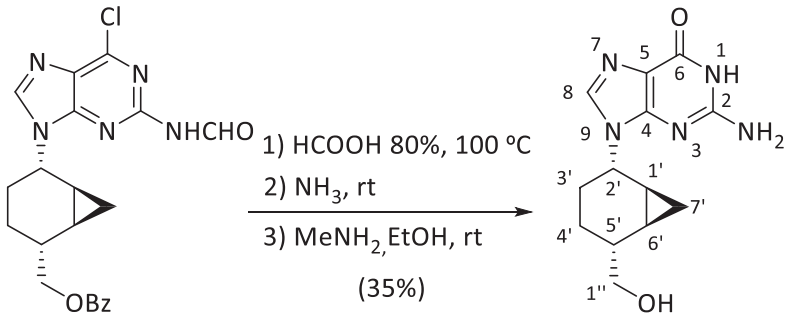

88 D-**2-G**

A solution of **88** (10 mg, 24 µmol) in 80% HCOOH (0.5 mL) was stirred at 100 °C for 1h. The solution was cooled, the solvent removed, and the residue coevaporated with water. The residue was dissolved in concentrated aqueous ammonia (0.5 mL) and stirred at room temperature for 1 h. The solvent was removed in vacuo and the residue coevaporated with toluene. The residue was dissolved in a 33% solution of methylamine in EtOH (6 mL) and stirred overnight. Then, the mixture was concentrated under reduce pressure and purified by column chromatography (CH_2Cl_2-MeOH, 15:1) to provide D-**2-G** (2.3 mg, 8.4 µmol, 35% yield) as a brown solid.

Physical and spectroscopic data of D-**2-G**

m.p.: 233-236 °C (MeOH); **$[\alpha]_D^{20}$=** +65.6 (*c* 0.89, $CHCl_3$); **^{1}H-NMR** (400 MHz, MeOD) δ: 8.04 (s, 1H, H-8), 4.86 (m, 1H, H-2'), 3.65 (dd, J_{gem}=10.7 Hz, $J_{1'',5'}$=5.9 Hz, 1H, H-1''), 3.61 (dd, J_{gem}=10.7 Hz, $J_{1'',5'}$=6.0 Hz, 1H, H-1''), 1.89 (dq, $J_{5',4'ax}$=10.7 Hz, $J_{5',1''}$=$J_{5',1''}$=$J_{5',4'eq}$=6.1 Hz, 1H, H-5'), 1.81 (dq, J_{gem}=13.8 Hz, $J_{3'eq,2'}$=$J_{3'eq,4'ax}$=$J_{3'eq,4'ax}$=3.8 Hz, 1H, H-3'eq), 1.57 (tt, J_{gem}=$J_{3'ax,4'ax}$=13.8 Hz, $J_{3'ax,4'eq}$=$J_{3'ax,2'}$=3.4 Hz, 1H, H-3'ax), 1.40 – 1.22 (m, 2H, H-1', H-4'eq), 1.18 (dddd, $J_{6',7'exo}$=9.3 Hz, $J_{6',1'}$=7.6 Hz, $J_{6',7'endo}$=5.4 Hz, $J_{6',5'}$=1.6 Hz, 1H, H-6'), 1.06 (tdd, J_{gem}=$J_{4'ax,3'ax}$=13.8 Hz, $J_{4'ax,5'}$=10.7 Hz, $J_{4'ax,3'eq}$=3.1 Hz, 1H, H-4'ax), 0.94 (td, $J_{7'exo,1'}$=$J_{7'exo,6'}$=9.3 Hz, J_{gem}=5.4 Hz, 1H, H-7'exo), 0.36 (q, J_{gem}=$J_{7'endo,1'}$=$J_{7'endo,6'}$=5.4 Hz, 1H, H-7'endo); **^{13}C-NMR** (100 MHz, MeOD) δ: 159.5 (C-6), 155.1 (C-2), 152.7 (C-4), 138.8 (C-8), 117.7 (C-5), 67.8 (C-1''), 51.0 (C-2'), 37.7 (C-5'), 25.4 (C-3'), 20.1 (C-4'), 15.8 (C-1'), 13.9 (C-6'), 10.5 (C-7'); **COSY**, **dept135**, **HSQC**, **HMBC** and **NOESY** experiments were recorded; **IR** (ATR): ν 3400, 3098, 2361, 2341, 1680, 1648, 1600 (cm^{-1}); **HRMS** (ESI+): Calcd. for $[C_{13}H_{17}N_5O_2+H]^+$: 276.1455, Found: 276.1455.

3.3.1.3. 1-((1'*S*,2'*S*,5'*R*,6'*R*)-5'-(hydroxymethyl)bicyclo[4.1.0]heptan-2'-yl)pyrimidine-2,4(1*H*,3*H*)-dione, D-**2-U**

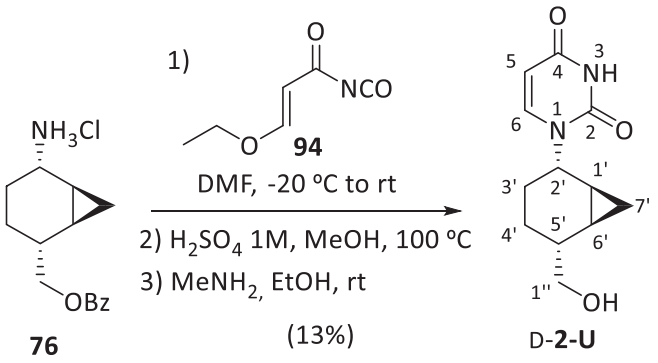

Sylver cyanate (86 mg, 0.57 mmol), previously dried over phosphorus pentoxide at 80 °C for 3h, in dry benzene (2 mL) was heated to reflux for 30 min and a solution of (2*E*)-3-ethoxyacryloyl chloride **92** (39 mg, 0.28 mmol) in dry benzene (0.8 mL) was then added dropwise. The mixture was stirred for 30 min before allowing the solid to settle out. The supernatant, which is a solution of the isocyanate **94**, was then decanted and used directly in the next reaction.

The ammonium chloride **76** (50 mg, 0.18) was dissolved in dry DMF (1.8 mL) and Et_3N (25 µL, 0.18 mmol) was added. The mixture was cooled to -20 °C and the supernatant was added slowly enough to avoid an increase on the temperature, and the reaction mixture was stirred overnight at room temperature. The solvent was evaporated in vacuo, and then water (2 mL) was added and the residue was extracted with EtOAc (2 x 2 mL), washed with brine, dried (Na_2SO_4), filtered, and evaporated in vacuo. The residue was dissolved in MeOH (0.42 mL), H_2SO_4 (1M, 0.76 mL) was added and the mixture was heated to reflux for 3 h. After the volatiles were removed in vacuo, the residue was dissolved in a 33% solution of methylamine in EtOH (27 mL) and stirred overnight. Then, the mixture was concentrated under reduce pressure and purified by column chromatography (CH_2Cl_2-MeOH, 15:1) to provide nucleoside analogue D-**2-U** (5.4 mg, 23 µmol, 13% yield) as a yellowish solid.

Physical and spectroscopic data of D-**2-U**

m.p.: 228-231 °C (MeOH); $[\alpha]_D^{20}$= +23.4 (*c* 0.13, MeOD); **^{1}H-NMR** (400 MHz, MeOD) δ: 8.05 (d, $J_{6,5}$=8.0 Hz, 1H, H-6), 5.69 (d, $J_{5,6}$=8.0 Hz, 1H, H-5), 4.86 – 4.79 (m, 1H, H-2'), 3.65 (dd, J_{gem}=10.7 Hz, $J_{1'',5'}$=5.8 Hz, 1H, H-1''), 3.60 (dd, J_{gem}=10.7 Hz, $J_{1'',5'}$=5.8 Hz, 1H, H-1''), 1.86 (dq, $J_{5',4'ax}$=11.3 Hz, $J_{5',1''}$=$J_{5',1''}$=$J_{5',4'eq}$=5.9 Hz, 1H, H-5'), 1.73 – 1.62 (m, 1H, H-3'eq), 1.56 – 1.42 (dddd, J_{gem}=14.5 Hz, $J_{3'ax,4'ax}$=12.3 Hz, $J_{3'ax,4'eq}$=4.1 Hz, $J_{3'ax,2'}$=3.2 Hz, 1H, H-3'ax), 1.38 – 1.30 (m, 1H, H-4'eq), 1.25 – 1.10 (m, 2H, H-4'ax, H-1'), 1.07 – 0.96 (m, 1H, H-6'), 0.89 (dt, $J_{7'exo,6'}$=$J_{7'exo,1'}$=9.3 Hz, J_{gem}=5.2 Hz,

1H, H-7'exo), 0.31 (q, $J_{gem}=J_{7'endo,1'}=J_{7'endo,6'}$=5.2 Hz, 1H, H-7'endo); **^{13}C-NMR** (100 MHz, MeOD) δ: 165.0 (C-4), 151.4 (C-2), 144.0 (C-6), 99.9 (C-5), 66.0 (C-1''), 51.1 (C-2'), 35.8 (C-5'), 23.1 (C-3'), 18.2 (C-4'), 13.8 (C-1'), 12.4 (C-6'), 8.8 (C-7'); **COSY**, **dept135**, **HSQC** and **HMBC** experiments were recorded; **IR** (ATR): ν 3393, 2925, 2361, 2341, 1678, 1260, 630 (cm^{-1}); **HRMS** (ESI+): Calcd. for $[C_{12}H_{16}N_2O_3+Na]^+$: 259.1053, Found: 259.1074.

3.3.1.4. Ethyl (*E*)-(3-ethoxy-2-methylacryloyl)carbamate, 101

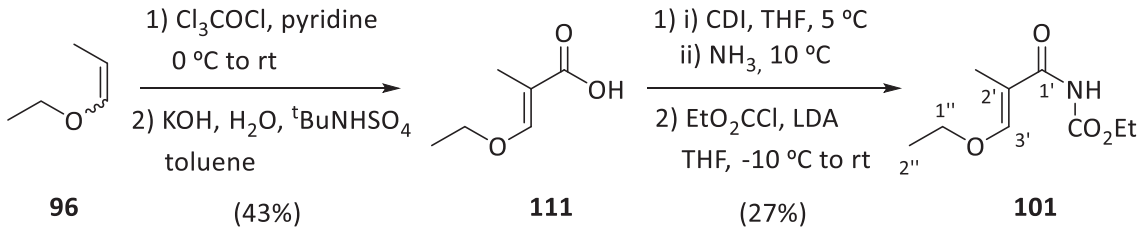

A mixture of **96** (0.5 mL, 4.43 mmol) and pyridine (360 µL, 4.43 mmol) was added to a cooled solution of trichloroacetyl chloride (0.5 mL, 4.43 mmol) in $CHCl_3$ (2.2 mL) at such a rate to keep the reaction temperature between 0-3 °C. After addition, the reaction was allowed to warm to room temperature and stirred for 16 h. Water (2 mL) was then added cautiously and the mixture was stirred for 5 min. The layers were separated and the aqueous phase was extracted with $CHCl_3$ (2 x 2 mL). The combined organic phases were successively washed with 0.1 M HCl (6 mL), 0.1 M KOH (6mL) and water (6 mL) and concentrated under reduced pressure. Then, water (0.11 mL) and tetrabutylammonium sulphate (406 g, 1.33 mmol) were added to a cooled mixture of the crude and KOH (175 mg, 2.66 mmol) on toluene (2.2 mL), and heated to 90 °C for 2 h. Afterwards, the reaction was cooled and extracted with water (2 mL) and diluted KOH (2 mL). The aqueous layers were washed with toluene (4 mL), combined and acidified with 5 M HCl (1 mL). The suspension was extracted with EtOAc (4 mL) and the combined extracts were washed with brine (4 mL) and stirred with charcoal. The mixture was then filtered through celite® and the filtrate evaporated to obtain carboxylic acid **111** which was used in the next step without further purification.

1,1'-Carbonyldiimidazole (CDI) (371 mg, 2.29 mmol) was added portionwise to a solution of **X100** (248 mg, 1.91 mmol) in THF (1.5 mL) at 5 °C. After 1 h, concentrated aqueous NH_3 (1 mL, 17.6 mmol) was added and the reaction stirred at 10 °C for a further 1 h. The reaction was then cooled to 5 °C and diluted with EtOAc (2 mL). The reaction was adjusted to pH 3.5 by the addition of 6 M HCl at such rate to maintain the temperature below 15 °C. The phases were

separated and the aqueous phase extracted with more EtOAc (3 x 2 mL). The combined organic layers were dried and evaporated to afford the corresponding amide which was used in the next step without further purification.

EtO_2CCl (0.56 mL, 5.72 mmol) was added over period of 15 min to a solution of the above residue and LDA (2.65 mL, 4.77 mmol) in THF (7 mL) at -10 °C under N_2 atmosphere. After 1h at -10 °C, the reaction mixture was allowed to warm to room temperature, stirred for a further 1 h and then quenched with aqueous NH_4Cl. The solution was extracted with EtOAc (2 x 7 mL) and the combined extracts were dried and evaporate. The residue was crystallised from EtOAc to afford **101** (105 mg, 0.56 mmol, 12% overall yield) as a white solid.

Spectroscopic data of **101**

^{1}H-NMR (400 MHz, $CDCl_3$) δ: 7.38 (q, $J_{3',CH3}$=1.2 Hz, 1H, H-3'), 4.25 (q, $J_{1'',2''}$=7.1 Hz, 2H, H-1''), 4.07 (q, $J_{1,2}$=7.1 Hz, 2H, H-1), 1.79 (d, $J_{CH3,3'}$= 1.2 Hz, 3H, -CH_3), 1.33 (t, $J_{2'',1''}$=7.1 Hz, 3H, H-2''), 1.32 (t, $J_{2,1}$=7.1 Hz, 3H, H-2).

3.3.1.5. 1-((1'*S*,2'*S*,5'*R*,6'*R*)-5'-(hydroxymethyl)bicyclo[4.1.0]heptan-2'-yl)-5-methylpyrimidine-2,4(1*H*,3*H*)-dione, D-2-T

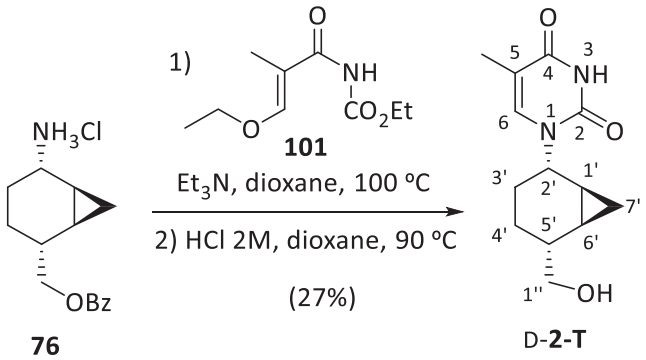

A solution of ammonium chloride **76** (50 mg, 0.18 mmol), ethyl carbamate **101** (36 mg, 0.18 mmol) and Et_3N (26 µL, 0.19 mmol) in 1,4-dioxane (0.5 mL) was heated at 100 °C for 3 h. The suspension was cooled, filtered and the collected solid was washed with more 1,4-dioxane (2 x 2.5 mL). The filtrates were combined, HCl 2M (5.6 mL) was added and the solution was heated to 90 °C overnight. The solution was extracted with CH_2Cl_2 (3 x 5 mL) and the combined extracts were dried and evaporated under reduced pressure. The crude was purified by column chromatography (EtOAc-MeOH, 20:1) to afford nucleoside analogue D-**2-T** (12.1 mg, 48 µmol, 27% yield) as a pale yellow syrup.

Physical and spectroscopic data of D-**2-T**

$[\alpha]_D^{20}$= +44.3 (*c* 0.72, $CHCl_3$); **^{1}H-NMR** (400 MHz, MeOD) δ: 7.92 (q, $J_{6,CH3}$=1.2 Hz, 1H, H-6), 4.80 (ddddd, $J_{2',3'ax}$=4.7 Hz, $J_{2',3'eq}$=4.1 Hz, $J_{2',1'}$=1.8 Hz, $J_{2',4'}$=1.1 Hz, $J_{2',4'}$=0.5 Hz, 1H, H-2'), 3.69 (dd, J_{gem}=10.7 Hz, $J_{1'',5'}$=5.3 Hz, 1H, H-1''), 3.61 (dd, J_{gem}=10.7 Hz, $J_{1'',5'}$=5.0 Hz, 1H, H-1''), 1.91 (d, $J_{CH3,6}$=1.2 Hz, 3H, -CH_3), 1.92 – 1.82 (m, 1H, H-5'), 1.66 (dq, J_{gem}=14.5 Hz, $J_{3'eq,2'}$=$J_{3'eq,4'ax}$=$J_{3'eq,4'eq}$=4.1 Hz, 1H, H-3'eq), 1.49 (ddt, J_{gem}=14.5 Hz, $J_{3'ax,4'ax}$=13.8 Hz, $J_{3'ax,4'eq}$=$J_{3'ax,2'}$=4.7 Hz, 1H, H-3'ax), 1.34 – 1.23 (m, 2H, H-4'), 1.18 (dddd, $J_{1',7'exo}$=9.4 Hz, $J_{1',6'}$=7.2 Hz, $J_{1',7'endo}$=5.3, $J_{1',2'}$=1.8 Hz, 1H, H-1'), 1.09 – 0.98 (m, 1H, H-6'), 0.89 (td, $J_{7'exo,6'}$=$J_{7'exo,1'}$=9.4 Hz, J_{gem}=5.3 Hz, 1H, H-7'exo), 0.30 (q, J_{gem}=$J_{7'endo,1'}$=$J_{7'endo,6'}$=5.3 Hz, 1H, H-7'endo); **^{13}C-NMR** (100 MHz, MeOD) δ: 166.6 (C-4), 153.0 (C-2), 141.5 (C-6), 110.1 (C-5), 67.3 (C-1''), 52.2 (C-2'), 37.0 (C-5'), 24.5 (C-3'), 19.6 (C-4'), 15.5 (C-1'), 14.0 (C-6'), 12.4 (-CH_3), 10.2 (C-7'); **COSY**, **dept135**, **HSQC** and **HMBC** experiments were recorded; **IR** (ATR): ν 3398, 3194, 3024, 2928, 2873, 2360, 2341, 1654, 1467, 1257 (cm^{-1}); **HRMS** (ESI+): Calcd. for $[C_{13}H_{18}N_2O_3Na]^+$: 273.1210, Found: 273.1193.

4. Study of antiviral activity of prodrug candidates

4.1. Activation process and DNA Polymerase interaction

Table VII-4. Predicted binding energies (score units) of synthesised compounds.

Compounds		Activation process			DNA polymerase
		OH → OMP	OMP → ODP	ODP → OTP	OTP
ACV	Binding energy	**-63.4**	**-86.7**	**-78.8**	**-91.4**
	Best pose	**-52.9**	**-86.7**	**-76.6**	**-91.4**
D-**2-A**	Binding energy	-63.5	-88.3	-78.6	-94.7
	Best pose	-63.5	-88.3	-76.2	-91.8
D-**2-G**	Binding energy	-70.1	-96.2	-79.9	-100
	Best pose	-66	-92.8	-79.9	-100
dT	Binding energy	**-69.8**	**-72.7**	**-93.9**	**-84.8**
	Best pose	**-69.8**	**-67.6**	**-89.3**	**-84.8**
D-**2-T**	Binding energy	-72.6	-80.4	-92.5	-91.8
	Best pose	-72.6	-79	-92.5	-91.8
D-**2-U**	Binding energy	-66.5	-74.2	-	-85.2
	Best pose	-62.3	-71.2	-	-82.9

5. References

(1) Klopman, G.; Li, J.; Wang, S.; Dimayugat, M. *J. Chem. Inf. Comput. Sci.* **1994**, *34*, 752–781.

(2) Viswanadhan, V. N.; Ghose, A. K.; Reyankar, G. R.; Robins, R. K. *J. Chem. Inf. Comput. Sci.* **1989**, *29*, 163–172.

(3) Tachihara, T.; Kitahara, T. *Tetrahedron* **2003**, *59*, 1773–1780.

(4) Jones, A. B.; Yamaguchi, M.; Patten, A.; Danishefsky, S. J.; Ragan, J. A.; Smith, D. B.; Schreiber, S. L. *J. Org. Chem.* **1989**, *54*, 17–19.

(5) Danishefsky, S. J.; Simoneau, B. *J. Am. Chem. Soc.* **1989**, *111*, 2599–2604.

(6) O'Byrne, A.; Murray, C.; Keegan, D.; Palacio, C.; Evans, P.; Morgan, B. S. *Org. Biomol. Chem.* **2010**, *8*, 539–545.

(7) Kitahara, Takeshi; Kurata, Hitoshi; Mori, K. *Tetrahedron* **1989**, *44*, 4339–4349.

(8) Kawasumi, M.; Kanoh, N.; Iwabuchi, Y. *Org. Lett.* **2011**, *13*, 3620–3623.

(9) Gais, H. J.; Jagusch, T.; Spalthoff, N.; Gerhards, F.; Frank, M.; Raabe, G. *Chem. - A Eur. J.* **2003**, *9*, 4202–4221.

(10) Touge, T.; Hakamata, T.; Nara, H.; Kobayashi, T.; Sayo, N.; Saito, T.; Kayaki, Y.; Ikariya, T. *J. Am. Chem. Soc.* **2011**, *133*, 14960–14963.

(11) Sundararaman, P.; Barth, G.; Djerassi, C. *J. Org. Chem.* **1980**, *45*, 5232–5236.

(12) Starodubtseva, E. V.; Turova, O. V.; Vinogradov, M. G.; Gorshkova, L. S.; Ferapontov, V. A.; Struchkova, M. I. *Tetrahedron* **2008**, *64*, 11713–11717.

Chapter VIII: Computational methods

The present chapter is devoted to provide a brief description of the molecular modelling techniques used in this dissertation, including the mathematical details and principles.

1. Molecular modelling

As stated in Chapter III, molecular modelling encompasses all theoretical methods and computational techniques used to model or mimic the behaviour of molecules. The computational methods can be split into two categories: molecular mechanics (MM) and quantum mechanics (QM). MM methods use equations based on classical physics to calculate force fields and apply them to nuclei without considering the electrons. Thus, molecules are treated as charged spheres (atoms) joined together by springs (bonds). By contrast, quantum mechanics use equations based on quantum physics to calculate the properties of a molecule taking into account both the nuclei and the electrons. As a result, models based on QM are more accurate than those based on MM but also required more computer time. Thus, QM methods are restricted to small systems (up to hundreds of atoms) whereas MM methods are used for large systems (up to millions of atoms).

The next sections aim at establishing the basic elements of those MM and QM methods most widely used in molecular modelling.

1.1. Molecular mechanics

MM embraces an ensemble of widely used methodologies that share the same approximation: atoms are considered as solid spheres with physical properties interacting with each other following the laws of classical physics.

Force fields (ff) are a set of parameters and equations derived from classical physics, which are used in MM approaches to calculate the potential energy of the system. Many of the force fields in use today consider that the potential energy V_{pot} of a system is composed by the potential energy from bonded and non-bonded interactions (1)

$$V_{pot} = V_{bonded} + V_{non-bonded} \quad (1)$$

where V_{pot} is the potential energy of a system, V_{bonded} the energy associated with bonded interactions and $V_{non\text{-}bonded}$ the energy related to non-covalent terms.

Bonded terms

The bonded term accounts for the interactions between the atoms that are directly linked. The potential energy is generally defined as a sum of four terms: bond stretching (V_{bond}), angle bending (V_{angle}), dihedral torsions ($V_{dihedral}$) and improper torsions ($V_{improper}$) (2).

$$V_{bonded} = V_{bond} + V_{angle} + V_{dihedral} + V_{improper} \quad (2)$$

All the bonded terms are represented in Figure VIII-1.

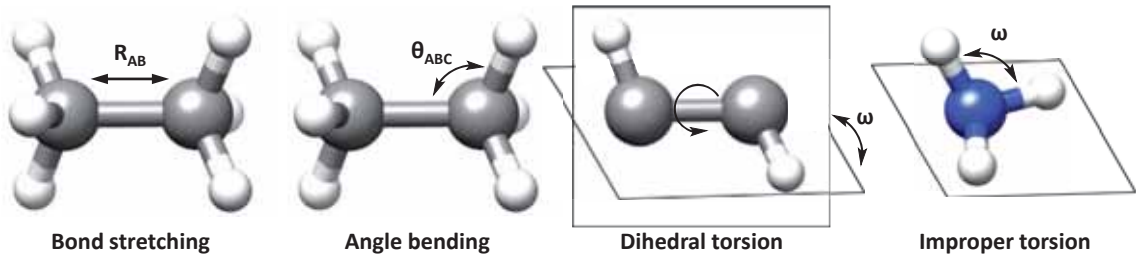

Figure VIII-1. Schematic representation of the four bonded terms to calculate the potential energy of a system in MM.

- ***Bond stretching (V_{bond})***. This term models the interaction between pairs of bonded atoms A-B, which vibrates around an equilibrium bond length ($R_{e,AB}$) using a harmonic function (3).

$$V_{bond} = \sum_{bonds} \frac{k_{AB}}{2}\left(R_{AB} - R_{e,AB}\right)^2 \quad (3)$$

  Here k_{AB} is the bond-stretching force constant, R_{AB} the instantaneous bond length and $R_{e,AB}$ the reference (equilibrium) value.

- ***Angle bending (V_{angle})***. This term is a sum of all valence angles in the molecule, again using a harmonic function. A valence angle is the angle formed between three atoms A-B-C, θ_{ABC}, which vibrates around an equilibrium value $\theta_{e,ABC}$ (4).

$$V_{angle} = \sum_{angles} \frac{k_{ABC}}{2}\left(\theta_{ABC} - \theta_{e,ABC}\right)^2 \quad (4)$$

- ***Dihedral torsions ($V_{dihedral}$)***. This term is a torsional potential that models how the energy changes as a bond rotates. To represent this bond rotation, dihedral angles between four bonded atoms A-B-C-D are used, using a periodic function to describe the potential energy (5).

$$V_{dihedral} = \sum_{torsions} \frac{V_n}{2}(1 + \cos(n\omega - \gamma)) \quad (5)$$

Here ω accounts for the actual A-B-C-D angle, n for the periodicity, γ for the equilibrium torsional angle (indicating where ω passes through a minimum) and V_n for the torsional barrier.

- ***Improper torsions ($V_{improper}$)***. Often it is necessary to consider also the out-of-plane potential term. There are several ways in which out-of-plane bending terms can be incorporated into a force field. One approach is based on improper dihedral angles. These angles are dihedrals where the rotation is limited. A torsional potential of the form described in equation (6) is used to maintain the improper torsion angle at 0º or 180º.

$$V_{improper} = k(1 - \cos 2\omega) \tag{6}$$

Non-bonded terms

The non-bonded term, also called non-covalent, accounts for the interactions between atoms that are not directly connected. The non-bonded potential energy is calculated for all pairs of atoms (A and B) that are in different molecules or in the same molecule but separated by at least three bonds. This energy is described as a sum of the van der Waals (V_{vdw}) and electrostatic (V_{el}) interactions (7).

$$V_{non-bonded} = V_{vdw} + V_{el} \tag{7}$$

- ***Van der Waals interactions (V_{vdw}).*** This term is the total energy contribution due to attractive and repulsive forces between two atoms approximating each other without forming a covalent bond. Attractive forces act at long distances and represent London dispersion forces, whereas the repulsive contribution is at short distances. These forces are commonly described using a *Lennard-Jones potential* (8)

$$V_{vdw} = \sum_{A}^{N} \sum_{B}^{N} \varepsilon \left[\left(\frac{r_{min}}{r_{AB}} \right)^{12} - 2 \left(\frac{r_{min}}{r_{AB}} \right)^{6} \right] \tag{8}$$

Here r_{min} is the distance between two atoms A and B when the energy is at a minimum potential, r_{AB} is the observable distance between A and B, and ε is the potential well depth.

- ***Electrostatic interactions (V_{el})***. The electrostatic term is calculated using the *Coulomb electrostatic law*. Equation (9) shows the Coulomb electrostatic potential between two atoms A and B, where atomic charges Q_A and Q_B are assigned according to the rules of the particular force field.

$$V_{el} = \sum_{A}^{N} \sum_{B}^{N} \frac{Q_A Q_B}{4\pi\varepsilon_0 r_{AB}} \quad (9)$$

Here Q_A and Q_B are the point charges of atoms *A* and *B*, r_{AB} is the distance between both atoms and ε_0 is the dielectric constant of the medium surrounding the charges.

Many force fields have been developed and nowadays it is widely accepted that they are accurate enough for the application in the biomolecular field.

2. Protein–ligand docking

Protein–ligand docking aims at predicting the most favoured ligand orientations when it is bound to a given target protein and estimate the binding affinity. The free energy associated to the binding process can be easily calculated by the Law of mass action (10)

$$\Delta G_{binding} = -RTlnK_{eq} \quad (10)$$

Where K_{eq} is the equilibrium constant associated to the binding process.

$$K_{eq} = \frac{[Complex]}{[Protein][Ligand]} \quad (10)$$

Docking protocols can be split into two different algorithm: a search algorithm, which is related to the conformational search, and a scoring function, which calculates the energy of the binding.[1–5]

2.1. Search algorithms

The search algorithm explores the conformational space available to the ligand in the binding site and generates all the possible orientations of protein-ligand complexes. As there are a huge number of degrees of freedom associated with both the ligand and the receptor, some approximations have to be applied in order to perform an effective sampling. Depending on which approximations are applied, search algorithms can be classified into three main groups: rigid-body, flexible-ligand and flexible-protein docking.

Rigid ligand docking is almost not currently used since treats both the ligand and the protein as rigid, only considering the translational and rotational degrees of freedom. The search algorithms used in rigid-body dockings are based on matching characteristic features of

the molecules in space in order to fit the ligand into the binding site. A more detailed description of these search algorithms may be found in the corresponding literature.[5]

Flexible-ligand docking considers a full or partial flexibility of the ligand. The main algorithms are divided into three general categories: systematic methods, random or stochastic methods, and simulation methods.[1–5]

2.1.1. Systematic methods

Systematic search algorithms try to explore most conformational degrees of freedom of the ligand and can be further divided into three main types: conformational search methods, fragmentation methods and database methods.

Conformational search methods

These methods are based on systematically rotating all rotatable bonds in the ligand through 360º using a fixed increment, until all possible combinations have been generated and evaluated. The major drawback is that a huge number of rotatable bonds increases the number of structures produced (combinatorial explosion). Thus, the application of these methods is very limited.

Fragmentation methods

This is one of the most commonly used approaches to tackle ligand flexibility. In this method, the ligand is somehow divided into small pieces, called fragments, which can be treated as conformationally rigid or by a small conformational ensemble. There are two strategies for handling the fragments: either by placing one fragment in the binding site and subsequently adding the remaining fragments (*incremental construction approach*, IC), or by placing all fragments into the binding site and try to reconnect them until they constitute a complete ligand (*place-and-join approach*). FlexX[6] and DOCK[7] are examples of docking programs that use a fragmentation search method.

Database methods

Database methods deal with the combinatorial explosion by using libraries of ligand conformations previously generated. An example of a docking program that makes use of this type of approximation is FLOG.[8]

2.1.2. Random methods

Random search algorithms sample the conformational space by performing random changes to one or more ligands. The alteration performed at each step is accepted or rejected

according to a predefined probability function. There are four basic types of random algorithms: Monte Carlo (MC), Tabu Search (TS), Swarm Optimization methods (SO) and Genetic Algorithms (GA). The Genetic Algorithms are implemented in the molecular docking program used in the present dissertation, GOLD[9] (Genetic Optimization for Ligand Docking).

Monte Carlo methods

Monte Carlo methods explore the thermodynamically accessible states of a system by generating small random changes in the system that are either accepted or rejected according to a Boltzmann probability function. This function depends on the difference in the energy score of the ligand before and after the random change. Examples of programs that use MC methods are DockVision[10] and ICM.[11]

Tabu search methods

Tabu search methods impose restrictions that prevent the search from revisiting previously explored areas of the conformational space. These methods start with an initial structure and generate new orientations by random moves, storing them in a list (tabu list). Thus, an alteration will be rejected if the resulting orientation is close to one already present in the tabu list, except if its scoring is better than the best scoring in the list. An example off docking program which uses a TS algorithm is PRO_LEADS.[12]

Swarm optimization methods

Similarly to the above described random methods, swarm optimization (SO) algorithms generate an ensemble of orientations that are randomly located in different regions of the search space. SO methods are bio-inspired, and the initial set of orientations represents a population of birds. Then, mimicking the movement of a swarm of birds when one of them finds food, the orientations are distorted so that they move through the search space in the direction of the fittest individuals (i.e. the best scored orientations) of this population. These movements are repeated until the scoring function converges.

Some examples of programs that have implemented a SO method are PLANTS[13] and a variation of the AutoDock program, PSO@AutoDock.[14]

Genetic algorithm methods

Genetic algorithms[15–17] apply ideas derived from genetics and the theory of biological evolution to docking. Starting from an initial population of different orientations of the ligand in the binding site, generic operators such as crossovers, mutations and migrations are applied

to the population in order to sample the conformational space until a final population that optimises a predefined fitness function is reached.

The general optimization scheme of genetic algorithms, which simulates the process of evolution, consists of three main steps:

- *Generation of the initial population* (step 1). An initial population of orientations of the ligand in the binding site is generated.
- *Fitness evaluation and parent selection* (step 2). The fitness function is used to decide which conformation survive and produce offspring. Thus, each orientation is initially scored and a selection scheme is subsequently applied to make sure that the best scored orientations have more opportunities to reproduce.
- *Breeding* (step 3). Genetic operators such as crossover, mutation and migration are used to provide the next generation of orientations.

Steps 2 and 3 are then repeated to score children, who will replace the least-fit members of the population, and produce the next offspring generation. Iteration of these two steps is performed a certain amount of times or until the fitness function converges.

The docking programs AutoDock,[18] DIVALI,[19] DARWIN[20] and GOLD, which has been used in this dissertation to perform all the protein-ligand docking studies, all use or include a GA or GA-like algorithm.

2.1.3. Simulation methods

Simulations methods are based on the calculation of the solutions to Newton's equation of motion. Molecular dynamics (MD) is one of the most widely used techniques. MD allows molecules to interact at a given temperature for a period of time, giving a view of the motion of the atoms through time. These molecules are interacting under a defined potential and moving according to the Newton's equation of motion. Although MD methods are a powerful tool in docking, they present several drawbacks. One of the main drawbacks is the high computational cost required to guarantee a reasonable exploration of the conformational sampling.

In general, MD simulations have been widely used before and after the protein–ligand docking: before docking, to optimise the protein receptor structure and account for protein flexibility; and after docking, to refine already docked complexes by incorporating solvent effects and flexibility of both the ligand and the receptor.

2.2. Scoring functions

Scoring functions are used to evaluate and rank the binding modes predicted on the basis of the search algorithm, being able to distinct between the true binding modes and all the alternative orientations explored. Ideally, a scoring function should be accurate and fast and easy to compute. However, the more accurate a scoring function is, the more computer-intensive.

Nowadays, there are several scoring functions available and they can be divided into three major classes: force field-based, empirical and knowledge-based.[4,21,22]

2.2.1. Force field-based scoring functions

Force field scoring functions are based on non-bonded terms of the molecular mechanics force field. The set of parameters used by these scoring functions are usually derived from both experimental data and QM calculations according to the principles of physics. Despite its physical meaning, there are some limitations in force field-based scoring functions related to solvation and entropic terms.

Some examples of force field-based scoring functions are GoldScore[9] and DOCK[7] scoring functions.

2.2.2. Empirical scoring functions

Empirical scoring functions estimate the binding affinity of a complex in the basis of a set of weighted energy terms:

$$\Delta G = \sum_i W_i \cdot \Delta G_i \qquad (10)$$

where ΔG_i represents individual energy terms such as van der Waals energy, electrostatics, hydrogen bond, desolvation, etc. and W_i the corresponding coefficients, which are determined by fitting the binding affinity data of a set of protein-ligand complexes with known three-dimensional structures.

Empirical scoring functions are much faster in binding score calculations due to their simple energy terms. However, the main disadvantage of these methods is their dependence on the experimental data set used in the parameterization process.

An example of empirical scoring function is ChemPLP[23] implemented in GOLD, which has been used in the present dissertation. Among the fitness functions available in GOLD,

ChemPLP has been found to give the highest rates for both pose prediction and virtual screening.

Concerning the ChemPLP equation, two separate terms are included by taking into account hydrogen bonds, metal atoms and steric effects.

$$f_{CHEMPLP} = f'_{PLP} - (f_{chem-hb} + f_{chem-cho} + f_{chem-met}) \quad (11)$$

Equation (11) is the general ChemPLP scoring function, where f'_{PLP} is the *piecewise linear potential* (PLP) fitness function and $f_{chem\text{-}hb}$, $f_{chem\text{-}cho}$ and $f_{chem\text{-}met}$ are terms of ChemScore scoring function, which are used to introduce distance- and angle-dependent terms for hydrogen bonding and metal binding.

The *Piecewise Linear Potential* (PLP) models the attraction and repulsion of the protein and the ligand atoms. The fitness function PLP equation can be separated in five different terms as it can be seen in Equation 11.

$$f'_{PLP} = -(w_{PLP} \cdot f_{PLP} + w_{lig-clash} \cdot f_{lig-clash} + w_{lig-tors} \cdot f_{lig-tors} + f_{chem-cov} + w_{prot} \cdot f_{prot} + w_{cons} \cdot f_{cons}) \quad (11)$$

Here f_{PLP} is used to model the steric complementarity between the protein and the ligand, $f_{lig\text{-}clash}$ and $f_{lig\text{-}tors}$ are the heavy-atom clash potential and the torsional potential used within ChemScore, $f_{chem\text{-}cov}$ is the term used to consider covalent docking, $f_{chem\text{-}prot}$ is the term used for flexible side-chains and f_{cons} is the term used to consider constraints. The mathematical functions of each term may be found in the corresponding literature.[23]

ChemPLP function assigns general atom types to all protein and ligand atoms. The atom types are:

- *H-bond donor*. Nitrogen atom with at least one attached hydrogen and no accessible lone pair.
- *H-bond acceptor*. Oxygen or nitrogen atoms not attached to hydrogen atoms with one or two connections, except -O- in ester groups.
- *H-bond donor/acceptor*. Oxygen and nitrogen that can act as both (e.g. hydroxyl, water).
- *Nonpolar*. Non-hydrogen atoms that are not classified according to the other rules. *Metal*. Metal atoms.
- *H*. Any hydrogen attached to oxygen or nitrogen.

- *Charged H*. donor's hydrogen neighbour has positive formal charge
- *CH*-donor. Hydrogen attached to a carbon atom neighboured to an aromatic ring nitrogen acceptor
- *Charged acc*eptor. Acceptor has negative formal charger

It is noteworthy that the final score ($f_{CHEMPLP}$) is dimensionless. In the present dissertation, this final score is referred to as "binding energy" for the sake of clarity, despite it should not be considered as an accurate value of binding energy.

ChemScore[24] and FlexX[6] are other examples of empirical scoring functions.

2.2.3. Knowledge-based scoring functions

Knowledge-based scoring functions, also known as statistical-potential based scoring functions, focus on predicting good orientations rather than binding affinities, employing energy potentials that are derived from the structural information contained in protein–ligand complexes of known structure available in the PDB. These methods are based on the assumption that the frequency of occurrence of individual contacts between protein and ligand atoms is related to their energetic contribution to binding.

DrugScore[25,26] and GOLD/ASP[27] are examples of this kind of scoring functions.

In the last years, protein-ligand docking approaches have achieved several improvements in both search and scoring algorithms, but some limitations are still a challenge in this field.

3. References

(1) Taylor, R. D.; Jewsbury, P. J.; Essex, J. W. *J. Comput. Aided. Mol. Des.* **2002**, *16*, 151–166.

(2) Sousa, S. F.; Fernandes, P. A.; Ramon, M. J. *Proteins: Struct., Funct., Bioinf.* **2006**, *65*, 15–26.

(3) Moitessier, N.; Englebienne, P.; Lee, D.; Lawandi, J.; Corbeil, C. R. *Br. J. Pharmacol.* **2008**, *153 Suppl.*, S7–26.

(4) Huang, S.-Y.; Zou, X. *Int. J. Mol. Sci.* **2010**, *11*, 3016–3034.

(5) Muegge, I.; Rarey, M. In *Reviews in Computational Chemistry*; John Wiley & Sons, Inc., 2001; Vol. 17, pp. 1–60.

(6) Rarey, M.; Kramer, B.; Lengauer, T.; Klebe, G. *J. Mol. Biol.* **1996**, *261*, 470–489.

(7) Lang, P. T.; Brozell, S. R.; Mukherjee, S.; Pettersen, E. F.; Meng, E. C.; Thomas, V.; Rizzo, R. C.; Case, D. A.; James, T. L.; Kuntz, I. D. *RNA* **2009**, *15*, 1219–1230.

(8) Miller, M. D.; Kearsley, S. K.; Underwood, D. J.; Sheridan, R. P. *J. Comput. Mol. Des.* **1994**, *8*, 153–174.

(9) Verdonk, M. L.; Cole, J. C.; Hartshorn, M. J.; Murray, C. W.; Taylor, R. D. *Proteins* **2003**, *52*, 609–623.

(10) Hart, T. N.; Read, R. J. *Proteins* **1992**, *13*, 206–222.

(11) Abagyan, R.; Totrov, M.; Kuznetsov, D. *J. Comput. Chem.* **1994**, *15*, 488–506.

(12) Baxter, C. A.; Murray, C. W.; Clark, D. E.; Westhead, D. R.; Eldridge, M. D. *Proteins* **1998**, *33*, 367–382.

(13) Korb, O.; Stützle, T.; Exner, T. E. In *Lecture Notes in Computer Science*; Springer, 2006; pp. 247–258.

(14) Namasivayam, V.; Günther, R. *Chem. Biol. Drug Des.* **2007**, *70*, 475–484.

(15) Clark, D. E.; Westhead, D. R. *J. Comput. Mol. Des.* **1996**, *10*, 337–358.

(16) Devillers, J. In *Genetic Algorithms in Molecular Modeling*; Elsevier Ltd, 1996; pp. 1–34.

(17) Venkatasubramanian, V.; Sundaram, A. In *Encyclopedia of computational chemistry*; John Wiley & Sons, Inc., 1998; pp. 1115–1127.

(18) Morris, G. M.; Goodsell, D. S.; Halliday, R. S.; Huey, R.; Hart, W. E.; Belew, R. K.; Olson, A. J.; Al, M. E. T. *J. Comput. Chem.* **1998**, *19*, 1639–1662.

(19) Clark, K. P. *J. Comput. Chem.* **1995**, *16*, 1210–1226.

(20) Taylor, J. S.; Burnett, R. M. *Proteins* **2000**, *41*, 173–191.

(21) Huang, S.-Y.; Grinter, S. Z.; Zou, X. *Phys. Chem. Chem. Phys.* **2010**, *12*, 12899–12908.

(22) Sousa, S. F.; Fernandes, P. A.; Ramos, M. J. *Proteins: Struct., Funct., Bioinf.* **2006**, *65*, 15–26.

(23) Korb, O.; Stu, T.; Exner, T. E. *J. Chem. Inf. Model.* **2009**, *49*, 84–96.

(24) Eldridge, M. D.; Murray, C. W.; Auton, T. R.; Paolini, G. V; Mee, R. P. *J. Comput. Aided. Mol. Des.* **1997**, *11*, 425–445.

(25) Gohlke, H.; Hendlich, M.; Klebe, G. *J. Mol. Biol.* **2000**, *295*, 337–356.

(26) Velec, H. F. G.; Gohlke, H.; Klebe, G. *J. Med. Chem.* **2005**, *48*, 6296–6303.

(27) Mooij, W. T. M.; Verdonk, M. L. *Proteins* **2005**, *61*, 272–287.

Formula Index

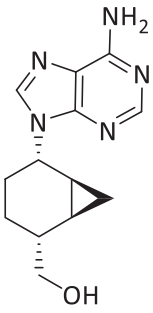
D-**2-A**

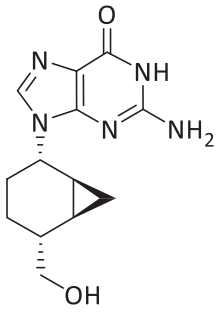
D-**2-G**

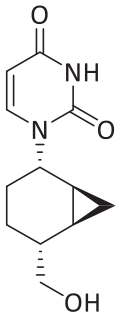
D-**2-U**

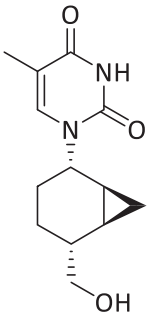
D-**2-T**

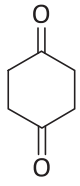
7

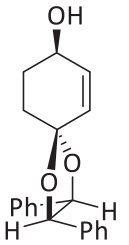
8

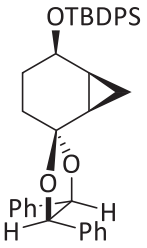
9

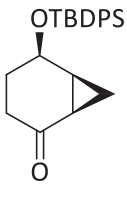
10

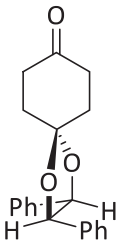
11

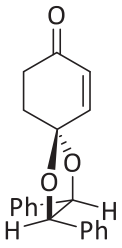
12

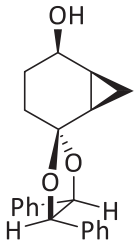
13

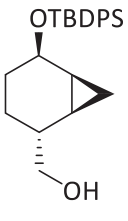
14


15

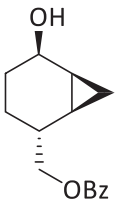
16

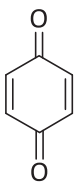
18

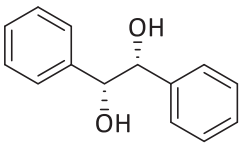
19

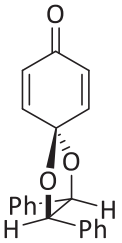
20

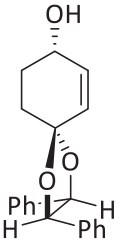
21

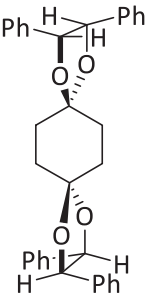
22

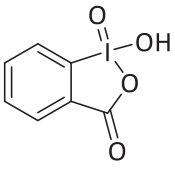
23

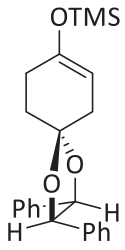
24

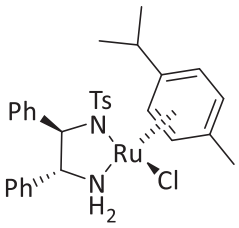
25

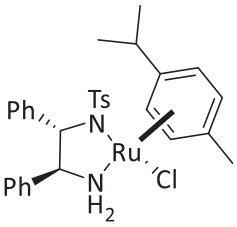
26

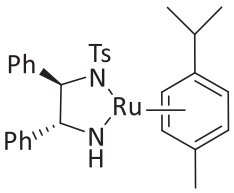
27

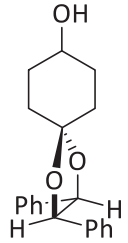
28

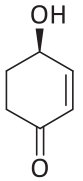
(*R*)-**29**

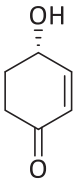
(*S*)-**29**

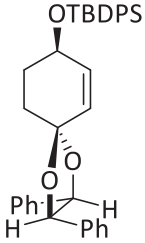
30

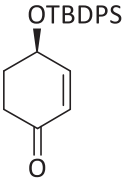
31

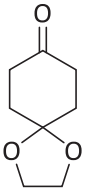
34

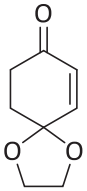
35

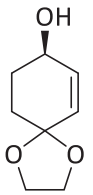

(*R*)-**36**

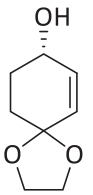

(*S*)-**36**

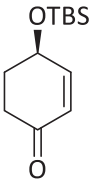

(*R*)-**37**

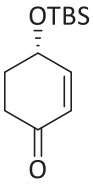

(*S*)-**37**

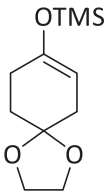

38

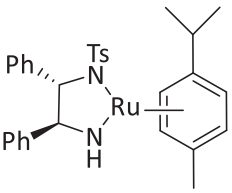

39

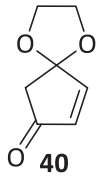

40

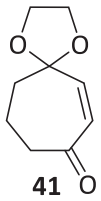

41

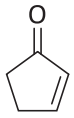

42

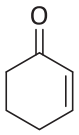

43

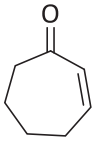

44

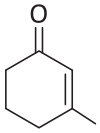

45

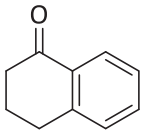

46

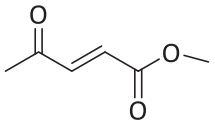

47

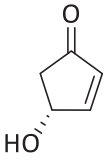

48

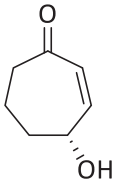

49

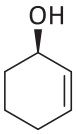

50

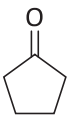

51

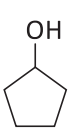

52

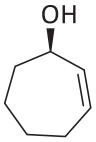

53

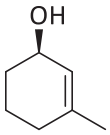

54

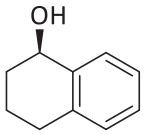

55

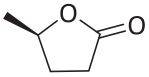

56

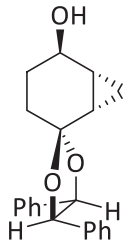

59

60

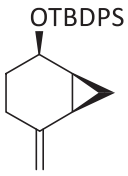

61

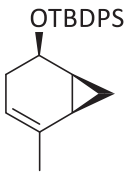

62

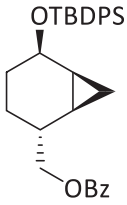

63

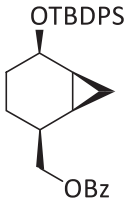

64

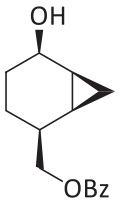

65

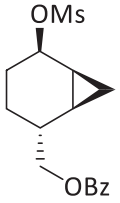

68

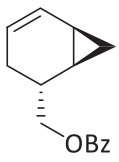

69

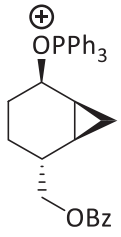

70

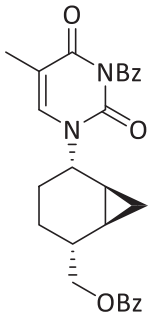

71

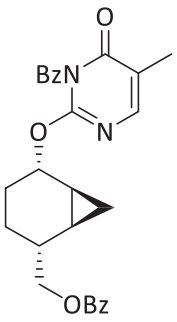

72

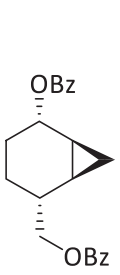

73

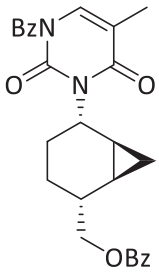

74

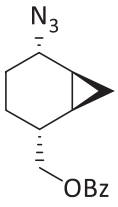

75

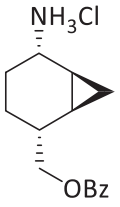

76

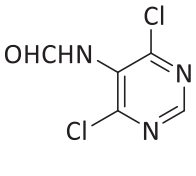

78

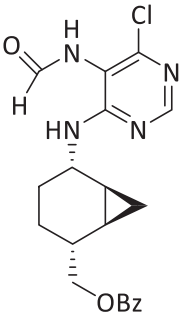

81

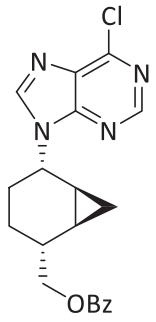

82

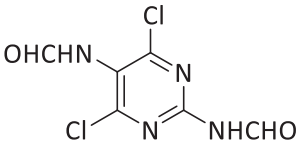

86

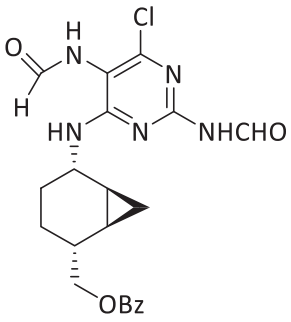

87

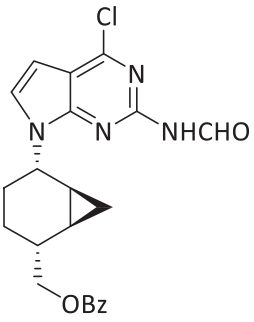

88

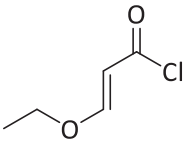

92

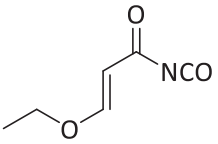

94

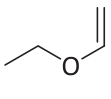

95

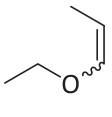

96

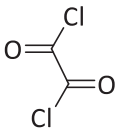

98

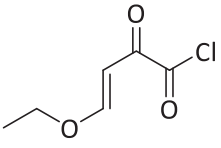

99

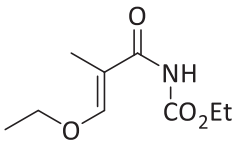

101

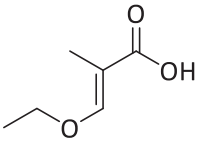

111